

**For Reference**


---

**NOT TO BE TAKEN FROM THIS ROOM**



Ex libris  
UNIVERSITATIS  
ALBERTAENSIS





Digitized by the Internet Archive  
in 2023 with funding from  
University of Alberta Library

<https://archive.org/details/Banka1970>





THE UNIVERSITY OF ALBERTA

PERFORMANCE OF TWO-PHASE REACTORS-  
OXIDATION OF ACETALDEHYDE TO ACETIC ACID

BY



RAJ K. BANKA

A THESIS

SUBMITTED TO THE FACULTY OF GRADUATE STUDIES  
IN PARTIAL FULFILLMENT OF THE REQUIREMENTS FOR THE DEGREE  
OF MASTER OF SCIENCE IN CHEMICAL ENGINEERING

DEPARTMENT OF CHEMICAL AND PETROLEUM ENGINEERING

EDMONTON, ALBERTA

FALL, 1970





Thesis  
1970 F  
10

UNIVERSITY OF ALBERTA

The candidate of FACULTY OF GRADUATE STUDIES

The undersigned certify that they have read, and recommend to the Faculty of Graduate Studies for acceptance a thesis entitled PERFORMANCE OF TWO-PHASE REACTORS - OXIDATION OF ACETALDEHYDE TO ACETIC ACID submitted by Raj K. Banka in partial fulfilment of the requirements for the degree of Master of Science in Chemical Engineering.





## ABSTRACT

The oxidation of acetaldehyde to acetic acid using a manganese(ous) acetate catalyst was studied in a single-orifice four-inch sparged reactor with a view to modelling the performance of a two-phase reactor.

The kinetic data were obtained in a stirred-tank reactor under conditions of high turbulence where chemical reaction was controlling. It was found that the over-all rate of oxidation could be described by a rate expression which is first order in oxygen, first order in acetaldehyde and first order in catalyst concentration.

In order to model gas-liquid reactors such parameters as gas hold-up, interfacial area and physical mass transfer coefficients must be known or estimated. A review of the literature concerning these parameters is presented along with values determined experimentally for the oxygen-acetic acid system. Calderbank's equation for interfacial area, Hughmark's equation for gas hold-up and Calderbank's correlation for mass transfer coefficients for bubble swarms (of average bubble diameter  $< 0.25$  cm) and Hughmark's equation for mass transfer coefficients for bubble swarms provide values which are in reasonable agreement with the experimental values.

A simple mathematical model was developed which predicts the performance of the sparged reactor satisfactorily under simple operating conditions, that is, for the case where the liquid may be assumed to be perfectly mixed and a pure gas is used.





## ACKNOWLEDGEMENT

The author is particularly indebted to Dr. F.D. Otto, for his encouragement, guidance and constructive criticism.

Acknowledgement is gratefully made to Dr. T. Akiyama for his suggestions and help in the theoretical analysis.

The author is indebted to Chemcell Limited for the supply of chemicals and to the National Research Council and the University of Alberta for the financial assistance during the course of this project.





## TABLE OF CONTENTS

|   | <u>Page</u> |
|---|-------------|
| LIST OF TABLES  | i           |
| LIST OF FIGURES   | iii         |
| I. INTRODUCTION   | 1           |
| II. OXIDATION OF ACETALDEHYDE   | 4           |
| A. Chemistry of Oxidation of Acetaldehyde and<br>the Reaction Mechanism         | 4           |
| B. Reaction Kinetics  | 14          |
| III. SIMULTANEOUS ABSORPTION AND CHEMICAL REACTION:<br>MATHEMATICAL DESCRIPTION | 21          |
| A. Slow Reaction Regime   | 23          |
| B. Fast Reaction Regime   | 27          |
| C. Transition from Slow to Fast Reaction  | 27          |
| D. Instantaneous Reaction Regime  | 28          |
| E. Transition from Fast to Instantaneous Reaction                               | 29          |
| IV. DESIGN OF TWO-PHASE REACTORS  | 30          |
| V. PARAMETER EVALUATION   | 39          |
| A. Bubble Behavior and Mechanics of Bubble Formation                            | 39          |
| B. Mass Transfer Coefficient  | 45          |
| C. Gas Hold-up  | 48          |
| D. Interfacial Area   | 52          |
| VI. EXPERIMENTAL  | 56          |
| A. Kinetic Measurements   | 56          |
| (a) Experimental Equipment  | 56          |
| (b) Experimental Procedure  | 58          |
| (c) Experimental Conditions   | 60          |





|   |     |
|---|-----|
| B. Sparged Reactor Study  | 60  |
| (a) Experimental Equipment  | 60  |
| (b) Measurement of Gas Hold-up                                      | 64  |
| (c) Measurement of Bubble Diameters                                 | 64  |
| (d) Measurement of Rate of Conversion of<br>Acetaldehyde            | 66  |
| C. Analysis of Liquid Components                                    | 67  |
| VII. RESULTS  | 70  |
| A. Kinetic Studies  | 70  |
| (a) Determination of Operating Conditions for<br>the Kinetic Regime | 70  |
| (b) Effect of Acetaldehyde Concentration                            | 76  |
| (c) Effect of Oxygen Concentration                                  | 76  |
| (d) Effect of Temperature   | 76  |
| (e) Effect of Catalyst Concentration                                | 76  |
| (f) Check of Reproducibility  | 76  |
| (g) Catalyst Activity   | 79  |
| (h) Determination of Rate Equation                                  | 79  |
| B. Sparged Reactor  | 91  |
| (a) Hold-up Measurements  | 91  |
| (b) Bubble Diameter and Interfacial Area                            | 94  |
| (c) Conversion of Acetaldehyde to Acetic Acid                       | 99  |
| 1. Experimental Results   | 99  |
| 2. Modelling Sparged Reactor  | 99  |
| VIII. DISCUSSIONS AND CONCLUSIONS                                   | 104 |
| LIST OF SYMBOLS   | 107 |



|   |     |
|---|-----|
| BIBLIOGRAPHY                                    | 112 |
| APPENDIX A                                      | 117 |
| DERIVATION OF CHEMICAL REACTION RATE EXPRESSION | 117 |
| SOLUBILITY OF OXYGEN IN ACETIC ACID             | 119 |
| DIFFUSIVITY OF OXYGEN IN ACETIC ACID            | 121 |
| DETERMINATION OF THE REACTION REGIME            | 122 |
| COMPUTER PROGRAMME FOR RUNGE KUTTA METHOD       | 124 |
| APPENDIX B - BASIC DATA                         | 127 |





LIST OF TABLES

|   | <u>Page</u> |
|---|-------------|
| Table Vll.1                                 |             |
| Bubble Diameters, Hold-up and Interfacial   |             |
| Area as a Function of Superficial Gas       | 96          |
| Velocity.                                   |             |
| Table Vll.2                                 |             |
| Physical Mass Transfer Coefficients.        | 102         |
| Table B.1                                   |             |
| The Effect of Agitation on Reaction Rate.   | 127         |
| Table B.2                                   |             |
| The Effect of Agitation on Reaction Rate.   | 130         |
| Table B.3                                   |             |
| The Effect of Agitation on Reaction Rate.   | 131         |
| Table B.4                                   |             |
| The Effect of Sample Size and Agitation     |             |
| on Reaction Rate.                           | 132         |
| Table B.5                                   |             |
| The Effect of Temperature on Reaction Rate  | 133         |
| Table B.6                                   |             |
| The Effect of Catalyst Concentration on     |             |
| Reaction Rate.                              | 134         |
| Table B.7                                   |             |
| Check of the Reproducibility.               | 135         |
| Table B.7'                                  |             |
| The Catalyst Activity.                      | 136         |
| Table B.8                                   |             |
| The Effect of AcH and $O_2$ Concentrations  |             |
| on Reaction Rate.                           | 137         |
| Table B.9                                   |             |
| The Effect of AcH and $O_2$ Concentrations  |             |
| on Reaction Rate.                           | 138         |
| Table B.10                                  |             |
| The Effect of AcH and $O_2$ Concentrations  |             |
| on Reaction Rate.                           | 139         |
| Table B.11                                  |             |
| The Effect of Temperature on Reaction Rate. | 140         |
| Table B.12                                  |             |
| The Effect of Temperature on Reaction Rate. | 141         |
| Table B.13                                  |             |
| The Effect of Catalyst Concentration on     |             |
| Reaction Rate.                              | 142         |





|            |  |     |
|------------|--|-----|
| Table B.14 | The Effect of Catalyst Concentration on<br>Reaction Rate.                                  | 143 |
| Table B.15 | Comparison of the Predicted and<br>Experimental Results.                                   | 144 |
| Table B.16 | Oxygen Flow Rate vs Fractional Gas Hold-up.  | 145 |
| Table B.17 | Comparison of the Experimental $\epsilon$ With the<br>Values Given by Hughmark's Equation. | 146 |
| Table B.18 | Individual Bubble Diameters.   | 147 |
| Table B.19 | Individual Bubble Diameters.   | 149 |
| Table B.20 | Individual Bubble Diameters.   | 150 |
| Table B.21 | Individual Bubble Diameters  | 151 |
| Table B.22 | Individual Bubble Diameters  | 153 |
| Table B.23 | Conversion of AcH to AcOH in Sparger Reactor.  | 154 |
| Table B.24 | Conversion of AcH to AcOH in Sparger Reactor.  | 155 |
| Table B.25 | Model Predicted Concentration Profile in<br>Sparged Reactor for $O_2 = 85$ ccs/sec.        | 156 |
| Table B.26 | Model Predicted Concentration Profile in<br>Sparged Reactor for $O_2 = 334$ ccs/sec.       | 157 |



LIST OF FIGURES

|  | Page |
|--|------|
| Figure 1   | 57   |
| Schematic of the Apparatus for Study of Kinetics.                                  |      |
| Figure 2   | 61   |
| Schematic of the Sparged Reactor.  |      |
| Figure VII.1   | 71   |
| Effect of Stirrer RPM on "Concentration of AcOH vs. Time" Curve.                   |      |
| Figure VII.2   | 73   |
| Effect of Stirrer RPM on "Concentration of AcOH vs Time" Curve.                    |      |
| Figure VII.3   | 74   |
| Effect of Stirrer RPM on 'Concentration of Acetic Acid vs. Time Curve'.            |      |
| Figure VII.4   | 75   |
| Effect of Sample Size and Stirring Rate on 'Concentration of AcOH vs. Time' Curve. |      |
| Figure VII.5   | 77   |
| Effect of Temperature on 'Concentration of AcOH vs. Time' Curve.                   |      |
| Figure VII.6   | 78   |
| Effect of Catalyst Concentration on 'Concentration of Acetic Acid vs. Time' Curve. |      |
| Figure VII.7   | 80   |
| Check of the Reproducibility.  |      |
| Figure VII.7'  | 81   |
| Catalyst Activity for Reaction.  |      |
| Figure VII.8   | 83   |
| Verification of the Assumed Rate Expression by the Integral Method.                |      |
| Figure VII.9   | 85   |
| Effect of Temperature on Reaction Rate Constant.                                   |      |
| Figure VII.10  | 86   |
| Effect of Temperature on $K_R$ .   |      |
| Figure VII.11  | 88   |
| Effect of Catalyst Concentration on $K_R$ .  |      |





|               |  |     |
|---------------|--|-----|
| Figure VII.12 | Check of the Reaction Order in Catalyst Concentration.                                 | 89  |
| Figure VII.13 | Dependence of the Reaction Rate on Catalyst Concentration.                             | 90  |
| Figure VII.14 | Comparison of the Predicted and the Experimental Kinetic Results.                      | 92  |
| Figure VII.15 | Hold-up Correlation for $O_2$ -AcOH System and Comparison With Hughmark's Correlation. | 93  |
| Figure VII.16 | Superficial Gas Velocity of $O_2$ vs. $d_{vs}$ .                                       | 97  |
| Figure VII.17 | Superficial Gas Velocity of $O_2$ vs. $a'$ .   | 98  |
| Figure VII.18 | Liquid Concentration Profiles in the Sparged Reactor.                                  | 103 |



## CHAPTER 1

### INTRODUCTION

Gas-sparged contacting devices or gas bubble columns, in which a gas is bubbled through a deep liquid without mechanical agitation, are commonly used in industrial practice as absorbers, strippers and reactors. Some of the current applications of gas-sparged contactor technology are listed below (1).

| <u>Process</u>         | <u>Reactants</u>                   |
|------------------------|------------------------------------|
| Acetaldehyde           | Oxygen, ethylene                   |
| Acetic Acid            | Oxygen, acetaldehyde               |
| Acrylonitrile          | Acetylene, hydrogen cyanide        |
| Ammonium Nitrate       | Ammonia, nitric acid               |
| Cyclohexane            | Hydrogen, benzene                  |
| Ethylene dichloride    | Ethylene, chlorine                 |
| Hydrogen Peroxide      | Air, hydroquinone                  |
| Oxo-processing         | Hydrogen, carbon monoxide, olefine |
| Phenol                 | Air, cumene                        |
| Synthetic hydrocarbons | Hydrogen, carbon monoxide          |

Fermentations, waste oxidations and the general hydrogenation-oxidation-chlorination of hydrocarbons are also carried out in sparged reactors.

Many reaction situations can occur in sparged contactors and no simple set of design procedures are available. A few typical situations are the following.

1. Reactants may be in the liquid phase, with the gas serving only as an agitating medium.





2. A component of the gas may react directly with a component of the liquid.
3. A component of the gas may react with a component of the liquid, the reaction taking place on the surface of a suspended solid catalyst.
4. Two (or more) components of the gas may react with a component of the liquid or a suspended solid serving as a catalyst but not otherwise participating in the reaction.

In order to be able to design a two-phase sparged reactor, one has to deal with gas dispersion, dynamic gas hold-up, mass transfer and chemical kinetics. In the case of simultaneous mass transfer and chemical reaction, one must determine the relative contribution of chemical reaction rate and mass transfer rate on the overall reaction rate. Rate of mass transfer is a function of gas hold-up and average bubble diameter. Gas hold-up and average bubble diameter are functions of hydrodynamic and geometric parameters.

A considerable volume of literature is now available that is concerned with the subject of two-phase flow. The majority of literature covers the area of hydrodynamics and heat transfer and a small amount of work is reported in the field of mass transfer with and without chemical reactions. Design-information on sparged reactors is scarce.

The main purpose of this work was to study the performance of a two-phase sparged reactor in which a desired product was formed by the reaction of gas and liquid reactants and to investigate possible design procedures. This involved studies to establish the reaction kinetics



determining suitable models for sparged reactors, evaluating procedures for the various design parameters and measuring conversions in a four inch diameter semibatch sparged reactor. Kinetic data were obtained in an intensively-stirred autoclave where an attempt was made to eliminate mass-transfer effects by creating a great deal of liquid turbulence.

The reaction chosen for this study was the oxidation of acetaldehyde to acetic acid because of the mild experimental conditions required and also because this reaction is industrially important. Chemcell Limited manufactures acetic acid by the oxidation of acetaldehyde in a sparged reactor and has a considerable interest in this reaction.





## CHAPTER II

OXIDATION OF ACETALDEHYDE

When exposed to oxygen or air, an aldehyde is slowly oxidized to the corresponding peracid, which may further react with the aldehyde to form the normal acid. The rate of oxidation is decreased by a long list of inhibitors and is increased by light and certain catalysts, for example, the acetates of Mn, Co and Cu (2). Further, depending on the experimental conditions, e.g. temperature, concentration of liquid and gas reactants, type of catalysts, purity of reactants, etc., different products are formed. For example, for the oxidation of acetaldehyde, the reaction can be controlled to give the desired product as peracetic acid, acetic anhydride or acetic acid. In the presence of manganese (ous) acetate catalyst, oxidation of acetaldehyde gives acetic acid as the main product. The over-all reaction is

A. Chemistry of Oxidation of Acetaldehyde and the Reaction Mechanism:Initiation and the Induction period:-

In the uncatalyzed oxidation there is always an induction period of unpredictable length (3,4). Use of a catalyst shortens the induction period and in its presence there may or may not be a measurable induction period depending on the catalyst concentration. For example, Bawn and Williamson (4) observed that with  $10^{-6}$  molar  $\text{Mn}(\text{OAc})_2$  there was an induction period, whereas with  $4 \times 10^{-2}$  molar there was not.

When using Mn salts, the end of the induction period occurs when there is a change in color of the reaction mixture from pink to dark brown (5). At this time there is a rapid uptake of oxygen and a considerable

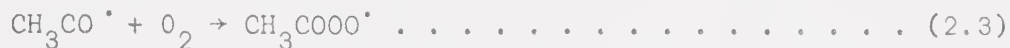


evolution of heat. The color changes noted are associated with a change in the valence of the catalyst from  $Mn^{++}$  to  $Mn^{+++}$  (6).

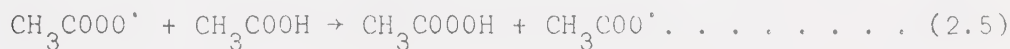
The first reaction in the initiation process is that of molecular oxygen with AcH (acetaldehyde) to give an acetyl radical:-



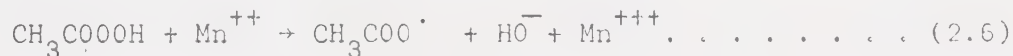
The acetyl radical reacts further with molecular oxygen to give the acetylperoxy radical:-



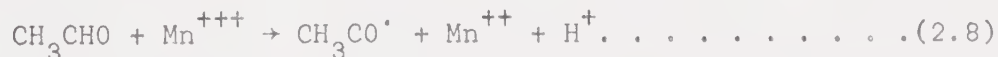
Peracetic acid is then formed from this latter radical either by reaction with acetaldehyde (reaction 2.4) or acetic acid (if acetic acid is used in the reaction mixture) or by a combination of both.



The  $HOOAc$  (peracetic acid) so formed then oxidizes the ionic catalyst, e.g.  $Mn^{++}$ , to its next highest valence state, either by reaction (2.6) or (2.7).



The resulting oxidized cation reacts with acetaldehyde (AcH) to form the acetyl radical (reaction 2.8) which initiates a chain reaction as depicted by equations (2.3) and (2.4)

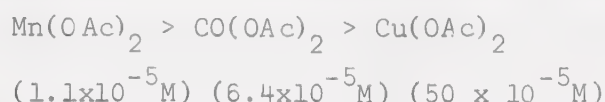


It should be noted that reaction (2.8) is much faster than reaction (2.2) and is more important than reaction (2.2) after the induction period is over. The reduced state of the cation (as formed in reaction (2.8), for example) is re-oxidized via reaction (2.6) or (2.7).





From the above reactions, it can be seen that the induction period is shortened or may be completely eliminated upon the addition of  $\text{Mn}(\text{OAc})_3$  to the reaction mixture (5). Conversely, it is lengthened substantially by the addition of benzoquinone. This latter substance is well-known for its ability to react with (i.e. destroy) free radicals. Many other cations have been proposed for the initiation reactions and the following order of activity is suggested (3):-



The presence of water in the reaction mixture causes an increase in the induction period, even when  $\text{Mn}(\text{OAc})_3$  is added (5). This effect may be due to the conversion of the Mn-salts to  $\text{Mn}(\text{OOH})_2$  which has in fact been isolated from oxidation mixtures and found to be inactive as a catalyst (5).

#### The Chain Reaction and Formation of Peracetic Acid:-

The following mechanism for the chain reaction is widely accepted for both the liquid and vapor phase oxidations (3,4). The acetyl radical formed in reaction (2.8) reacts with oxygen as described previously (reaction 2.3) and the resulting acetylperoxy radical reacts with  $\text{AcH}$  to give  $\text{HOOAc}$  (reaction 2.4). Reactions (2.3) and (2.4) together constitute the "chain reaction" - in other words one of the reactants in reaction (2.3) is produced in reaction (2.4) and one of the reactants in reaction (2.4) is produced in reaction (2.3). The overall effect is the production of  $\text{HOOAc}$  from  $\text{AcH}$  and  $\text{O}_2$  (reaction 2.9).





This reaction will be maintained as long as AcH and  $O_2$  are provided, and as long as no  $CH_3CO^\bullet$  or  $CH_3COOO^\bullet$  are consumed by routes other than reaction (2.3) or (2.4). This latter requirement is not always met because of the chain termination reactions (discussed later) and in order to sustain the chain reaction, reaction (2.8) is called into play to replenish the supply of acetyl radicals. However, reaction (2.8) can function only with a supply of AcH and  $Mn^{+++}$  ions, the latter being obtained by reaction (2.6) or (2.7).

It should be noted that  $Mn^{+++}$  (or  $Co^{+++}$ ) does not affect reaction (2.3) or (2.4) but is partly responsible for the formation (in reaction 2.8) of one of the reactants in reaction (2.3) and, as will be shown later for the decomposition of  $HOOAc$ . Therefore, the metal ion concentration enters into the overall kinetic rate equation for the oxidation.

#### The Chain Termination Reaction:-

As mentioned earlier any reaction which consumes the  $CH_3CO^\bullet$  and  $CH_3COOO^\bullet$  radicals will inhibit the chain reaction (reactions 2.3 and 2.4). The effect of this chain inhibition will be much greater for a batch reaction than for a continuous one. Some biacetyl may form as a reaction product via reaction (2.10).

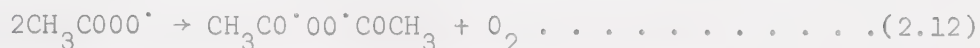


Carbon monoxide and products produced from methyl radicals are also noted as oxidation by-products. These would result from reaction (2.11)





It is more likely that the decomposition of the acetylperoxy radicals is the main chain-breaking reaction. They can, for example, react according to reaction (2.12),



to give an unstable product, which breaks down further to stable products like  $\text{CH}_3\cdot$ ,  $\text{CO}$ ,  $\text{O}_2$ , etc. Further, since  $\text{H}_2\text{O}$  inhibits the uncatalyzed as well as the catalyzed oxidation, it is possible that a reaction such as (2.13) is involved.



The  $\cdot\text{OH}$  radical formed does not participate in the chain reaction.

#### Conditions For Maximising Peracetic Acid:-

Yau et al. (7) studied oxidation of acetaldehyde with a view to maximising peracetic acid as the final product and maintained the following experimental conditions:

1. Temperature:  $5 - 15^\circ\text{C}$ , so that peracetic acid formed in reaction (2.9) is stable. At higher temperatures, peracetic acid will decompose easily to acetic acid (reaction 2.20, given later).
2. Catalyst type and concentration:  $\text{CO}(\text{OAc})_2$ , 20 - 40 ppm, which is good for the initiation and low concentration is used so that there is no further catalytic decomposition of peracetic acid by reaction (2.20).
3. AcH Concentration: 5 - 10% by volume supported by industrial practice.





### Formation of Acetic Acid and Acetic Anhydride:-

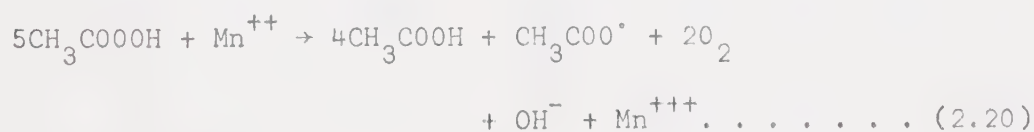
In this section the formation of acetic acid and acetic anhydride as the main products from the principal intermediate peracetic acid will be discussed.

#### (1) The Catalytic Decomposition of Peracetic Acid (HOOAc):-

It is well known that a solution of HOOAc in HOAc is stable for long periods of time (4); however, in the presence of over  $1.3 \times 10^{-6} \text{M}$  of  $\text{Mn}(\text{OAc})_2$  or over  $1.3 \times 10^{-5} \text{M}$  of  $\text{CO}(\text{OAc})_2$  (6) a vigorous reaction occurs (accompanied by a color change associated with the appearance of a trivalent cation). The products of the reaction are HOAc,  $\text{O}_2$  and small amounts of  $\text{CO}_2$ , CO and gaseous hydrocarbons (5). No acetic anhydride ( $\text{Ac}_2\text{O}$ ) was found as a product (5). It is suggested that the decomposition of peracetic acid to acetic acid proceeds by the steps (2.6) plus (2.14) to (2.19),



The overall reaction is given by equation (2.20):-





(2) Direct Reaction of Acetaldehyde and Peracetic Acid to Give Acetic Acid and/or Acetic Anhydride:-

The decomposition of HOOAc by AcH was originally believed to occur by reaction (2.21) and was studied by observing the action of AcH on HOOAc dissolved in HOAc (5).



HOAc catalyzes the above reaction. Further studies (3,4) indicated that the reaction proceeded in two steps:-



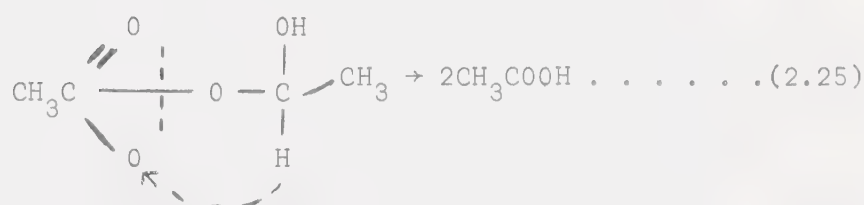
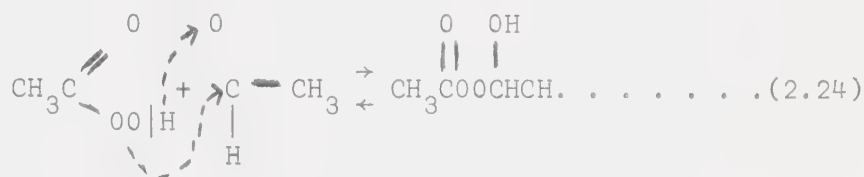
Either one or both reactions (2.22 and 2.23) are catalyzed by acid. It has been contemplated (2,3,5) that one peracid and one aldehyde molecule react to form a complex (reaction 2.22) which decomposes into two acid molecules (reaction 2.23). These two reactions were studied at low temperatures (5), in the expectation that while the fast reaction (2.22) would be substantially slowed, reaction (2.23) would stop altogether. This was indeed found to be the case; and at  $-61^\circ\text{C}$ , a bimolecular velocity constant of  $0.031/\text{mole}/\text{cm}^3/\text{sec}$  was found, while at  $-41^\circ\text{C}$  it was  $0.132/\text{mole}/\text{cm}^3/\text{sec}$  (5). By calculation, the velocity constant for reaction (2.22) at  $20^\circ\text{C}$  was  $3.1/\text{mole}/\text{cm}^3/\text{sec}$ , at least fifteen times that of the overall reaction.

Kagan and Lubarsky (5) isolated a peroxide, m.p.  $-20^\circ\text{C}$ . Bawn and co-workers (4) obtained a peroxide (m.p.  $22^\circ\text{C}$ ) and found it to have the empirical formula  $\text{C}_6\text{H}_{12}\text{O}_5$ . On examining its reactions they came to the conclusion that there was a molecule of "AcH of crystallization"



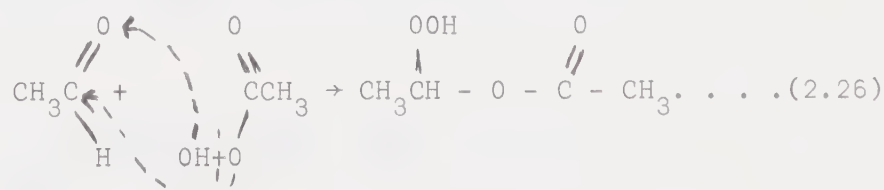
involved, so that the formula became  $C_4H_8O_4 \cdot CH_3CHO^-$ . The peroxide was decomposed to HOAc solution on the addition of  $CO(OAc)_2$ .

Kagan and Lubarsky (5) thought the peroxide had the structure shown in reaction (2.24) and that it was decomposed to HOAc according to reaction (2.25).

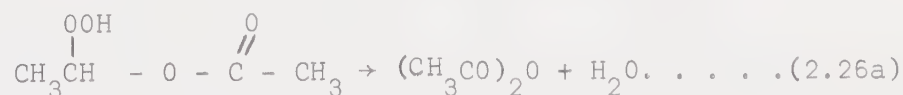


They based their proposed structure for the peroxide on the structure of analogous compounds formed by the action of  $H_2O_2$  on AcH or  $C_2H_5OOH$  on AcH (4).

Bawn's group believes that the peroxide breaks down to give  $Ac_2O$  first and that a peroxide of the structure suggested would not give  $Ac_2O$  so readily. They, therefore, proposed a reaction, such as (2.26), for the formation of the peroxide.



The product of (2.26) would easily give  $Ac_2O$  by splitting off  $H_2O$



Carpenter (8) recently studied the catalytic oxidation of AcH to  $Ac_2O$





and found that the reactions (2.26) and (2.26a) are most favorable at  $56^{\circ}\text{C}$  and in the presence of cobalt and copper acetate catalysts, whereas reaction (2.23) was found to be (9) favorable at  $40 - 60^{\circ}\text{C}$  and in the presence of  $80 - 250$  ppm  $\text{Mn}(\text{OAc})_2$  catalyst. Also water formed in reaction (2.26a) must be continuously removed, if  $\text{Ac}_2\text{O}$  is to be obtained as a major product. This could be done by separating the oxidation products into gas and liquid and then by dehydrating the liquid products by means of some water-carrying agent; many patents have been issued on this process (10). Allen (9) studied the catalytic oxidation of  $\text{AcH}$  to  $\text{AcOH}$  and found that the main role of the metal-ion (besides initiation) is to catalyze the reaction of  $\text{AcOOH}$  with  $\text{AcH}$  so effectively that it becomes the main route to  $\text{AcOH}$ . The catalytic decomposition of  $\text{AcOOH}$  is relatively too slow to be of any significance.

#### Conditions for Maximising Acetic Acid Production:-

1. Catalyst: manganese (ous) acetate (2,9,11)
2. Temperature:  $40 - 60^{\circ}\text{C}$  (1,9) which increases the rate of decomposition of peroxide.
3. Catalyst Concentration:  $80 - 240$  ppm (9) which is enough for both initiation and the decomposition of peroxide.
4. No water in the reactants since water can make the catalyst inactive.
5. Oxygen content in the reacting gases high: 90% oxygen and 10% nitrogen (9,12), supported by industrial practice.
6.  $\text{AcH}$  content low:  $2 - 10\%$ , supported by industrial practice, probably to lessen the chance of by-products formation.



### Conditions for Maximising Acetic Anhydride:-

The following conditions should be maintained (10) for obtaining a high yield (50 to 80%) of acetic anhydride:-

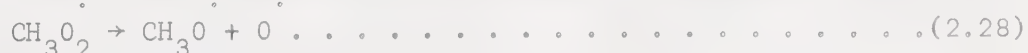
1. Oxygen content: 7 - 9% by volume as supported by industrial practice.
2. A mixture of Co and Cu-acetates in certain proportions to be established by experiments.
3. The reaction temperature: about 55°C, so that the decomposition of peroxide will be faster.
4. The acetaldehyde content in the reaction bath: 4 - 6%, supported by industrial practice, which will probably lessen the possibility of any by-products formation.
5. Continuous removal of water formed in reaction 26 (a).

### The Formation of By-products:-

Some by-products, whose concentration is generally small, may also be formed depending on the experimental conditions.

Carbon monoxide may be formed at 100°C by the decomposition of methyl radical. Carbon dioxide is formed at about 80°C (13). At low temperatures, e.g. 30° - 40°C, the probability of their formation is small (13).

Methanol, formaldehyde and formic acid could be formed (5) through the following reaction sequence:



Formic acid is probably formed by direct oxidation of formaldehyde.



B. Reaction Kinetics for Oxidation of Acetaldehyde to Acetic Acid:-

Laboratory stirred-tank reactors have often been used in order to obtain kinetics of gas-liquid reactions (11, 14, 15, 16). In this an attempt is made to eliminate mass-transfer effects by creating a great deal of liquid turbulence and interfacial area (11). Van De Vusse (17) has shown that at higher transfer rates the overall reaction rate approaches the chemical reaction rate. This is in agreement with the concept given by Astarita (15) that when two phenomena occur in series, the overall driving force is, in practice used entirely by that phenomenon which has a much smaller specific rate. Reaction kinetics have to be determined under the conditions when chemical reaction is controlling.

In aldehyde oxidation, the order of reaction has been found by the method of measuring the initial rate for various initial concentrations rather than by studying the change of rate during one complete run (2, 3, 11). However, Allen (9) and Yau et al (7) have successfully studied the reaction by following the concentration vs time curve.

Experimental techniques used by other workers, to determine the kinetics will be discussed now.

Since the reaction of acetaldehyde is extremely fast and highly exothermic (11), the acetaldehyde is generally diluted with acetic acid to give measurable rates of oxidation.





### Purity of Reactants:

Aldehyde oxidation is very sensitive to traces of metal ions (2) and a large number of other substances and hence it is necessary that the apparatus for the purification of aldehyde and the vessel in which the reaction is carried out should be scrupulously clean (2).

### Oxygen:

The oxygen should be ozone-free and also dust-free since dust could be a catalyst for aldehyde oxidation (2).

### Acetaldehyde:

The acetaldehyde must be purified in the absence of air and both the catalysts and inhibitors must be removed from it (2, 4). The same source of acetaldehyde, if possible, should be used for all the experimental runs so that purity of acetaldehyde is same for all the runs (4).

### Acetic Acid:

Analytic reagent grade glacial acetic acid which should be free from peroxides and water content (usually 0.001%) should be used. In view of the pronounced effects of water on the oxidation reaction, the same sample or source of acetic acid must be used in all experimental runs (4).

### Dissolution Rate:

Since the reaction takes place between aldehyde and dissolved oxygen, it is evident that a quiescent volume of aldehyde may quickly exhaust the dissolved oxygen, and the rate of absorption of the oxygen from the gas phase becomes controlled by the rate of diffusion of the oxygen from the surface into the volume of aldehyde. It is



quite clear that if the rate of reaction is to be measured, the aldehyde must be kept physically saturated with oxygen. The rate of oxidation has been shown to be a function of the rate of agitation (2, 16, 18, 19). The amount of agitation to maintain saturation depends largely upon the volume employed (19), the means of agitation, and the rate of reaction as controlled by catalysts and light.

In the photochemical oxidation of heptaldehyde (2), it was shown that a shaking speed of 350 rpm was sufficient to insure saturation of 2 ml. of aldehyde during photooxidation at a rate of oxygen uptake of about 8 ml per min. It is evident that the average surface:volume ratio when 2 ml. of aldehyde is shaken is far greater than when 20 ml. is stirred. Hence a shaking technique using small volumes of liquid appears to insure rapid saturation of aldehyde with oxygen more efficiently and conveniently than does rapid stirring of large volumes of aldehyde(2).

Cooper and Melville (18) conducted experiments to determine the effect of varying the stirrer speed on the overall rate of oxygen uptake for the oxidation of n-decanal and the results obtained show that the oxygen uptake keeps on increasing as the stirring speed is increased from 100 rpm to 350 rpm but then above 350 rpm, the uptake is lowered. The length of the stirring rod used was 2.5 cm. and its thickness 3 m.m. so that the liquid surface was continuously being broken as the rods rotated. At the lower speeds, its action amounted to the transmission of waves across the aldehyde layer and so the whole sample was being subjected to disturbance. At the higher speeds, there was not sufficient time during a revolution for the aldehyde swept aside by the stirrer to be replaced and so the resultant effect was the formation of a vortex



in the film, the surrounding liquid being almost unaffected.

Unfortunately, the onset of the phenomenon of vortex formation makes it difficult to tell whether, at this speed, the observed rates of oxidation are really independent of the rate of dissolution of oxygen. However, a consideration of the effect of sample size on the rate of reaction showed them that this required condition was indeed satisfied. It was found that the specific rate of oxygen uptake was independent of the quantity of material, other factors, e.g. temperature, pressure and stirring speed being constant.

#### Selection of Catalyst:-

According to the patent literature, manganese salts are said to be very effective catalysts for the production of acetic acid, whereas cobalt salts, a mixture of cobalt and copper salts and vanadium salts are stated to oxidise the aldehyde to acetic anhydride in high yield (11). The salts of iron, chromium and nickel are less effective catalysts. Cobaltous acetate gives high yield of peracetic acid (7).

#### Order in Aldehyde:-

Bowen and Tietz (20) reported that the photooxidation of acetaldehyde is first order in aldehyde. However, the rates are reported ambiguously and it is impossible to tell whether they are reported per unit volume of solution or per unit volume of aldehyde. The oxidation of benzaldehyde in benzene solution (21) with benzoyl peroxide as initiator was found to be first order in aldehyde. The cobalt ion-catalyzed oxidation of solutions of acetaldehyde in acetic acid (4) was also found to be first order in acetaldehyde. A later





paper by Ingles and Melville (22) states that the oxidation of benzaldehyde in decane is first order in benzaldehyde, but the authors give no data in support of this statement. Venugopal et al (11) also found the manganese acetate catalyzed oxidation of acetaldehyde to be first order in acetaldehyde. In some exceptional cases (3), the order of acetaldehyde was found to be  $3/2$ .

#### Order in Oxygen:-

Almquist and Branch (23) found that the thermal oxidation of benzaldehyde is first order in oxygen. The photo-oxidation of heptaldehyde (2) was found to be a zero-order reaction between 250 and 400 m.m and a first order reaction above 400 m.m. At  $16^{\circ}\text{C}$  the thermal oxidation of benzaldehyde was zero order in oxygen over a large pressure range (16). As the temperature was raised, the reaction approached a first-order relation. Venugopal et al (11) found the oxidation of acetaldehyde to be a first order reaction in oxygen.

#### Order in Catalyst:-

Bawn and Williamson (4) found the oxidation of acetaldehyde to be first order in catalyst concentration, using cobaltous acetate. Allen (9) studied the oxidation of acetaldehyde to acetic acid in the presence of manganese, cobalt and copper acetates and found the reaction to be first order in catalyst. Venugopal et al (11) found the oxidation of acetaldehyde to be independent of catalyst concentration in the range of 0.2 to 1.6% by weight and they used  $\text{Mn}(\text{OAc})_2$  as the catalyst.



### Inhibitors:-

Ethanol changed the order of oxidation of acetaldehyde from 0.5 to 1 in light intensity (2), anthracene to 0.65, diphenylamine and hydroquinone to 0.9. It has been suggested (2) that these differences are due to two different mechanisms involved. Adducts changing the initiator order to 1 are chain-ending inhibitors; those in whose presence the order remains 0.5 are chain-transfer retarders. Intermediate orders are due to both mechanisms operating simultaneously.

### Rate Equation:-

As mentioned earlier, the rates of photooxidation of acetaldehyde reported by Bowen and Tietz (20) are ambiguous and it is impossible to tell whether they are reported per unit volume of solution or that of aldehyde. Bawn and Williamson (4) studied the kinetics of oxidation of acetaldehyde in presence of cobaltous acetate and hence peracetic acid was one of their final products and the rate constant found by them cannot be used for oxidation of acetaldehyde to acetic acid in the presence of manganese(ous) acetate. Venugopal et al. (11) recently studied the kinetics of oxidation of acetaldehyde to acetic acid in the presence of manganese(ous) acetate and found the rate expression as follows:-

$$r_{O_2} = 3.02 \times 10^3 e^{-3980/RT} C_{O_2}^i \cdot b_{AcH}^o$$

where  $r_{O_2}$  = rate of reaction,  $\frac{\text{g-mole } O_2}{\text{c.c. min}}$

$C_{O_2}^i$  = volume % of  $O_2$  in gas

$b_{AcH}^o$  = volume % of acetaldehyde in liquid feed.

$T = ^\circ K.$



However, they found that the reaction rate was independent of catalyst concentration when the catalyst concentration was varied from 0.2 to 1.6% by weight, which is contrary to the results obtained by other workers (2, 3, 4, 5). Also they used the volume % of  $O_2$  in the gas-phase instead of dissolved  $O_2$ -concentration to determine the rate equation and the pressure was not mentioned so that the solubility of  $O_2$  in the liquid mixture cannot be estimated. Further, the values of the reaction rate constant given in their data cannot be calculated by the rate equation given by them.

Reaction rate data is scarce and the reliability for design purposes of that which is available is questionable.



### CHAPTER III

#### SIMULTANEOUS ABSORPTION AND CHEMICAL REACTION: MATHEMATICAL DESCRIPTION

The differential equation representing the phenomenon of simultaneous diffusion and chemical reaction in a liquid phase may be written for any reacting gas component C, in the form

$$D_1 \frac{\partial^2 C}{\partial x^2} = \frac{\partial C}{\partial t} + r \quad \dots \dots \dots (3.1)$$

$$\begin{array}{l} \text{Molecular} \\ \text{Transport} \end{array} = \begin{array}{l} \text{Accu-} \\ \text{mula-} \\ \text{tion} \end{array} + \text{reaction rate}$$

in the case of the penetration theory, under the simplifying assumption that the gas-liquid interface is plane, where C = instantaneous concentration of reacting gas component in the liquid and r = reaction rate.

A general solution of the above equation involves a number of analytical problems whenever r has other than the simplest relationship (i.e. first order) to the concentration of the reactants. However, it is possible to find asymptotic solutions of the above equation for very simple expressions of r, using the concept of reaction regimes as given by Astarita (15). Two time parameters i.e. "Diffusion Time" and "Reaction Time" have been defined (15) to assist in recognizing the reaction regimes in which a system is operating.

#### Diffusion Time:-

Astarita (15) has defined "diffusion time",  $t_D$  through the equation

$$t_D = \frac{D_1}{K_L} \quad \dots \dots \dots (3.2)$$





where,  $K_L^{\circ}$  = Physical mass tr. co-efft.

$D_L$  = Diffusivity of the reacting component into the liquid

$t_D$  = diffusion time.

The physical meaning of the "Diffusion time" is the average life of the surface elements, that is to say the interval of time among successive mixing processes which make the concentration within the liquid elements uniform. The range of values for  $t_D$  for any practical absorber is

$$0.005 < t_D < 0.04 \text{ sec.} \dots \dots \dots (3.3)$$

and for a reasonable value of  $D$ , limits of  $K_L^{\circ}$  can be obtained from equations (3.2) and (3.3) as:

$$0.015 < K_L^{\circ} < 0.04 \text{ cm/sec.} \dots \dots \dots (3.4)$$

Available experimental evidence confirms this range of values (15).

#### Reaction Time:-

The reaction time,  $t_R$ , represents the amount of time which is required by the reaction to proceed to an appreciable extent and is given (15) by

$$t_R = \frac{C - C'}{r} \dots \dots \dots (3.5)$$

where,  $C'$  = Equilibrium concentration of the gas-reactant in the liquid.

For the case of a first order reaction,

$$t_R = \frac{1}{K_r}$$

Depending on the relative values of  $t_D$  and  $t_R$ , reaction regimes are defined (15) as follows:



### A. Slow Reaction Regime:-

The value of the bulk concentration of the liquid-phase reactant ( $b_o$ ) is much larger than the value of the bulk-liquid concentration of the absorbing gas ( $C_o$ ) in many practical cases. Except for very fast reactions, which will be considered later, it may be assumed that the depletion of the liquid-phase reactant near the gas-liquid interface is negligible as compared to its bulk concentration. Thus  $b$  may be assumed equal to  $b_o$  throughout the liquid-phase, and therefore the reaction rate is only a function of  $C$ . Let it now be assumed that

$$t_D \ll t_R = \frac{C_o' - C'}{r(C_o - C')} \dots \dots \dots (3.6)$$

where the reaction time has been calculated at the interface concentration level, i.e. the average life of surface elements is much less than the time required by the reaction to take place appreciably even if the concentration were equal to  $C_o'$  throughout the surface element of the liquid. In other words, the reaction may be assumed not to take place at all during the diffusion time.

Thus the equation (3.1) reduces to

$$D_L \frac{\partial^2 C}{\partial x^2} = \frac{\partial C}{\partial t} \dots \dots \dots (3.7)$$

Astarita (15) concludes that, whatever the kinetics of chemical reaction, if the reaction is slow enough for the condition (3.6) to be fulfilled, the chemical absorption coefficient  $K_L$  is equal to the physical absorption coefficient  $K_L^o$ . This does not mean that the reaction does not take place at all in the absorber; it does take place in the liquid phase, but it is slow enough to be negligible during the short life of the surface elements



of liquid.

The analysis of such processes is entirely based on the determination of the bulk-liquid concentration of dissolved gas.

Let  $\bar{N}$  = average rate of chemical absorption ( $\text{ML}^{-3}\text{T}^{-1}$ )

then the absorption rate is given by  $\bar{N} = K_L^0 \cdot a \cdot (C_O' - C_O)$  and can be calculated provided the value of  $C_O$  is known. At the gas-liquid interface, the concentration of the absorbing component ( $C_O'$ ) is assumed equal to its solubility under the assigned interface partial pressure.

(a) Diffusional Regime:-

$$\text{Reaction rate, } r = r(C_O - C') \dots \dots \dots (3.8)$$

If the following condition is fulfilled:

$$r(C_O' - C') \gg a \cdot K_L^0 \cdot (C_O' - C') \dots \dots \dots (3.9)$$

then the reaction rate per unit interfacial area is much larger than the absorption rate. It may be noted that the fulfilment of condition (3.9) does not conflict with the fulfilment of condition (3.6) and the contemporary fulfilment of both conditions implies that

$$t_D \ll \frac{C_O' - C'}{r(C_O' - C')} \ll \frac{1}{K_L^0 \cdot a} \dots \dots \dots (3.10)$$

This condition may easily be fulfilled in any practical absorber (15).

In such a case, the reaction rate is high enough to keep the unreacted gas concentration,  $C_O$ , practically equal to the equilibrium value  $C'$  and then in this regime,

$$C_O - C' \ll C_O' - C_O$$

If condition (3.9) is fulfilled, the rate controlling phenomenon is





diffusion, so that the overall driving force is completely used up by the diffusion process. This condition has been called the "Diffusional regime" by Astarita (15).

The absorption rate in the diffusional regime is given by:

$$\bar{N} = K_L^{\circ} a. (C_O' - C'). \quad \dots \dots \dots (3.11)$$

In this regime, though the chemical reaction does not influence the value of  $K_L^{\circ}$ , it keeps the bulk-liquid concentration down to its equilibrium value  $C'$ , although absorption takes place at a finite rate.

(b) Kinetic Regime:-

This regime occurs when the chemical reaction rate is low enough so that:

$$r(C_O' - C') \ll K_L^{\circ} a. (C_O' - C'). \quad \dots \dots \dots (3.12)$$

The overall driving force is entirely used up by the reaction, i.e.  $C_O' - C_O \ll C_O - C'$  so that, in practice the liquid phase is everywhere saturated with the absorbing gas,  $C_O = C_O'$ .

The absorption rate under these conditions is given by:

$$\bar{N}.a = r(C_O' - C') \quad \dots \dots \dots (3.13)$$

This equation shows that the total absorption rate in this regime is:

- (i) independent of interfacial area
- (ii) proportional to liquid hold-up
- (iii) independent of  $K_L^{\circ}$
- (iv) proportional to  $r$ , and
- (v) influenced by the overall driving force  $C_O' - C'$ .



It is important to note that only in the kinetic regime is the rate proportional to the liquid hold-up. This fact can be used to determine when one is operating in the kinetic regime. Operation in this regime is a widely accepted procedure for obtaining kinetic data for gas-liquid reactions (15) and has also been used in this work for the same purpose.

(c) Intermediate Regime:-

This regime occurs when the chemical reaction rate and diffusion rate are of the same order. For a first order reaction and under the quasi-stationary hypothesis, the absorption rate is given by

$$\bar{N} = \frac{K_L^o \cdot (C_o' - C')}{1 + \frac{a \cdot K_L^o}{K_R}} \dots \dots \dots (3.14)$$

It should be noted that

$$K_L \neq \frac{K_L^o}{1 + \frac{a \cdot K_L^o}{K_R}} \quad \text{as incorrectly taken by Schafteilen and}$$

Russel (24).  $K_L$  is still equal to  $K_L^o$ , being in the slow reaction regime, irrespective of the subregimes.

For any other order  $n$ ,  $0 < n < 1$ , the total absorption rate is given by

$$\bar{N} = K_L^o (C_o' - C') (1 - \xi) = \frac{K_R}{a} \cdot (C_o' - C')^n \xi^n$$

where  $\xi = (C_o - C') / (C_o' - C')$ .  $\xi \rightarrow 1$  gives kinetic regime while  $\xi \rightarrow 0$  gives diffusional regime.



B. Fast Reaction Regime:-

In this reaction regime,  $t_R \ll t_D$  and it is assumed that the reaction is fast enough to keep the bulk-liquid concentration equal to its equilibrium value,  $C_o \approx C'$

$$N = \bar{N} = \sqrt{2D_1 \int_{C_o}^{C_o'} r(C) dC} \dots \dots \dots (3.15)$$

(for penetration theory), which for a first order reaction reduces to

$$\bar{N} = \sqrt{D_1 K_R} (C_o' - C') \text{ by which } K_L = \sqrt{D_1 K_R}$$

For any reaction order n, the absorption rate is given by (15)

$$\bar{N} = \frac{\sqrt{2D_1 K_R}}{n+1} (C_o' - C')^{n-1} \cdot (C_o' - C')$$

C. Transition From Slow To Fast Reaction:-

In this case,  $t_R \approx t_D$  and the mean absorption rate for a first order reaction is given by (25)

$$\begin{aligned} \bar{N} = a. \{ & (C_o' - C') \sqrt{K_R \cdot D_1} \{ \text{erf} \sqrt{K_R t^*} (1 + \frac{1}{2K_R t^*}) \\ & + \frac{\exp(-K_R t)}{\sqrt{(K_R t^* \pi)}} \} - (C_o - C') \sqrt{K_R D_1} \frac{\text{erf} \sqrt{K_R t^*}}{K_R t^*} \} \end{aligned}$$

(which is for Higbie's model). . . . . (3.16)

or

$$\bar{N} = a \{ (C_o' - C') \sqrt{D_1 (S + K_R)} - (C_o - C') \sqrt{D_1 S} \frac{\sqrt{S}}{S + K_R} \}$$

(which is for Danckwert's model). . . . . (3.17)



where  $t^*$  = total time elapsed from the moment the surface element considered has been brought to the surface and  $S$  = Danckwert's model parameter,  $T^{-1}$ .

For an  $n$ -th order reaction,

$$\bar{N} = \frac{\sqrt{2D_1}}{n+1} K_R (C_O' - C')^{n+1} + AD_1^2 \dots \dots \dots (3.18)$$

where  $A$  is an integration constant and can be calculated as a function of  $K_L^O$  as shown by Astarita (15).

#### D. Instantaneous Reaction:-

In this case, the absorbing component and the liquid-phase component cannot co-exist in the same region of liquid. The condition  $t_R \ll t_D$  is fulfilled and whenever  $C \neq 0$ ,  $b = 0$  and vice-versa. The

condition  $\sqrt{\frac{t_D}{t_R}} \gg \frac{b_O}{qC_O'}$ ,

where  $q$  = stoichiometric coefficient, is fulfilled. The instantaneous absorption rate is given by

$$N = \sqrt{\frac{D_1}{\pi t}} \cdot \frac{C_O'}{\text{erf}\sqrt{(\alpha/D_1)}} \dots \dots \dots (3.19)$$

where  $\alpha$  can be calculated from

$$\frac{q \cdot \sqrt{D_1} \cdot C_O'}{\text{erf}\sqrt{(\alpha/D_1)}} \exp\left(\frac{-\alpha}{D_1}\right) = \frac{\sqrt{D_2} \cdot b_O}{\text{erf}\sqrt{(\alpha/D_2)}} \exp\left(\frac{-\alpha}{D_2}\right) \dots \dots \dots (3.20)$$

If  $D_1 = D_2$  is assumed then

$$\bar{N} = K_L^O \left\{ \frac{b_O}{q} + C_O' \right\} \dots \dots \dots (3.21)$$





### E. Transition From Fast To Instantaneous Reaction:-

No analytical solutions are available, though numerical methods can be applied under very crude simplifying assumptions (15).

All the absorption rate expressions above were derived from Penetration theory.

The following table (15) summarizes the conditions necessary for any chemical absorption regime:

| <u>Regime</u>          | <u>Conditions to be Fulfilled</u>                          |
|------------------------|--|
| Kinetic                | $r(C_o' - C') \ll K_L^o \cdot a \cdot (C_o' - C')$         |
| Diffusional            | $t_D \ll t_R \ll \frac{1}{K_L^o \cdot a}$                  |
| Fast Reaction          | $1 \ll \frac{\sqrt{t_D}}{\sqrt{t_R}} \ll \frac{b_o}{qC_o}$ |
| Instantaneous Reaction | $\frac{\sqrt{t_D}}{\sqrt{t_R}} \gg \frac{b_o}{qC_o}$       |



## CHAPTER IV

### DESIGN OF TWO-PHASE REACTORS

The two-phase tank-type reactors of interest can be classified in three groups (24) as follows:

- (1) Continuous flow tank reactors (CFTR), in which both the liquid and gas flow through the reactor,
- (2) Semiflow batch reactors (SFBR), in which only the gas flows through the reactor and the liquid is held in the reactor.
- (3) Batch reactors, in which both phases are charged in the reactor and there is no net flow of either phase from or to the reactor.

The general mass balance equation for the reacting gas component C in the liquid-phase in any of the well-stirred tank-type reactors listed above and operating in the 'Slow reaction regime' can be represented by the following equation:-

$$Q(C_i - C_o) + K_G \cdot Pa V_L (Y_C - \frac{C_o \cdot H}{P}) - r_C V_L = \frac{d}{dt}(V_L \cdot C_o) \dots (4.1)$$

where  $a$  = interfacial area per unit volume of liquid,  $L^2/L^3$ .

$C_i$  = inlet concentration of C in the liquid, Moles/vol.

$V_L$  = volume of liquid phase,  $L^3$

$Y_C$  = mole-fraction of component C in the gas-phase

$C_o$  = bulk-liquid concentration of C, Moles/vol.

$K_G$  = overall mass transfer coefficient, mole/area-time-pressure.

For a system operating in the 'Fast Reaction Regime', the reaction is fast enough to take place appreciably during the life of surface elements



and the concentration  $C_o$  of the reacting gas-component (C) can be approximated to zero (15,27) and there is no accumulation of the gas-component C in the bulk liquid. Hence the general mass-balance for the gas-phase reactant in the liquid phase can be written as:-

$$Q(C_i - 0) + K_G \cdot a \cdot P \cdot V_L (Y_C - 0) - \bar{N}_C = 0 \dots \dots \dots (4.2)$$

where  $\bar{N}_C$  = Average chemical absorption rate of the gas-component C, Moles/ volume-time

If the gas-component C reacts with the liquid-component b such that one mole of C reacts with one mole of b then

$$r_b = \bar{N}_C = \frac{db}{dt}$$

where  $r_b$  = rate of depletion of b by chemical reaction.

The general mass balance for the liquid-phase reactant can then be written

$$Q(b_i - b_o) - \bar{N}_C \cdot V_L = \frac{d(b_o V_L)}{dt} \dots \dots \dots (4.3)$$

The equations (4.2) and (4.3) are also valid in the instantaneous reaction regime and the mass flux  $\bar{N}_C$  can be obtained from the last chapter.

The liquid-phase behavior of any of the two-phase reactors can be obtained, in the slow reaction regime, from equation (4.1) and in the fast and instantaneous reaction regimes from equation (4.2) or (4.3) by deleting the appropriate terms. For a steady state continuous flow tank reactor, equation (4.1) is applicable if the time-derivative is set equal to zero. For a batch or semiflow batch reactor the terms containing the input and output flow rate, Q, are eliminated.



Schaftlein and Russel (24) incorrectly presented equation (4.1) as a general mass-balance equation irrespective of the reaction regime. They did not seem to realize the difference between the "mass flux across the interface" and the "absorption rate due to chemical reaction in the bulk phase".

Several different models have been employed to describe the gas-phase behavior.

In the absence of mechanical agitation the bubbles of gas will rise in a swarm through the reactor and their spatial variation over the reactor length must be considered. The total mass of the component C in the bubble,  $PV_b Y_C / RT$ , is dependent upon both  $z$  and  $t$ . For a single bubble the differential change in the liquid  $(z_1, t_1)$  and  $(z_2, t_2)$  is equal to the mass of C transferred to the liquid,  $-K_G a_b PV_b (Y_C - CH/P)$ , and since the mass of C in the bubble is a function of both  $z$  and  $t$ ,

$$\frac{d(PV_b Y_C / RT)}{dt} = \frac{\partial(PV_b Y_C / RT)}{\partial z} \cdot \frac{dz}{dt} + \frac{\partial(PV_b Y_C / RT)}{\partial t}$$

since  $U_b = \frac{dz}{dt}$ , the following equation results:

$$-K_G a_b PV_b (Y_C - \frac{CH}{P}) - U_b \frac{\partial}{\partial z} \left( \frac{PV_b}{RT} \cdot Y_C \right) = \frac{\partial}{\partial t} \left( \frac{PV_b}{RT} \cdot Y_C \right) \dots (4.4)$$

where  $a_b$  = ratio of surface area to volume of a single bubble

$V_b$  = volume of a bubble

$U_b$  = rise velocity of the bubble

If there is mechanical agitation and deliberate dispersion of the gas,





it is possible that the gas-phase may behave as if it were well-mixed; an unsteady state mass-balance for this situation yields a second gas-phase model:

$$G_1 Y_{ic} - G_2 Y_C - K_G a V_L (P Y_C - CH) = \frac{d}{dt} \left[ (N_b V_L V_b) \frac{P Y_C}{RT} \right] \dots (4.5)$$

where,  $a V_L$  = total surface area for mass-transfer

$N_b V_L V_b$  = total gas volume

$K_G$  = overall gas-phase mass-transfer co-efficient, moles/ area-time-pressure.

These two equations (4.4) and (4.5) represent the limiting configuration for the gas-phase and should provide, when combined with the liquid-phase equation of interest, two-phase models which can be solved to indicate performance limits for a reactor in which the gas-phase doesn't behave "ideally".

Schaftlein and Russel (24) have summerized the two-phase model developments for three reactor types: (1) CFTR, (2) SFBR and (3) Batch reactors, and have also discussed the various possible cases for each of the reactor types. Only a semi-flow batch reactor (SFBR) and its various possible cases will be discussed here.

#### Semiflow Batch Reactor:

In this case liquid is charged in the reactor and gas flows through it. Because of this, the liquid concentrations are time-dependent but spatially invariant for constant gas flow rate. The gas-phase may be described by either the plug-flow or well-mixed models.

#### Case A: Plug-flow Gas-Well-Mixed

##### Batch Liquid:

The liquid is assumed to be well-mixed and the general mass



balance equation for the gas-phase (4.4) can be written as

$$K_G a_b V_b (Y_C - \frac{CH}{P}) + U_b \frac{d}{dz} (\frac{PV_b}{RT} \cdot Y_C) = 0 \dots \dots \dots (4.6)$$

which can be combined with the mass-balance equation for the liquid phase to give overall model equations. Special cases for the SFBR are considered below, assuming a first-order reaction.

Case A-(1)  $V_b = \text{constant}$ , first order reaction.

Here it is assumed that the bubble volume remains practically constant. This will be true if the gas-phase reactant concentration,  $Y_C$ , is small or if the amount of mass transferred from the bubble is small. In this case then  $a_b$  and  $U_b$  are also constant and equation (4.6) can be integrated to give

$$Y_C = \frac{CH}{P} + (Y_{ic} - \frac{CH}{P}) \exp (-K_G a_b RT z/U_b) \dots \dots \dots (4.7)$$

The gas-phase concentration is a function of  $z$  and therefore it is necessary to define an average value of  $Y_C$  for the driving force of the liquid-phase model, i.e.

$$\bar{Y}_C = \frac{1}{L} \int_0^L Y_C(z) dz \dots \dots \dots (4.8)$$

The average values  $\bar{a}_b$  and  $\bar{V}_b$  can be obtained in the same manner. Thus  $\bar{Y}_C$  is obtained (24) from equations (4.7) and (4.8) as:

$$\bar{Y}_C = C(1 - \frac{1 - e^{-n_1}}{n_1}) \frac{H}{P} + Y_{ic} (\frac{1 - e^{-n_1}}{n_1}) \dots \dots \dots (4.9)$$

where  $n_1 = K_G a_b RT L/U_b$

By substituting equation (4.9) for  $\bar{Y}_C$  in the liquid-phase model of



interest, the solution for the two-phase model can be obtained.

Case A-(2)  $V_b = \text{constant}$ ,  $Y_C = 1$ , pure gas-phase, first order reaction.

In this case the bubble volume changes significantly because of mass transferred from the bubble into the liquid. Both  $a_b$  and  $V_b$  are functions of the distance the bubble has travelled,  $z$ . For this situation equation (4.6) can be solved for  $V_b(z)$ , if  $a_b$  and  $U_b$  can be expressed as functions of  $V_b$ .

From the definition of  $a_b$  and the assumption that all bubbles are spherical,  $a_b$  can be expressed as follows (24):

$$a_b = S_1 V_b^{-1/3} \quad \text{where } S_1 = 6^{2/3} \pi^{1/3} \dots \dots \dots (4.10)$$

If the rise velocity of bubbles through liquid is assumed to follow the Davies-Taylor equation discussed in Davidson and Harrison (26), then

$$U_b = W V_b^{1/6} \dots \dots \dots (4.11)$$

$$\text{where } W = 0.711 \text{ g}^{1/2} \left(\frac{6}{\pi}\right)^{1/6} \dots \dots \dots (4.12)$$

The gas-phase model (equation 4.6) can be integrated after the proper substitution (from equations 4.10 to 4.12) to yield  $V_b(z)$  (24):

$$V_b = \{V_{ob}^{1/2} - \frac{1}{2} K_G RT \frac{S_1}{W} (1 - \frac{CH}{P}) z\}^2 \dots \dots \dots (4.13)$$

$\bar{V}_b$  and  $\bar{a}_b$  can be obtained as in equation (4.8):

$$\bar{V}_b = V_{ob} + \left(\frac{L^2 F^2}{3} - V_{ob}^{1/2} L F\right) \dots \dots \dots (4.14)$$

$$F = \frac{1}{2} K_G RT \frac{S_1}{W} \left(1 - \frac{CH}{P}\right) \dots \dots \dots (4.15)$$

$$\bar{a}_b = S_1 \bar{V}_b^{-1/3} \dots \dots \dots (4.16)$$



These previous results can then be substituted in the liquid-phase model of interest and solution for  $C(t)$  can then be obtained.

Case A-(3)  $V_b \neq \text{constant}$ ,  $Y_C \neq 1$ , first-order reaction.

In this case the change in bubble volume cannot be neglected. The overall gas-phase balance is then:

$$K_G a_b P V_b (Y_C - \frac{CH}{P}) + U_b \frac{d}{dz} (\frac{P V_b}{RT}) = 0 \dots \dots \dots (4.17)$$

Equation (4.17) and equation (4.6) then give:

$$K_G a_b RT (Y_C - \frac{CH}{P}) + \frac{U_b}{(1-Y_C)} \cdot \frac{dY_C}{dz} = 0 \dots \dots \dots (4.18)$$

This gas-phase model can then be solved for  $Y_C(z)$  and then average values of  $\bar{a}_b$ ,  $\bar{V}_b$  and  $\bar{Y}_C$  must be used in the liquid-phase model of interest to solve for  $C(t)$  or  $b(t)$ .

Case B: Well-mixed Gas-Well-Mixed Batch Liquid:-

In this configuration both phases are intimately mixed by mechanical agitation and the action of the gas on the liquid. The concentrations in both phases are assumed to be time-dependent but spatially invariant.

The gas-phase model equation is then

$$G_1 Y_{1C} - G_2 Y_C - K_G a V_L P (Y_C - \frac{CH}{P}) = 0 \dots \dots \dots (4.19)$$

This gas-phase equation is for the steady state but is coupled with the time-dependent liquid phase concentration  $C(t)$ .

This equation can be solved for  $Y_C$ , substituted in the liquid-phase equation of interest, and the resulting differential equation solved for





$C(t)$ .

### Flow Patterns in Two-phase Flow and their Importance:-

Two phases flowing together in a tube assume various different flow patterns or regimes depending on the relative flow rates, pressure drops and tube orientations. The actual conditions which cause the existence of individual flow patterns are not completely understood (27). Indeed, the transition from one flow pattern to another is difficult to identify. It is customary however to identify the flow patterns in the manner indicated below (27).

| <u>Flow Patterns</u>                           |                             |                           |
|--|-----------------------------|---------------------------|
| <u>Horizontal and Helical<br/>Coiled Tubes</u> | Increasing<br>Gas      Flow | <u>Vertical<br/>Tubes</u> |
| Bubble   | ↓                           | Bubble                    |
| Plug   |                             | Slug                      |
| Stratified                                     |                             | Semi-annular              |
| Wavy   |                             | Annular                   |
| Slug   |                             | Dispersed                 |
| Dispersed                                      |                             |                           |

The well-known Baker plot first developed for horizontal low pressure two-phase flow (28) and subsequently for vertical and helical coil flow data (29) is the most widely used method for mapping flow patterns (27). This chart can be used in conjunction with the reactor model to decide which flow regime should be most profitably used for particular types of chemical reaction. In certain flow patterns, for example, in slug or plug-flow, the



hold-up at a given point fluctuates with time. In these cases, time-averaged values are used.

Depending on the flow rates and phase properties of liquid and gas, the flow-patterns in the reactor vary and so do the various model parameters, e.g. interfacial area, mass-transfer co-efficient, hold-up, etc., affecting the reactor performance directly. Details of various flow patterns and their effects on two-phase reactor performance can be found in the papers by Cichy et al (30) and Roseheart et al (27).



## CHAPTER V

### PARAMETER EVALUATION

In addition to kinetic data one must have values for the physical mass transfer coefficient and the interfacial area. The interfacial area can be estimated from information on gas hold-up and average bubble size. This section deals with the bubble behavior and mechanics of bubble formation as well as the evaluation of mass transfer coefficient and hold-up. The discussion is limited to consideration of the bubble regime.

#### A. Bubble Behavior and Mechanics of Bubble Formation:-

Although a single orifice would not normally be used to form bubbles in any practical piece of equipment, an understanding of the process of bubble formation at a single orifice is a preliminary to the study of disperison devices containing multiple orifices.

The simplest mechanism of bubble formation is that in which the bubble is formed very slowly at the open end of a tube immersed vertically in a liquid. In this case the bubble will grow until its buoyancy exceeds the surface tension forces tending to hold it onto the tube, when it will detach. Assuming the bubble to be spherical, a force balance considering only buoyancy and interfacial tension yields the following expression for initial bubble diameter  $d_{ob}$  (31):-

$$\frac{\pi}{6} d_{ob}^3 (\rho_l - \rho_g) g = \pi d_o \sigma$$

or

$$d_{ob} = \frac{6 d_o \sigma}{g (\rho_l - \rho_g)} \dots \dots \dots (5.1)$$



where,  $d_{ob}$  = initial bubble diameter at the orifice

$d_o$  = orifice diameter

$\rho_{l, g}$  = density of liquid and gas respectively

$\sigma$  = surface-tension of liquid

$g$  = acceleration due to gravity.

Datta, Napier and Newitt (32) obtained a large amount of experimental data for the air-water system. Working with orifice diameters ranging from 0.022 - 0.519 cm (made from glass capillary tubes) they confirmed that the above equation was approximately correct. They also found that the bubble size from an inclined orifice was smaller than a vertical one. This could be explained by the tendency of the buoyancy forces to drag the bubble across the orifice thus allowing the surface forces to operate over only a portion of it (33).

As the gas flow is increased, the bubble diameter at first remains reasonably constant while the frequency of bubble formation increases. Then at higher gas flows the frequency of formation becomes approximately constant while the bubble diameter increases with gas flow rate. At still higher flows bubbles of a single size are no longer produced; there is a considerable spread of bubble sizes with production of numerous small bubbles (33). Most research workers e.g. Coppock and Micklejohn (34), Benzing and Myers (35), Leibson et al. (36), Davidson and Amick (37) agree with this behavior of the bubbles with respect to gas flow.

#### Bubble Formation Regimes:-

Based on the gas-flow rate and hence the orifice Reynolds number, four bubble formation regimes are defined (33):-





(a) Constant Volume Region: - This region has been defined to extend up to an orifice Reynolds number of about 200 (33). In this region both gas rate and liquid viscosity have negligible effect on bubble diameter and equation (5.1) would be expected to hold approximately.

(b) Slowly Increasing Volume Region:- Davidson and Shuler (38) carried out experiments in this region and the following equation is suggested for the bubble diameter.

$$d_{ob} = \text{const.} \left\{ \frac{d_o \sigma}{\rho_l - \rho_g} \right\}^{1/3} \{ G \mu_l \}^{1/4} \dots \dots \dots (5.2)$$

where, G = volumetric flow of gas

and  $\mu_l$  = viscosity of liquid.

This is a modification of equation (5.1), which takes into account the effects of viscosity and gas-rate on bubble diameter.

(c) Constant Frequency (Laminar) Region:- As the gas-rate increases to correspond to orifice Reynolds number in the range of 1000-2000, the frequency becomes independent of gas flow rate and approaches a constant value depending on orifice diameter. It ranges from 15/sec, for large diameter orifices (35) to 45/sec, for small capillaries (39) being about 20/sec, for 1/15-1/4 inch diameter vertical orifices (40); the bubble volume then increases with increasing gas rate. Only one correlation has been developed for  $d_{ob}$  (41) which is claimed to hold for gases at orifice Reynolds numbers between 1000 and 2000:

$$d_{ob} = 0.18 d_o^{0.5} N_{Re}^{0.33} \dots \dots \dots (5.3)$$

Although the observed size of bubbles formed at an orifice is reproducible, considerable coalescence and bubble break-up begins to



occur in this region so that equation (5.3) may not give a good estimate of the bubble diameter in a bubble column. The above behavior is supported by Davidson and Amick (37), Benzing and Myers (35), Calderbank (40), Leibson et al. (36), and Valentin (31). The fraction of the small bubbles gradually increases with increasing gas flow rate.

(d) Turbulent Region: - At gas flow rates corresponding to an orifice Reynolds number greater than about 2100, gas bubbles break up due to turbulence. This transition point cannot be taken to be a sharp one, since a certain amount of bubble break-up may take place even at a lower Reynolds number. Also in this region bubble coalescence begins to take place closer and closer to the orifice and a variety of sizes of bubbles are formed. Leibson et al. (36) have classified another region above a Reynolds number greater than 10,000, where turbulence is considered to be fully developed, and the gas jet disintegrates into a range of fine and coarse bubbles near the orifice. Siems (42) has named this zone as 'jet gassing'. However, according to Rennie and Evans (43) even at Reynolds number of 40,000 there is still bubble formation followed by bubble break-up, the bubbles now being all toroidal.

Leibson et al. (36) measured the average bubble size for the air-water system by a photographic method and found a sharp fall over the Reynolds number region 2100-10,000 from the 'laminar' values (given by equation 5.1) to an approximately constant value given by

$$d_{vs} = 0.71 (N_{Re})^{-0.05} \dots \dots \dots (5.4)$$

$$d_{vs} = \text{volume surface mean diameter of the bubble, also called Sauter mean diameter} = \frac{\sum n_i d_{bi}^3}{\sum n_i d_{bi}^2}$$



Rennie and Evans (43) have approximately confirmed the above equation. Although this equation applies strictly to single orifices operating at 10,000, there is reasonable agreement in the range 2000-10,000 for the frothing systems which have been studied.

Bubble Swarms:-

Koide et al. (44) give the following equation and limits for calculating the average bubble diameter of bubble swarms in air-water system, generated from perforated plates

$$d_{ob} = 2.94 \left( \frac{N_{We}}{N_{Fr}^{\frac{1}{2}}} \right)^{0.071} \left( \frac{g\rho}{\sigma\delta} \right)^{-1/3}$$

$$0.07 < N_{We}/N_{Fr}^{\frac{1}{2}} < 64 \dots \dots \dots (5.5)$$

where  $N_{We}$  = Weber number =  $\frac{gu\rho}{\delta}$

$N_{Fr}$  = Froude Number =  $\frac{u^2}{g\delta}$

- $\rho$  = density
- $\delta$  = pore diameter
- $u$  = gas velocity through orifice.

The average bubble diameter of bubble swarms from porous plates generally ranges from 0.05 to 0.5 cm. and may be estimated by the equation given below (44).

$$d_{ob} = 1.35 \left( \frac{N_{Fr}}{N_{We}^{\frac{1}{2}}} \right)^{0.278} \left( \frac{g\rho}{\sigma\delta} \right)^{-1/3} \dots \dots \dots (5.6)$$

At the present time it appears that the initial bubble diameters generated in bubble column are not easily estimated unless one has a fairly low gas rate through the orifice. Experimental studies may have



to be conducted to evaluate mean bubble diameters unless the specific system of interest has been investigated and reported in the literature. A comprehensive listing of literature sources related to bubble motion is presented by Baker and Chao (45), Peebles and Barber (46) and Galore (47).

#### Bubble Size Distribution:-

Houghton et al. (48) examined a large number of bubbles in both fluidized and foam beds and determined the bubble size distribution. The bubble sizes followed a typical probability distribution about the most probable value, which was found to vary with plate porosity, gas velocity and the properties of the liquid phase. The relationship between bubble size and the cumulative percentage of bubbles of a smaller size than this, when plotted on log-probability paper is linear, which confirms the presence of a probability function. Observed bubbles smaller than the most probable size may have been formed at very small pores, or may have been broken off from other bubbles; those larger than the most probable size could be produced either by large pores or by coalescence. Coalescence seems less probable in the main body of the liquid than close to the bubbler plate, since most bubbles seem to coalesce by being pulled into the slip stream of the bubble ahead. Coalescence of bubbles moving in opposite directions appears unlikely, since the moving films of liquid around the front and sides would appear to repel them. Gal-Or (49) and Ho and Prince (50) have analyzed the effect of taking bubble size distribution into account when calculating the overall physical mass transfer coefficient from empirical correlations for single bubble and





have concluded that the effect is negligible if the volume surface mean diameter is used for calculating the mass transfer coefficient.

#### B. Mass Transfer Coefficient:-

The usual combined resistance approach is employed to define the overall gas-phase mass transfer coefficient,  $K_G$  in terms of gas-phase and liquid-phase resistances, i.e.

$$\frac{1}{K_G} = \frac{H}{K_L} + \frac{1}{K_g} \quad \dots \dots \dots (3.8)$$

where,  $K_L$  = individual liquid-phase chemical absorption coefficient,  
length/time

$K_g$  = individual gas-phase mass transfer coefficient, mole/  
area-time-pressure.

In any 'bubble-type' gas-liquid reaction system in which a pure gas is employed, the gas-phase resistance,  $1/K_g$  can be neglected; for systems in which there is more than one component in the gas-phase,  $1/K_g$  is generally small enough to be neglected when compared with  $H/K_L$ . The possible exception is the case in which  $K_L$  is very large because of a fast reaction in the liquid phase.

Values of  $K_L$  are often given as enhancement factor defined as  $K_L/K_L^{\circ}$  where  $K_L^{\circ}$  is the physical mass transfer coefficient or in case of slow reaction regime  $K_L = K_L^{\circ}$ . Thus the determination of  $K_L$  generally depends on the evaluation of  $K_L^{\circ}$ .

A variety of empirical correlations have been proposed for  $K_L^{\circ}$  in bubbling systems, without any mechanical agitation. Calderbank and Moo-Young (51), Griffith (52), Johnson and Akheta (53), Miller (54), Soo (55) and Teller (56) have proposed the following type of correlation:-



$$\frac{K_L^o}{U_L} = a_1 \left( \frac{L U_L}{v_L} \right)^{a_2} \left( \frac{v_L}{D} \right)^{a_3} \dots \dots \dots (5.7)$$

where  $U_L$  and  $L$  are characteristic of the liquid velocity and a dimension, respectively;  $a_1$ ,  $a_2$  and  $a_3$  are constants. A literature review on various equations is given by Valentin (31).

A correlation proposed by Hughmark (57) appears to be useful. This correlation applies to single bubbles in liquids, for liquid drops in liquids, and for single spherical surfaces exposed to flowing air or liquid streams. The predictions are claimed to deviate by 15% from experimental data. The general form of the correlation for liquid-phase mass-transfer coefficients is presented as:

$$N_{Sh} = 2 + a_k \{ N_{Re}^{0.484} \cdot N_{Sc}^{0.339} \left( \frac{d_b g^{1/3}}{L^{2/3}} \right)^{0.072} \}^{b_k} \dots (5.9)$$

where,  $D$  = diffusivity

$d_b$  = bubble diameter

$a_k$ ,  $b_k$  are constants

for single bubbles  $a_k = 0.061$ ,  $b_k = 1.61$

for bubble swarms  $a_k = 0.0187$ ,  $b_k = 1.61$

For bubble swarms the velocity in the Reynolds number is represented by the slip velocity between the bubbles and the liquid.

For cases where

$$N_{Re}, N_{Sc} \text{ and } \frac{d_b g^{1/3}}{L^{2/3}} \text{ are } \gg 2,$$

the liquid-phase mass-transfer coefficients for single bubbles (SB)



and bubble swarms (BS) are related as follows:

$$\frac{(K_L^o)_{BS}}{(K_L^o)_{SB}} = \frac{(a_k)_{BS}}{(a_k)_{SB}} = 0.326 \dots \dots \dots (5.10)$$

Hughmark's correlation thus indicates that mass transfer coefficients for single bubbles are greater than those for bubble swarms.

Lochiel and Calderbank (58) present theoretical equations for calculating mass transfer from single bubbles in gas-absorption. According to them, when the continuous phase is pure water at 20°C,

$$N_{Sh} = 1.13 \left\{ 1 - \frac{2.96}{N_{Re}^{1/2}} \right\}^{1/2} N_{Pe}^{1/2} \dots \dots \dots (5.11)$$

and for very high Reynolds number

$$N_{Sh} = 1.13 N_{Pe}^{1/2} \dots \dots \dots (5.12)$$

which is the solution of Boussinesq equation (58) for transfer around spheres in potential flow.

$$\text{Here } N_{Pe} = \frac{d_b U_L}{D}$$

Calderbank and Moo-Young (51) have suggested the following equation for bubble swarms of average bubble diameter < 0.25 cm,

$$K_L^o = 0.31 \left\{ \frac{(\rho_c - \rho_d) \mu_c g}{\rho_c^2} \right\}^{1/3} \left\{ \frac{D \rho_c}{\mu_c} \right\}^{2/3} \dots \dots \dots (5.13)$$

and for average bubble diameter > 0.25 cm,

$$K_L^o = 0.42 \left\{ \frac{(\rho_c - \rho_d) \mu_c g}{\rho_c^2} \right\}^{1/3} \left\{ \frac{D \rho_c}{\mu_c} \right\}^{1/2} \dots \dots \dots (5.14)$$



where,  $\rho_c$  = density of continuous phase, gm/cc

$\rho_d$  = density of dispersed phase, gm/cc

$\mu_c$  = viscosity of continuous phase, gm/cm.sec.

$g$  = acceleration due to gravity, cm/sec<sup>2</sup>

$D$  = diffusivity, cm<sup>2</sup>/sec.

Sharma et al. (50) have given a graphical correlation for  $K_L a$  vs  $U_{SG}$  using various two-phase systems. Braulick et al. (60) have given some interpretation of literature data enabling one to calculate  $K_L a$  corresponding to any superficial gas velocity.

Most of the correlations for  $K_L^o$  have been developed for the air-water system. Extension of these equations to other systems is not definite. The conversion from one system to another could be made by the following relationship developed by the AIChE Distillation Committee (60).

$$(K_L^o)_{\text{system}} = (K_L^o)_{O_2 - H_2O} \left\{ \frac{D_{\text{system}}}{D_{O_2 - H_2O}} \right\}^{\frac{1}{2}} \dots \dots \dots (5.15)$$

### C. Gas Hold-up:-

The gas hold-up in a sparged contactor is important in determining residence time and interfacial area for mass transfer and has generally been determined by directly measuring the height of aerated liquid and that of clear liquid without aeration. Thus the average fractional gas hold-up is given as

$$\epsilon = \frac{Z_f - Z_l}{Z_f} \dots \dots \dots (5.16)$$





$\epsilon$  = fractional gas hold-up

$Z_f$  = the expanded (aerated) liquid height

$Z_1$  = the clear liquid height.

Yoshida and Akita (61) have determined experimentally the effects of various parameters on gas hold-up, a summary of which is given below.

#### Effect of Electrolytes on Gas Hold-up:-

Yoshida and Akita (61) found that the fractional gas hold-up in water and electrolyte solutions in a 7.7 cm diameter column was slightly larger than in columns having a larger diameter, probably due to wall effects. This observation is in agreement with that of Fair et al. (62). Yoshida and Akita also observed that gas bubbles in water were generally less than 10 mm in size, whereas bubbles in electrolyte solutions consisted mostly of very fine bubbles and were dotted with larger ones of several millimeter diameter. The occurrence of small bubbles in electrolyte solutions can be explained by the electrostatic potential at the gas-liquid interface.

#### Effect of Gas Rate:-

Gas hold-up in sparged contactors varies directly with superficial gas velocity for the air-water system and for the air-sodium sulfite system. Graphs of gas hold-up vs superficial gas velocity have been given by Yoshida and Akita (61), Fair et al. (62) and Hughmark (57).

#### Effect of Nozzle Diameter:-

According to Yoshida and Akita (61), fractional gas hold-up is independent of nozzle diameter (range: 0.2 to 0.4 cm.). This can be explained by the fact that, in the range of gas rates studied in



their work, gas flows out of the nozzle as a continuous jet stream and is then split into bubbles by the turbulent motion of liquid in a zone several inches above the nozzle.

#### Effect of Liquid Height:-

Yoshida and Akita (61) found that fractional gas hold-up did not depend on the liquid height when the column height was over one meter. Since conditions in the vicinity of the gas inlet nozzle are different from other parts of the column, some end-effects are expected in shorter columns. This observation agrees with results given by Fair (12), according to whom the fractional gas hold-up increases as length-diameter ratio ( $Z_1/d_t$ ) is decreased, but is practically independent for  $Z_1/d_t$  at 10 and above 10.

#### Effect of Temperature:-

Fractional gas hold-up is unaffected by temperature in the range of 10° to 30°C (61).

#### Hold-up Determination from Empirical Correlations:-

Koide et al. (44) have suggested the following correlation for estimating fractional gas hold-up. The slip velocity,  $U_S$  for bubble swarms is defined by

$$U_S = \frac{U_G}{\epsilon} - \frac{U_L}{1-\epsilon} \dots \dots \dots (5.17)$$

where  $U_L, U_G$  = linear liquid or gas velocity. The ratio of bubble slip velocity to terminal velocity,  $V_t$  was correlated with the liquid properties for two ranges of average bubble diameter:

Small Bubbles:  $d_b < 0.04$  cm.

$$U_S/V_t = 0.27 + 0.73 (1 - \epsilon)^{2.80}$$



$$\frac{d_b^2 \epsilon \rho}{\sigma} < 2.7, 0.240 < (1 - \epsilon) < 1.0 \dots \dots \dots (5.18)$$

Large Bubbles:-  $d_b > 0.4$  cm.

$$U_S/V_t = \left\{ 1 + 0.0167 \left( \frac{d_b^2 \epsilon \rho}{\sigma} \right)^{2.16} \right\} \{ 0.27 + 0.73 (1 - \epsilon)^{2.80} \}$$

$$\frac{d_b^2 \epsilon \rho}{\sigma} < 8.0, 0.250 < (1 - \epsilon) < 1.0 \dots \dots \dots (5.19)$$

The terminal velocity may be determined experimentally, obtained from the literature (63) or estimated as shown by Perry (41).

The average fractional gas hold-up of bubble swarms can now be estimated if negligible bubble coalescence is assumed. The procedure is: (a) Find  $d_b$  using an appropriate correlation, (b) determine a value of  $V_t$  based on  $d_b$ , and (c) estimate  $\epsilon$  by trial and error from equations (5.17) and (5.18) or (5.17) and (5.19). Koide et al. claim an accuracy of  $\pm 30\%$ .

Another recent correlation and probably the most useful is that of Hughmark (57). He obtained data in the bubble regime for air with water, a sodium sulfate solution, kerosine and a light oil in a 1-inch tube. Gas hold-up was found to be correlated as a function of the superficial gas velocity for the air-water system at zero liquid flow. The correlation applies to cocurrent liquid systems if the hold-up is defined by

$$\epsilon' = \frac{U_{SG}}{U_S} \dots \dots \dots (5.20)$$

The Hughmark data were used to evaluate the effect of liquid physical properties. The data indicate that hold-up for these systems can be correlated with the term



$U_{SG} \left( \frac{62.4}{\rho_L} \cdot \frac{72.0}{\sigma} \right)^{1/3}$ , where  $\sigma$  = surface tension and  $\rho_L$  = density of liquid, which reduces to  $U_{SG}$  for air-water system.

From Highmark's correlation for  $\epsilon'$  vs  $U_{SG} \left( \frac{62.4}{\rho_L} \cdot \frac{72.0}{\sigma} \right)^{1/3}$ ,  $\epsilon$  can be back-calculated by trial and error for any particular  $U_{SG}$  and  $U_{SL}$ , using the following relation (57):

$$\epsilon' = U_{SG} / \left( \frac{U_{SG}}{\epsilon} - \frac{U_{SL}}{1-\epsilon} \right) \dots \dots \dots (5.21)$$

Gas hold-up data of other workers e.g. Fair et al. (62), Yoshida and Akita (61) and Towell et al. (64) compare pretty well with this correlation within a maximum absolute deviation of 21.5%. All these data were taken at 1 atm. pressure. However, the Neusen data (65) for steam-water at 600 psi in 2.9 inch pipe show an average absolute deviation of 32.5%.

#### D. Interfacial Area:

The first attempt to measure interfacial area was made only in 1955 (66) and to date some independent techniques have been developed. Measurement techniques may be broadly divided into three different categories namely (a) optical methods, (b) photographic methods and (c) analytical-cum experimental methods. The details of optical methods can be found in the reference (67). Only photographic techniques and empirical correlations will be discussed here.

#### Photographic Techniques:-

This involves actually photographing the dispersions and then measuring the size of dispersion by either optical methods (e.g. a cathetometer or a microscope) or other precision instruments. In addition, the number of spherical particles per unit volume of the mixture may





be actually counted, once the hold-up of gas is determined by any of the previously described methods. A mean bubble diameter called the volume surface mean diameter may be calculated by the following equation:

$$d_{VS} = \frac{\sum n_i d_{bi}^3}{\sum n_i d_{bi}^2}$$

and then  $a' = 6\varepsilon/d_{VS}$  gives the interfacial area per unit volume of mixture where  $\varepsilon$  is the fractional volume gas hold-up.

Sharma et al. (59) recently studied the effects of various parameters on interfacial area in a variety of gas-liquid systems in bubble-columns. The values of 'a' were evaluated by using the theory of absorption accompanied by fast pseudo-first order reaction. A summary of the effects observed by them is presented below.

#### Effect of $Z_1/d_t$ Ratio:-

For a column diameter of 6.6 cm and superficial gas velocity  $\approx$  21 cm/sec, effective interfacial area was unaffected when  $Z_1/d_t$  was varied from 4 to 12. Similar observations have been reported by other workers (61,62,64).

#### Effect of Column Diameter:-

The values of effective interfacial area obtained at the same superficial velocity of gas were found to be practically the same in the range of their (59) experimental conditions which were: superficial gas velocity = 15 cm/sec to 40 cm/sec and column diameters = 6.6 cm to 38.5 cm.

#### Effect of the Type of Distributor:-

The values of effective interfacial area obtained by using different designs of spargers (59) (single-tube distributor, cross-type



distributor, ring-type distributor) in a 9 cm- diameter column were found to be the same when system properties and hydrodynamic conditions were unchanged. Similar observations were reported by other workers (68).

#### Effect of Gas Velocity and Gas Density:-

Sharma et al. (59) found that the effective interfacial area varies as the 0.7 power of the superficial gas velocity.

When  $\text{CO}_2$  diluted with  $\text{H}_2$ , air, or Freon-12 was absorbed in aqueous NaOH solution in the 6.6 cm. diameter column, at constant superficial gas velocity, the effective interfacial area,  $a$ , was found to remain physically constant. This indicates that the change in the density of the gas is unlikely to affect 'a'.

#### Effect of Pressure:-

Tadao and Takeya (69), who studied the hydro-dynamics in a gas bubble column under pressures of 1 atm. to 6 atm., found no effect of pressure on bubble size or bubble rise velocity. Thus at a given superficial velocity of the gas, when the column is operated under pressure, it is very probable that the values of 'a' will be practically the same as in a column working at atmospheric pressure for equal values of the superficial velocity of the gas.

#### Effect of Ionic Strength and Nature of Ions:-

Yoshida and Akita (61), Braulick et al. (60) and Marrucci and Nicodemo (70) have stressed the importance of the effects of ionic strength and nature of ions on gas hold-up and gas-liquid interfacial area. Sharma et al. (59) show that with an increase



in both viscosity and the ionic strength of the solution, the effective interfacial area increases considerably. When the viscosities of the solution are the same, aqueous non-electrolyte solutions give a value of effective interfacial area much lower than that in the case of electrolyte solutions.

#### Effect of Non-aqueous Solvents:-

It was found (59) that at equal viscosities the effective interfacial area increased from  $1.7 \text{ cm}^{-1}$  to  $2.73 \text{ cm}^{-1}$  when the solvent was water and isopropanol respectively (surface tension: 22 dyne/cm). A decrease in surface tension thus leads to an increase in the effective interfacial area.

#### Empirical Correlations:-

Using an extensive collection of experimental data from tanks in which gas was dispersed by an agitator, Calderbank (71) obtained the interfacial area for mass transfer:-

$$a = 1.44 \left( \frac{P_a}{V_a} \right)^{0.4} \rho_l^{0.2} \mu_l^{-0.6} \left( \frac{U_{SG}}{V_t} \right)^{0.5} \dots \dots \dots (5.22)$$

where  $P_a$  = agitator shaft power during dispersion

$V_a$  = volume of agitated mass

$U_{SG}$  = superficial gas velocity.

$V_t$  = terminal velocity of bubble

$a$  = interfacial area per unit volume of liquid-phase.

The shaft power per unit volume of agitated mass can be estimated by the following equation given by Towell et al. (64).

$$P_a/V_a = U_{SG} \rho_l \cdot \frac{g}{g_c} \dots \dots \dots (5.23)$$

where  $g_c$  = conversion factor,  $\frac{\text{Ft. lbm}}{\text{lbf. sec}^2}$ .



## CHAPTER VI

### EXPERIMENTAL

#### A. Kinetic Measurements:-

This section describes the experimental equipment and operating procedures used to study the kinetics of the oxidation of acetaldehyde to acetic acid.

(a) Experimental Equipment:- Figure 1 is a schematic of the equipment used.

The reactor used in this study was a Parr-high-pressure reactor which had a capacity of 2000 ml. It was constructed of carpenter 20 stainless steel and the pressure and temperature limits were 2000 psig and 350°C respectively. The reactor was equipped with an adjustable speed stirrer and stirring speeds up to 3500 rpm could be attained. An electric heater was used to heat the bomb. Water was circulated through a coil in the reactor to provide cooling. Temperature was measured by an iron-constantan thermocouple (type J) and controlled by (1) an on-off automatic temperature controller actuated by the controlling thermocouple and (2) by manually adjusting the cooling water flow rate. A refrigeration unit was used to produce cooling water (temperature 1-4°C) for the reactor.

Charcoal and calcium chloride absorbers - 2"O.D. x 18" high lucite cylinders - were used to remove moisture and oily substances from oxygen to be used for the reaction. Glass wool was used to prevent entrainment of particles.

The reactor pressure was maintained constant by means of a





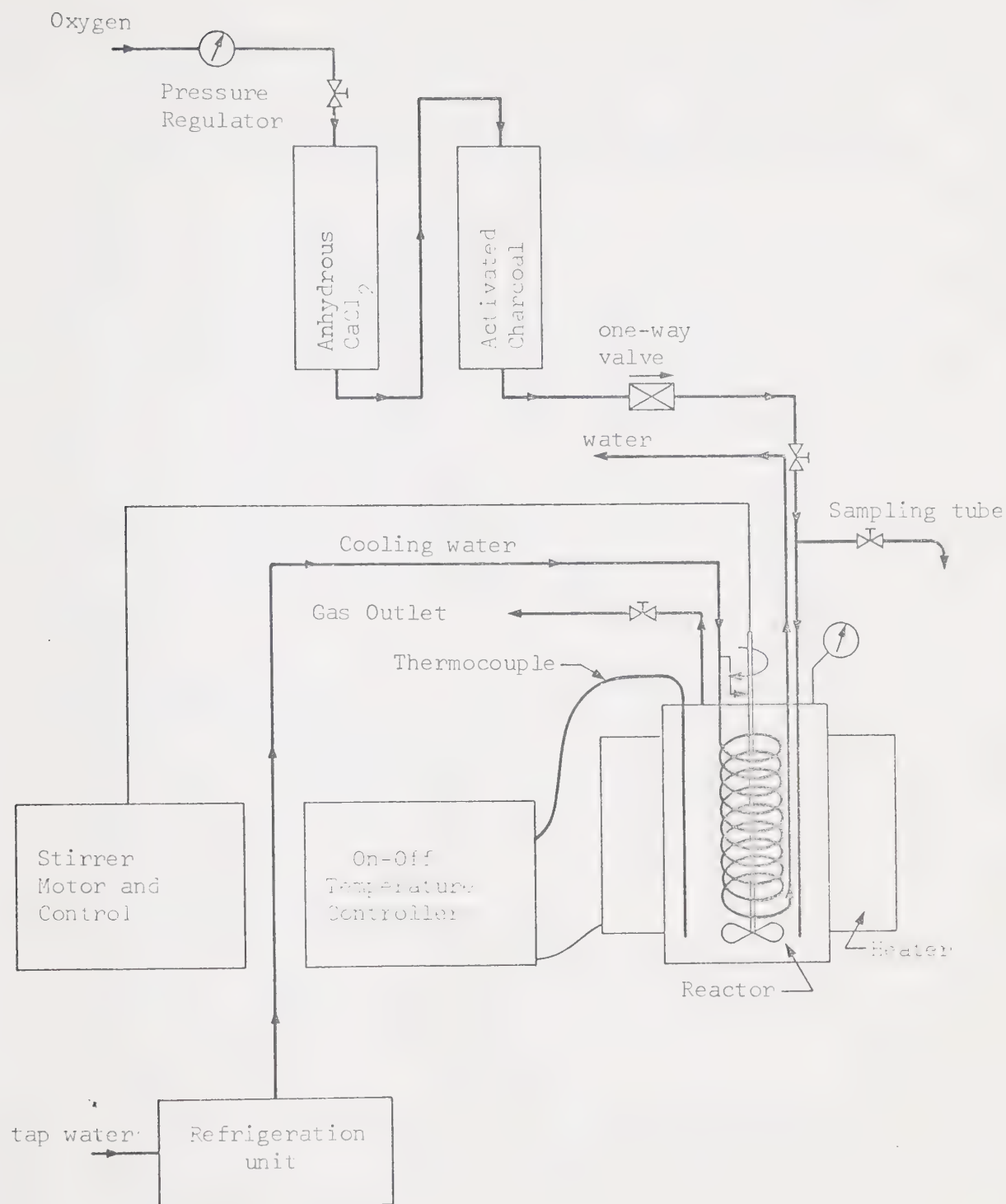


FIG. 1. SCHEMATIC OF THE APPARATUS FOR STUDY OF KINETICS.



pressure-regulator in the oxygen-inlet line. A one-way valve prevented the back-flow of liquid reactants from the reactor into the gas inlet line. Heat from packing glands was removed by cooling water circulating around them.

Sampling of the reaction mixture could be accomplished by means of a sampling tube built in the reactor. Any leaks through the packing glands (in the stirrer assembly) could be detected by means of a gas-leak detector plastic tube immersed in water. During or after the reaction, as the need may be, the gases in the reactor could be purged through the gas-outlet valve. The gas-outlet line was connected through tygon tubing to the exhaust hood to prevent dispersion of chemicals in the laboratory.

(b) Experimental Procedure:- The following steps were followed to carry out the reaction in the stirred-tank reactor.

1. The reactor was cleaned thoroughly by using distilled water and dried with air.
2. The system was checked for leaks.
3. The pressure regulator, stirrer-speed controller and the temperature controller were set at the pre-determined values.
4. The heater was brought to temperature.
5. The bomb was charged with measured volumes of acetaldehyde and acetic acid containing a known weight of dissolved catalyst.
6. The bomb was closed quickly and placed in the heater.
7. Oxygen gas-flow was started, purging out the air from the top of the reactor and pressure in the reactor was raised to a fixed value, keeping in mind that any further temperature



increase would increase the pressure; the gas outlet valve was then closed.

8. As soon as or just a little before the temperature and pressure in the reactor had been achieved, cooling water lines were opened and the stirrer was started.
9. The pressure gauge on the reactor had to be watched continuously and the pressure readjusted by releasing some gas through the gas-outlet.
10. Liquid samples were taken initially and at intervals of 5, 10, or 20 minutes as the situation warranted.
11. The sampling test-tubes were stored in the deep-freeze so that they were cold prior to use.
12. Before collecting any sample in the test-tube, a little bit of the first part of the liquid coming out of the sampling tube was discarded so that the sample collected was representative of the liquid inside the reactor at that time.
13. Since the boiling point of acetaldehyde is  $21^{\circ}\text{C}$ , the samples in test-tubes were quenched immediately by placing them in an ice-bath or deep-freeze. The temperature of the liquid samples was reduced to about  $0^{\circ}\text{C}$  within 2-3 minutes.
14. The reaction was run until the conversion of acetaldehyde was almost complete, which had to be determined by analyzing the liquid samples, consequently sample analysis was carried out while the run was in progress.



15. At the conclusion of the reaction the heater and the stirrer were shut down, the bomb was cooled, the gases in the bomb were released to the exhaust and the bomb was cleaned.

(c) Experimental Conditions Used in the Stirred-Tank Reactor:-

On the basis of the literature review and the features of experimental apparatus, the following range of experimental conditions were used.

|  |       |       |      |
|--|-------|-------|------|
| Pressure, psia   | 24.7, | 34.7, | 44.7 |
| Temperature, °C  | 30 ,  | 40 ,  | 50   |
| Catalyst ( $\text{Mn}(\text{OAc})_2$ concentration, ppm. | 80    | →     | 250  |
| Volume % of AcH<br>( $b_{\text{AcH}}$ )                  | 10    | ,     | 20   |
| R.P.M.   | 500   | →     | 3000 |
| Volume of Liquid Mixture, ccs.                           | 500   | ,     | 1000 |

Manganese(ous) acetate (powdered) was used as a catalyst for this reaction because it gives the highest efficiency for the production of acetic acid.

B. Sparged Reactor Study

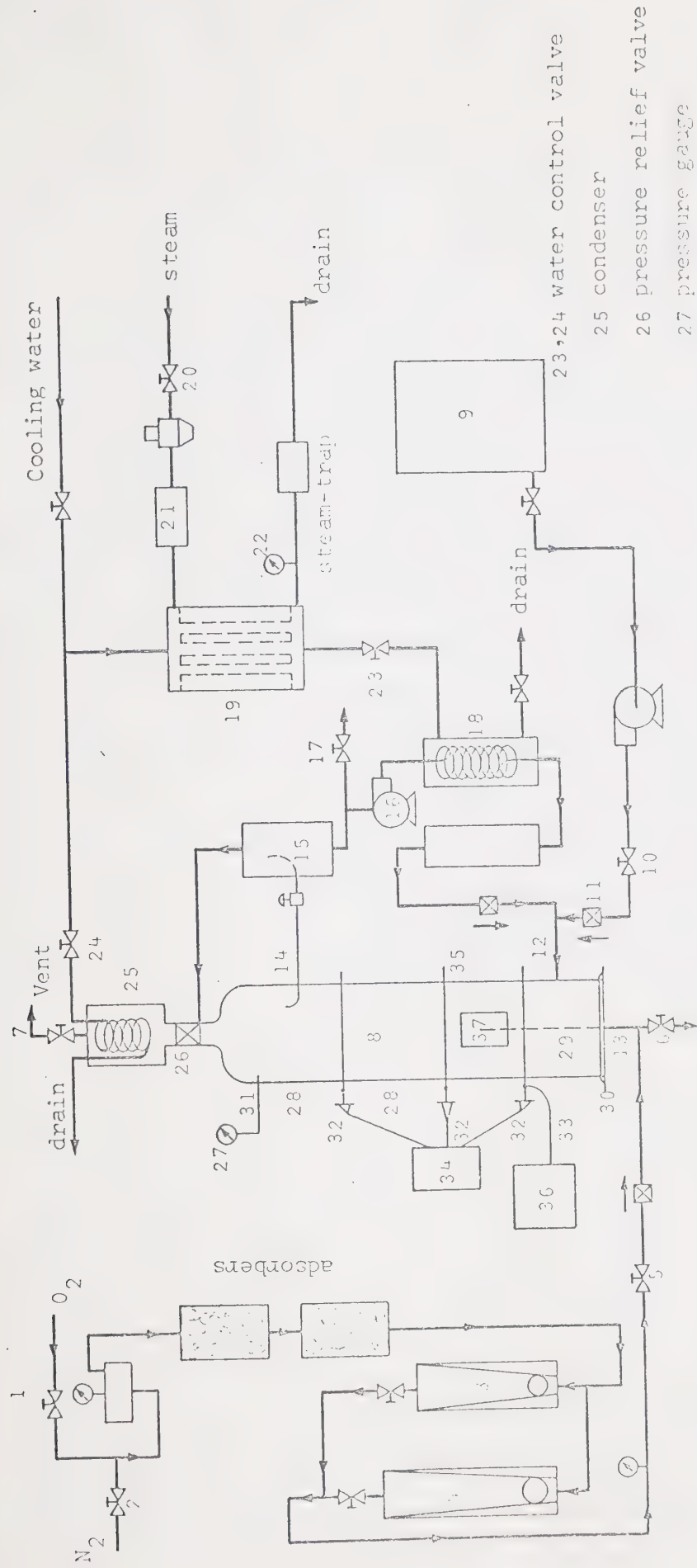
In this section the equipment and the operating procedures used for the sparged reactor study are described.

(a) Experimental Equipment:- Figure 2 is a schematic of the bubble reactor and associated equipment.

The bubble column was 4 ft. high and was constructed of four-inch







Legend:

- |     |                       |    |                      |    |                     |    |               |
|-----|-----------------------|----|----------------------|----|---------------------|----|---------------|
| 1   | O <sub>2</sub> -value | 9  | acetic acid tank     | 16 | recycle pump        | 30 | steel section |
| 2   | N <sub>2</sub> -value | 10 | acetic acid valve    | 17 | sampling valve      | 31 | guage line    |
| 3,4 | rotameter             | 11 | one-way valve        | 18 | recycle heat exchr. | 32 | thermocouples |
| 5   | gas-line valve        | 12 | liquid entrance      | 19 | water heat exchr.   | 33 | temp. probe   |
| 6   | drain valve           | 13 | orifice plate        | 20 | steam valve         | 34 | potentiometer |
| 7   | column vent           | 14 | liquid overflow line | 21 | solenoid valve      | 35 | steel section |
| 8   | bubble column         | 15 | surge tank           | 22 | pressure gauge      | 36 | temp. control |
|     |                       |    |                      |    |                     | 37 | glass window  |

FIG. 2. SCHEMATIC OF THE SPARGED REACTOR.



I.D., Q.V.F. pyrex glass (72) sections and was capable of withstanding up to 40 psig working pressure. The bottom section 30 of the column was a 6" long x 4" I.D. 316-stainless steel section. An orifice plate of any desired design could be inserted at the bottom of the column. The second section 35 of the column was also a 4" I.D. x 6" long stainless steel 316 pipe, which had two pyrex glass windows through which the bubble streams at the orifice tips could be observed and photographed. The temperature of the column was controlled by recirculating the reaction mixture at high rate through a heat exchanger where heat could be added or removed as required. Liquid was withdrawn from the top of the column at the point 14 through a 3/4" flexible 316 stainless steel pipe and through a gate valve to a surge tank 15 where the liquid and any entrained gas-bubbles were separated. This vapor returned to the column through a line. The recycle line from the surge tank was connected via a 3/4" flexible 316 stainless steel pipe to a centrifugal pump 16. Flexible stainless steel pipes were used to minimize the transmission of vibrations of the pump to the glass column. The recycle liquid was pumped through a coil and shell-type heat exchanger 18, where it was heated or cooled depending on the requirements. It then flowed through a rotameter and an one-way valve to the liquid entrance line 12 near the bottom of the column.

Three thermocouples (Iron-constantan, type J) 32 were inserted in the column through 1/2" thick stainless steel 316 rings placed between each section of the column. Cold water was used for cooling the recycle liquid whereas hot water was used for heating. The hot water was obtained by heating cold water with steam in a shell and tube-type heat



exchanger 19. A solenoid valve 21 was installed in the steam line and was connected to an automatic on-off temperature controller 36 actuated by a temperature probe 33 inserted in the column. The solenoid valve opened when the temperature in the column was lower than the set value. Thus a constant temperature could be maintained in the column by heating or cooling the recycle liquid. The flow rate of water and the steam pressure had to be adjusted manually. The recycle liquid flow rate was about 2 gals/min.

Oxygen gas at a constant pressure flowed from a gas cylinder through the needle valve 1 and similarly nitrogen gas flowed through the needle valve 2. Both gases were passed through a pressure-regulator to an activated charcoal absorber and to an anhydrous calcium chloride-absorber, where oily substances and moisture from the gas were removed, respectively. Dry and oil-free gas then passed either through rotameter 3 or 4 and through a pressure gauge, through a needle valve 5 and through a one-way valve to the orifice plate 13 in the bottom of the column. The one-way valve prevented any back-flow of liquids from the reactor into the gas-inlet line. All gas-inlet lines from needle valves 1 to 5 were 1/4" copper lines and from needle valve 5 to the column entrance, they were 1/4" 316 stainless steel.

The equipment used was capable of handling continuous flow of both gas and liquid. However, in this study the system used was 'continuous gas but batch liquid'. Glacial acetic acid (99.99%) was stored in a polyethene carboy 9 and was charged to the column with a centrifugal pump. A single orifice 29, 0.095" O.D. (0.078" I.D.) x 4" long constructed of 316 stainless steel tube was used. The gas-



phase flowed in the column through the orifice at 13 and liquid-phase flowed through a side entrance at 12 and through a number of holes in the top surface of the section 30.

A pressure gauge (0 - 100 psi) 27 was installed in the top section of the column. The pressure gauge could be screwed out from the tube 31 and acetaldehyde was introduced into the reactor through this opening. A pressure-relief valve 26 was installed at the top of the column and could be set at 30-40 psig. A shell and coil type condenser 25 (stainless steel 316) was employed to condense vapors in the exit gases. Cold water was used for condensing the vapors. A drain valve 6 was installed at the bottom of the column. Liquid samples were withdrawn through a needle valve 17.

(b) Measurement of Gas Hold-up:-

Gas hold-up measurements were made for the oxygen-acetic acid system at 20 psig and 40°C. These were the conditions at which the reaction was carried out in the column.

Operating Procedure:-

The column was filled with acetic acid to a height of about 40 inches. Oxygen was obtained by opening the valve 1 and the flow rate was recorded with one of the rotameters 3 or 4. Liquid levels at various gas flow rates were measured using a cathetometer. Measurements were made with the recycle pump in operation.

(c) Measurement of Bubble Diameters:-

The bubble diameters for various gas flow rates were measured by a direct photographic technique. A high speed (1/1000 sec) camera





was used with a flood light at the back of the column. A concavo-plano lens was designed of lucite with water in the lens to fit one side of the column, through which preliminary photographs of bubbles were taken. The lens was expected to reduce the distortion of bubbles in the photographs, but significant distortion did not occur in the absence of the lens. The inside diameter of the column was determined by placing a scale horizontally in the centre of a section of the column with water inside it and taking photographs from various distances. From four different photographs taken from varying distances, the following relation was calculated.

$$\frac{\text{Diameter of the column in the photograph}}{\text{Actual inside diameter of the column}} = \frac{\text{Length of one inch scale division in the photograph}}{\text{one inch}}$$

The length of both the 1-inch scale division and the diameter of the column in the photographs were measured and the actual inside diameter of the column (x) could be calculated from the above relation, i.e.

$$x = \frac{\text{length of 1-inch in the photograph}}{\text{diameter of the column in the photograph in inches}}$$

From the four different photographs mentioned above, it was found that  $x = 3.42", 3.48", 3.40", 3.50"$  and hence an average value of  $x = 3.45"$  was used as the actual inside diameter of the column. This also proved that there was not any appreciable distortion when photographs were taken from varying distances. The following relation was used for calculating the actual diameter of each bubble.

$$\text{Actual diameter of a bubble} = \frac{x(\text{bubble diameter in the photograph})}{\text{diameter of the column in the photograph}}$$

The bubble sizes were measured by means of a microscope.



(d) Measurement of Rate of Conversion of Acetaldehyde:-

The reaction: oxidation of acetaldehyde to acetic acid was carried out in the sparged reactor at the following conditions: 20 psig, 40°C, 140 ppm catalyst concentration, constant liquid height but at two different oxygen flow rates. The initial concentration of acetaldehyde in the mixture of acetaldehyde and acetic acid was approximately 10% by volume and pure oxygen was used.

The column was initially cleaned by charging it with acetic acid and passing nitrogen through it. The liquid was circulated so that any water that might have remained in the column was dissolved in the acetic acid. The column was charged with acetic acid and drained 2-3 times to make sure that there was no water in the system.

The following steps were taken to carry out the actual reaction run:-

1. The system was charged with acetic acid. The condenser cooling water inlet valve 24 was opened. A predetermined volume of pure acetaldehyde (99.98%+), which was stored at about 0°F in a deep-freeze, was then poured in the column. The recycle pump was started.
2. Nitrogen gas-flow was then started and its flow-rate was adjusted to a known value. Pressure in the column was raised to 20 psig.
3. The temperature-control system was switched on, and the temperature in the column was raised to 40°C.

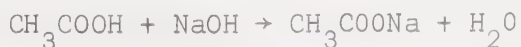


4. Nitrogen-flow was stopped and oxygen flow was started. Since the reaction is exothermic, the temperature in the column has to be re-adjusted to 40°C by adjusting the cooling water valve 23 and the steam-pressure-regulator. All these steps of bringing the system back to 40°C and 20 psig had to be done as quickly as possible.
5. Samples of liquid were withdrawn initially and after intervals of 5, 10 or 20 minutes, as required and were quenched in a deep-freeze.
6. Analysis of liquid samples were done as soon as possible.

After the completion of the reaction, oxygen flow was stopped and the temperature-control system was switched off. The system was drained after the liquid in the column was back at room temperature.

C. Analysis of Liquid Components:-

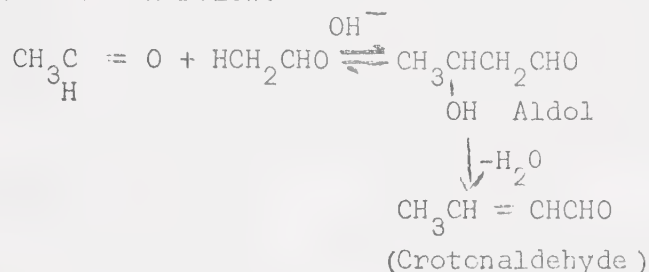
The liquid mixture contained mainly acetaldehyde and acetic acid and had to be analyzed for acetic acid content. This was done simply by titrating the liquid sample against standard sodium hydroxide solution:



Phenolphthalein was used as an indicator. A magnetic stirrer was used to stir the liquid. Titration was done in an inert atmosphere of nitrogen to reduce the possibility of any further oxidation of acetaldehyde while titrating. However, if the titration was done quickly enough, it was found that there wasn't any appreciable difference in the results when titration was done in an inert atmosphere or an ordinary atmosphere.



It may be noted that in the presence of dilute sodium hydroxide solution (10%) which acts only as a catalyst, aldol condensation would take place between the aldehyde molecules. However, it will not interfere with the titration because sodium hydroxide does not react with acetaldehyde but only acts as a catalyst. The aldol condensation reaction is shown below:



This was checked by titrating 1 cc of acetic acid with N/1 sodium hydroxide solution and then 1 cc of acetic acid + 1 cc of acetaldehyde mixture against N/1 sodium hydroxide. In both cases, sodium hydroxide consumed was the same. Thus acetic acid was analyzed by titration in this work.

#### Analysis for Acetic Anhydride, Peracetic Acid, Water and or other By-products:

As was seen in section 2, depending on the experimental conditions, e.g. temperature, catalyst, purity of reactants, there could be products other than acetic acid in the oxidation of acetaldehyde to acetic acid. To make sure that the products did not contain any appreciable amounts of these by-products, occasional checks were made on the samples by gas-chromatograph and mass spectrometer. In the products formed in various reaction runs, no traces of peracetic acid or acetic anhydride were found. In some cases, only traces of water were found but the percentage of water was less than 0.1% and thus within the limits of experimental error, it was assumed that there was complete conversion of acetaldehyde to acetic acid.





Gas-Chromatograph:-

Poropack-S column, 6' x 1/8", was employed at 120-180°C using helium (carrier gas) at the rate of 30 c.cs/min for analyzing the reaction mixture in the gas-chromatograph. The elution times at 150°C for water, acetaldehyde and acetic acid peaks were 0.4 min, 0.6 min and 3.2 minutes, respectively. Mass spectrometer was used to detect any acetic anhydride content.

Chemicals:

Acetaldehyde and acetic acid were supplied by Chemcell Limited, Edmonton and were reported to be over 99.9% pure. The catalyst, manganese(ous) acetate, powdered, was purchased from Fisher Scientific Company.



CHAPTER VIIRESULTSA. Kinetic Studies:-

Kinetic data for the oxidation of acetaldehyde to acetic acid were measured in the stirred-tank gas-liquid contactor described in section VIA. The effect of the following variables on the reaction rate were investigated:-

1. Concentration of acetaldehyde
2. Concentration of oxygen
3. Temperature
4. Catalyst concentration.

(a) Determination of Operating Conditions for the Kinetic Regime:-

Measurements were made at different stirring speeds to determine operating conditions in which the kinetic regime theory could be applied. In this regime the liquid must be physically saturated with oxygen and thus the reaction rate should be independent of the degree of agitation. In addition the rate of reaction per unit volume of liquid should be independent of the volume of liquid used.

Stirring speeds ranging from 600 to 3000 rpm were used. The reaction conditions for initial runs were:

Catalyst concentration = 140 ppm

Initial acetaldehyde concentration = 10 vol % approximately

Initial volume of liquid = 500 ccs.

Pressure = 24.7 psia.

Data are shown in appendix B, table B.1 and the results are shown on figure VII.1. It is seen from this figure that the conversion of



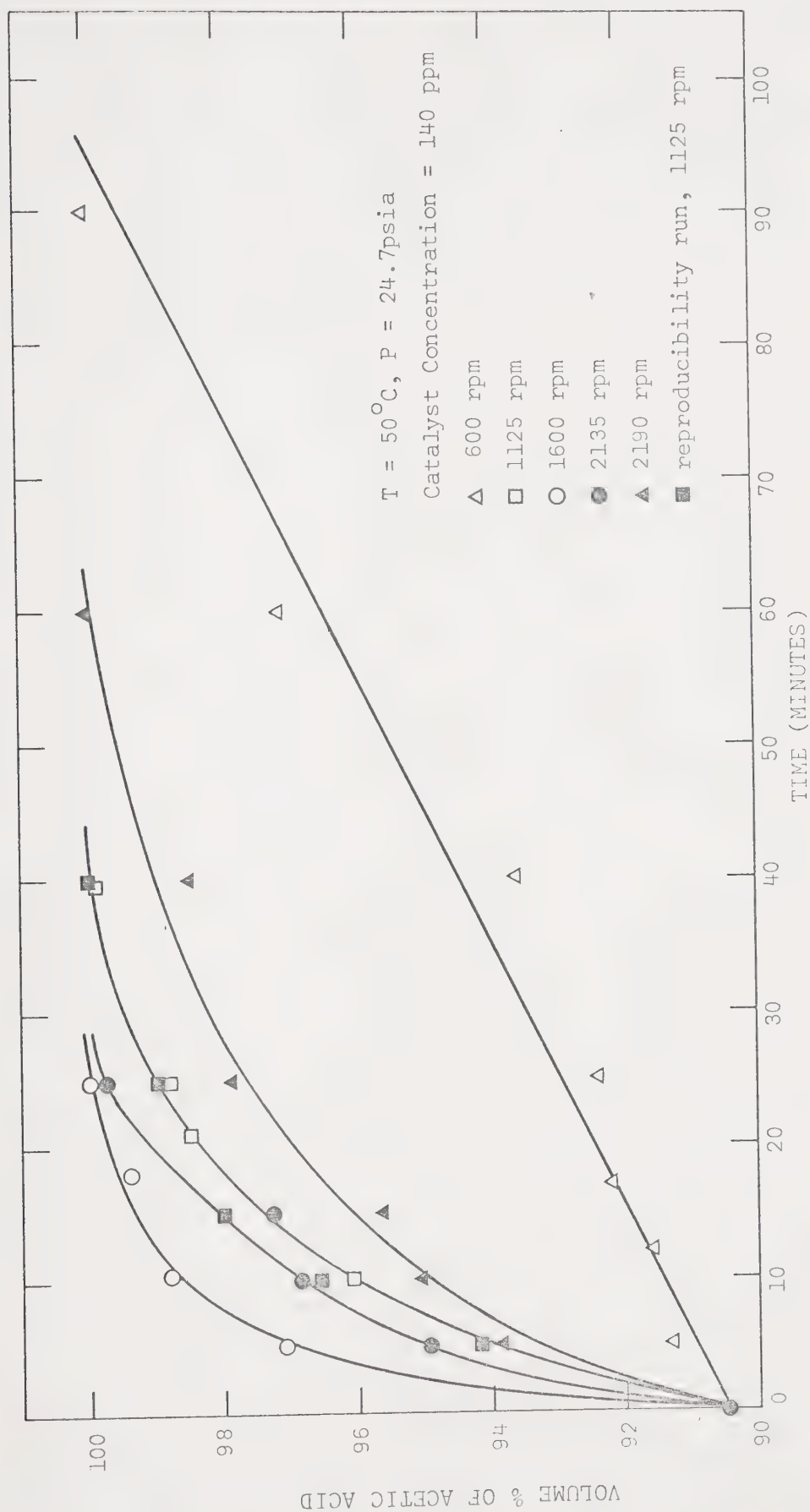


FIG. VII.1 EFFECT OF STIRRER RPM ON "CONCN. OF ACOH VS. TIME" CURVE



acetaldehyde to acetic acid increases as the stirring speed is increased from 600 to 1600 rpm but then decreases at higher stirring speeds.

The decreasing reaction rate observed at high stirring speeds can be explained by assuming that vortex-formation was taking place causing a decrease in interfacial area.

Additional runs were made at 34.7 psia and 44.7 psia. Data are shown in tables B.2 and B.3 and the results are shown on figures VII.2 and VII.3, respectively. The reaction rates for the 24.7 psia and 34.7 psia were highest at 1600 rpm but for 44.7 psia, it was highest at 2135 rpm. It appears that the stirring effect on the liquid particles decreases at high pressures and a high stirring rate is required to achieve saturation of the liquid with oxygen. It was also observed that the reaction rate did not decrease appreciably as the stirring rate was increased from 2135 rpm to 2900 rpm.

The highest concentration vs time curve was taken to represent the chemical reaction controlled regime. To further check this assumption runs were made using a larger volume of reaction mixture (i.e. 1000 ccs). One run was made at 1600 rpm and the other at 2135 rpm, both at a pressure of 24.7 psia. Data are shown in table B.4 and the results are shown on figure VII.4. The reaction rate at 1600 rpm was the same for both the 500 ccs. and the 1000 ccs runs, thus supporting the conclusion that the reaction rate was independent of the degree of stirring at this condition. At 2135 rpm, this was not the case. Thus the reaction rate was independent of liquid volume at 1600 rpm and 24.7 psia and the kinetic regime theory could be applied at the condition where the highest reaction rate was obtained.





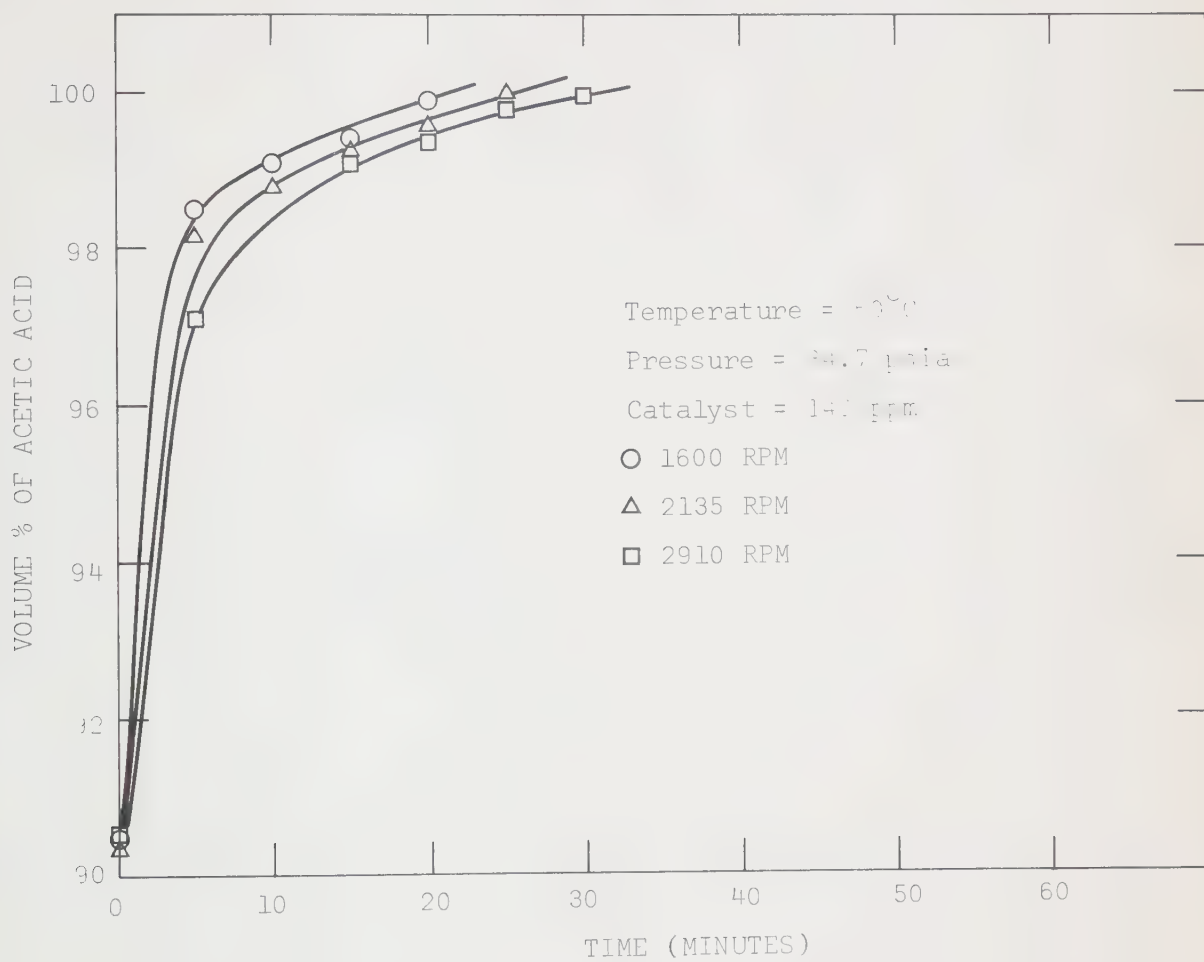


FIG. VII.2 EFFECT OF STIRRER RPM ON 'CONCENTRATION OF AcOH VS. TIME' CURVE.



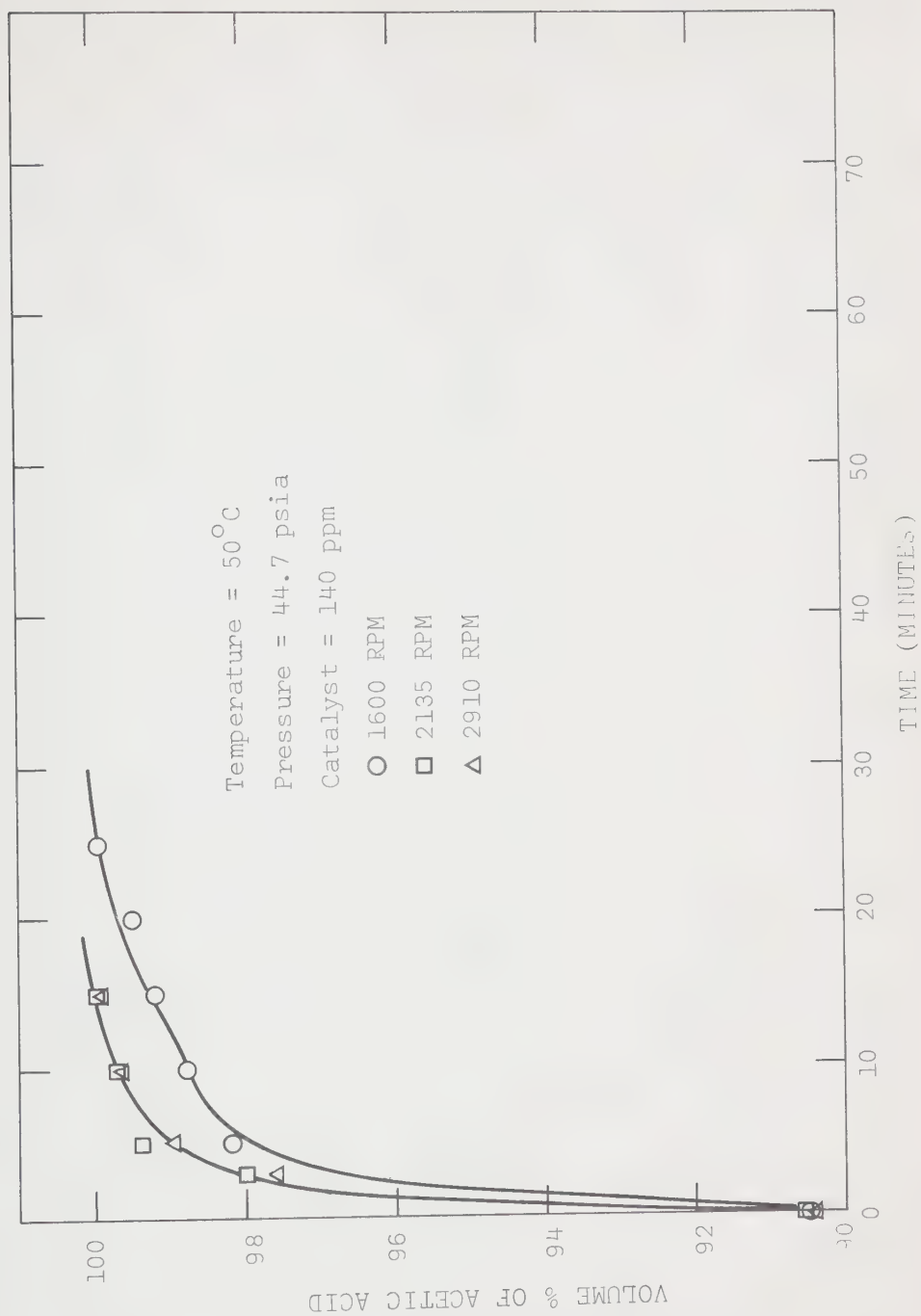


FIG. VII.3 EFFECT OF STIRRER RPM ON 'CONCENTRATION OF ACETIC ACID VS. TIME CURVE'.



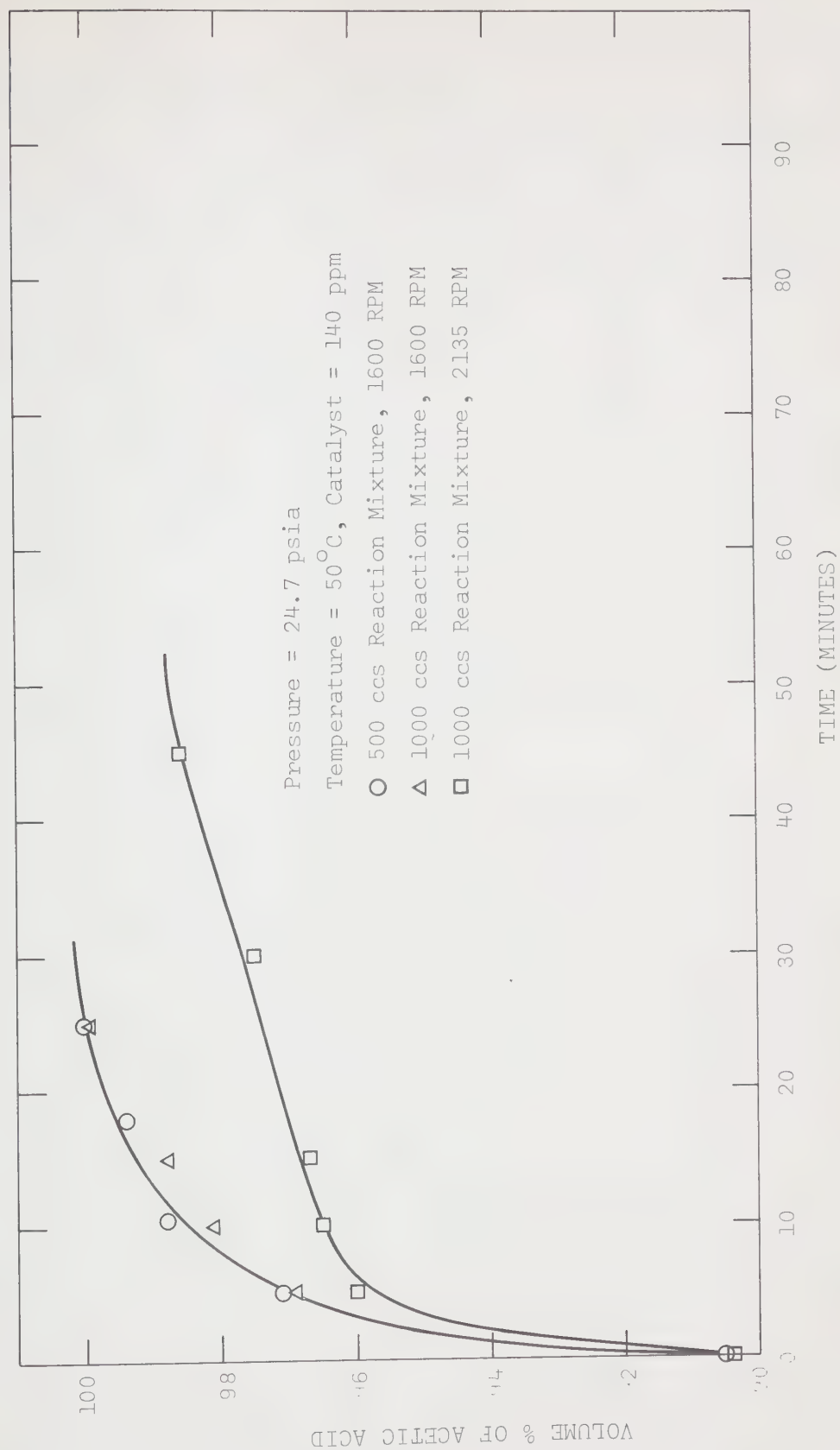


FIG. VII.4 EFFECT OF SAMPLE SIZE AND STIRRING RATE ON 'CONCENTRATION OF ACOH VS. TIME CURVE'.



(b) Effect of Acetaldehyde Concentration:-

The effect of acetaldehyde concentration on the reaction rate could be obtained from any of the acetic acid concentration vs time curves obtained by operating in the kinetic regime. Either a differential or an integral method of analysis could be used.

(c) Effect of Oxygen Concentration:-

The equilibrium concentration of oxygen-gas in the liquid mixture varies with pressure and therefore by carrying out the reaction at different pressures, the effect of oxygen concentration on the reaction rate could be studied. The results obtained at three different pressures: 24.7 psia, 34.7 psia and 44.7 psia are shown by the highest curves on figures VII.1, VII.2 and VII.3 respectively.

(d) Effect of Temperature:-

Since the chemical reaction rate is higher at higher temperature, the stirring rate required to achieve the kinetic regime at a higher temperature should also be sufficient at a lower temperature. Thus stirring rates used at 50°C were also used for lower temperatures. Runs were made at 30°C and 40°C, both at 34.7 psia. Data are given in table B.5 and results are shown on figure VII.5 for 30°C, 40°C and also 50°C.

(e) Effect of Catalyst Concentration:-

Reaction runs were carried out at two other catalyst concentrations 83 ppm and 249 ppm, both at 34.7 psia and 40°C. Data are given in table B.6 and results are shown on figure VII.6.

(f) Check of Reproducibility:-

A run was repeated at 140 ppm catalyst concentration and 40°C,





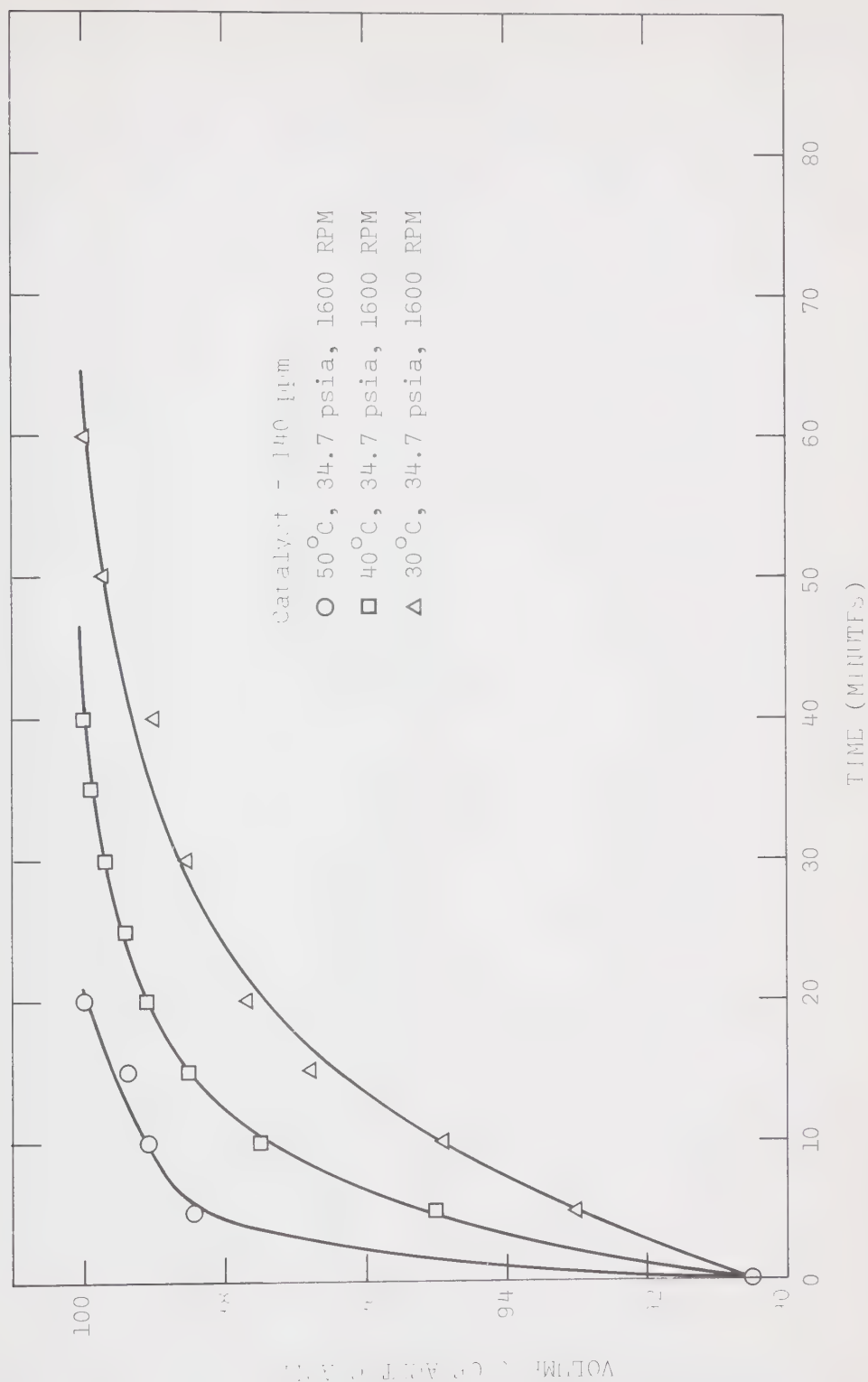


FIG. VII.5 EFFECT OF TEMPERATURE ON "CONCN. OF ACOH VS. TIME" CURVE.



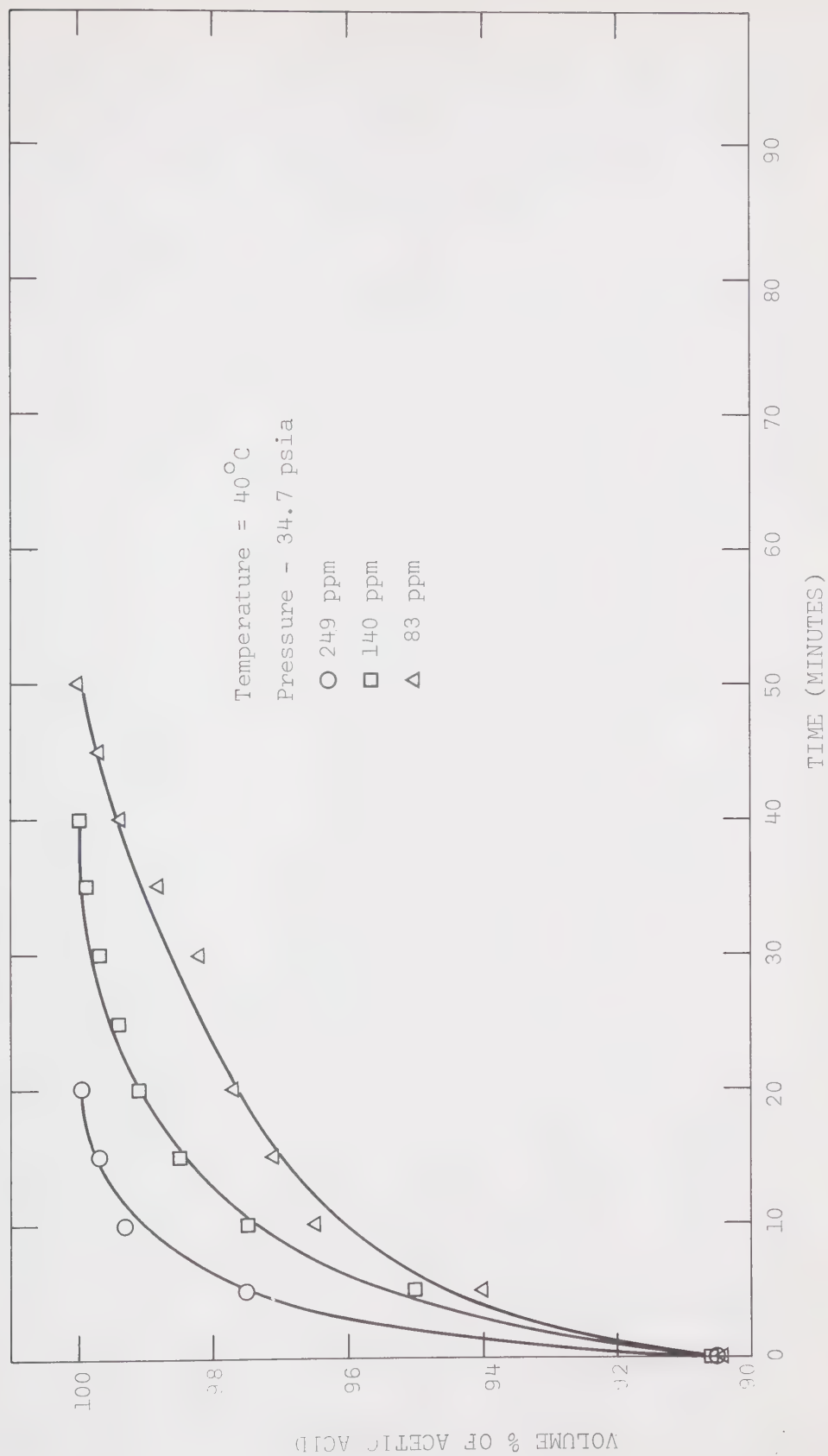


FIG. VII.6 EFFECT OF CATALYST CONCENTRATION ON 'CONCENTRATION OF ACETIC ACID VS. TIME CURVE'.



34.7 psia and 1600 rpm. Data are given in table B.7 and the results are shown on figure VII.7 which also shows the run taken earlier at the same conditions. The reproducibility is seen to be good.

(g) Catalyst Activity:-

A reaction run was made at  $40^{\circ}\text{C}$ , 34.7 psia, 140 ppm catalyst concentration, 1600 rpm and initial acetaldehyde concentration of 20% by volume. Data are shown in table B.7' and the results are plotted on figure VII.7' as concentration of acetic acid vs time. Acetic acid formed in this run was used for the next run. Fresh acetaldehyde was used and the make-up catalyst (since there was some loss of catalyst due to sampling) was added to bring the catalyst concentration to 140 ppm. The run was taken at exactly the same conditions as the previous run. Data are shown in table B.7' and the results are plotted on figure VII.7'. It can be seen from this figure that the 'concentration vs time' curve for the second run is lower than that for the first run indicating that the catalyst is deactivated after one run.

(h) Determination of Rate Equation:-

The review of literature in section II indicates that an assumption that the overall rate of reaction is first order in both oxygen concentration and acetaldehyde concentration may be justified. A rate expression, based on this assumption, was used to derive the following relationship between acetaldehyde concentration and time. The derivation, given in appendix A, takes into account the fact that the partial pressure of acetaldehyde decreases (partial pressure of oxygen increases) as the reaction proceeds. Acetic acid was supposed



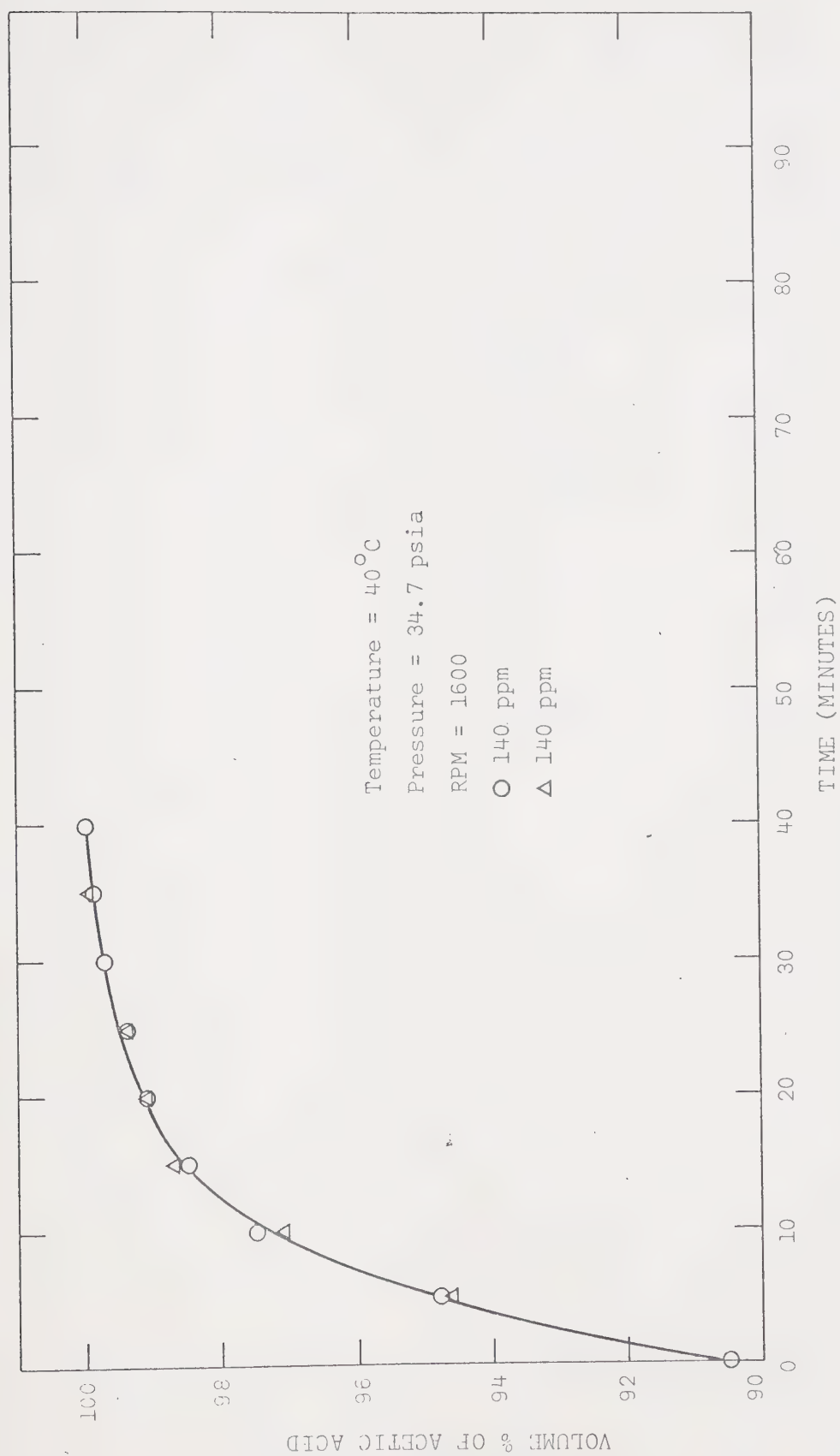


FIG. VII.7 CHECK OF THE REPRODUCIBILITY





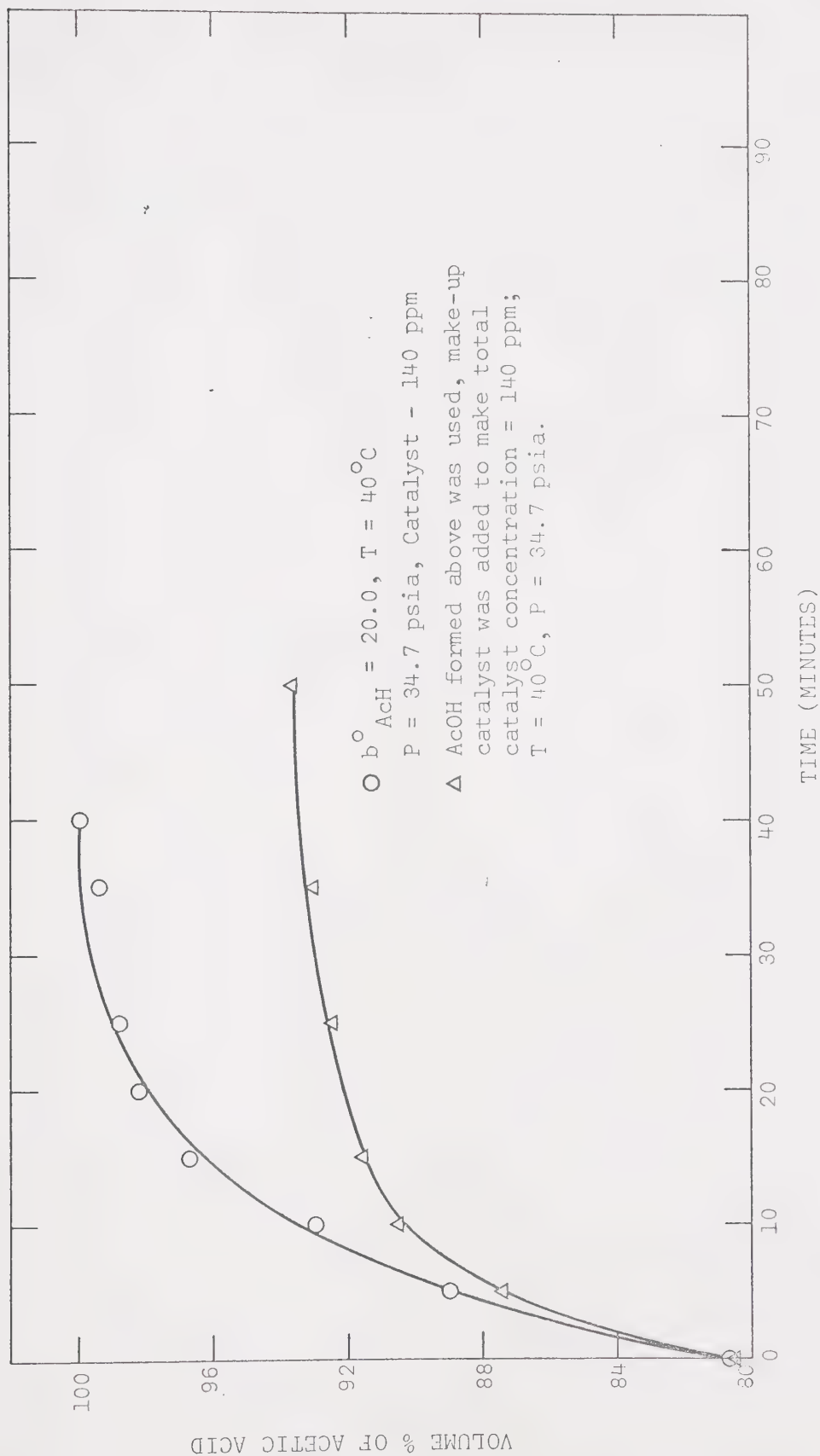


FIG. VII.7' CATALYST ACTIVITY FOR REACTION



to be the only product

$$\ln \left( \frac{P' - 1.015 \times 10^{-2} (V_1 - V_2) b_{\text{AcH}}}{P' - 1.015 \times 10^{-2} (V_1 - V_2) b_{\text{AcH}}^0} \right) \left( \frac{b_{\text{AcH}}^0}{b_{\text{AcH}}} \right) = K_R t P'$$

where  $b_{\text{AcH}}$  = concentration of acetaldehyde (volume %) at any time  $t$

$b_{\text{AcH}}^0$  = initial value of  $b_{\text{AcH}}$

$V_1$  = vapor pressure of AcH at reaction temperature, psia

$V_2$  = vapor pressure of AcOH at reaction temperature, psia

$P' = (P - V_2)$ , psia

$$\text{Let } I' = \left( \frac{P' - 1.015 \times 10^{-2} (V_1 - V_2) b_{\text{AcH}}}{P' - 1.015 \times 10^{-2} (V_1 - V_2) b_{\text{AcH}}^0} \right) \left( \frac{b_{\text{AcH}}^0}{b_{\text{AcH}}} \right)$$

$$\therefore \ln I' = K_R t P'$$

The assumed rate expression will be consistent with the data if the plot of  $\ln I'$  vs  $t.P'$  gives a straight line. The slope of this line then gives the value of  $K_R$ .

Tables B.8, B.9 and B.10 show the processed data for runs at 50°C, 140 ppm catalyst concentration and at three different pressures 24.7, 34.7 and 44.7 psia, respectively. Figure VII.8 shows the plot of  $\ln I'$  vs  $t.P'$  for runs at 50°C, 140 ppm catalyst concentration and at all three pressures 24.7 psia, 34.7 psia and 44.7 psia. It is seen that the plot is a straight line and thus the assumed rate expression is consistent with the data. The slope of the line ( $K_R$ ) was calculated to be  $7.64 \times 10^{-3} / (\text{psia})(\text{min})$  by a least square fit of first order. Because of the high



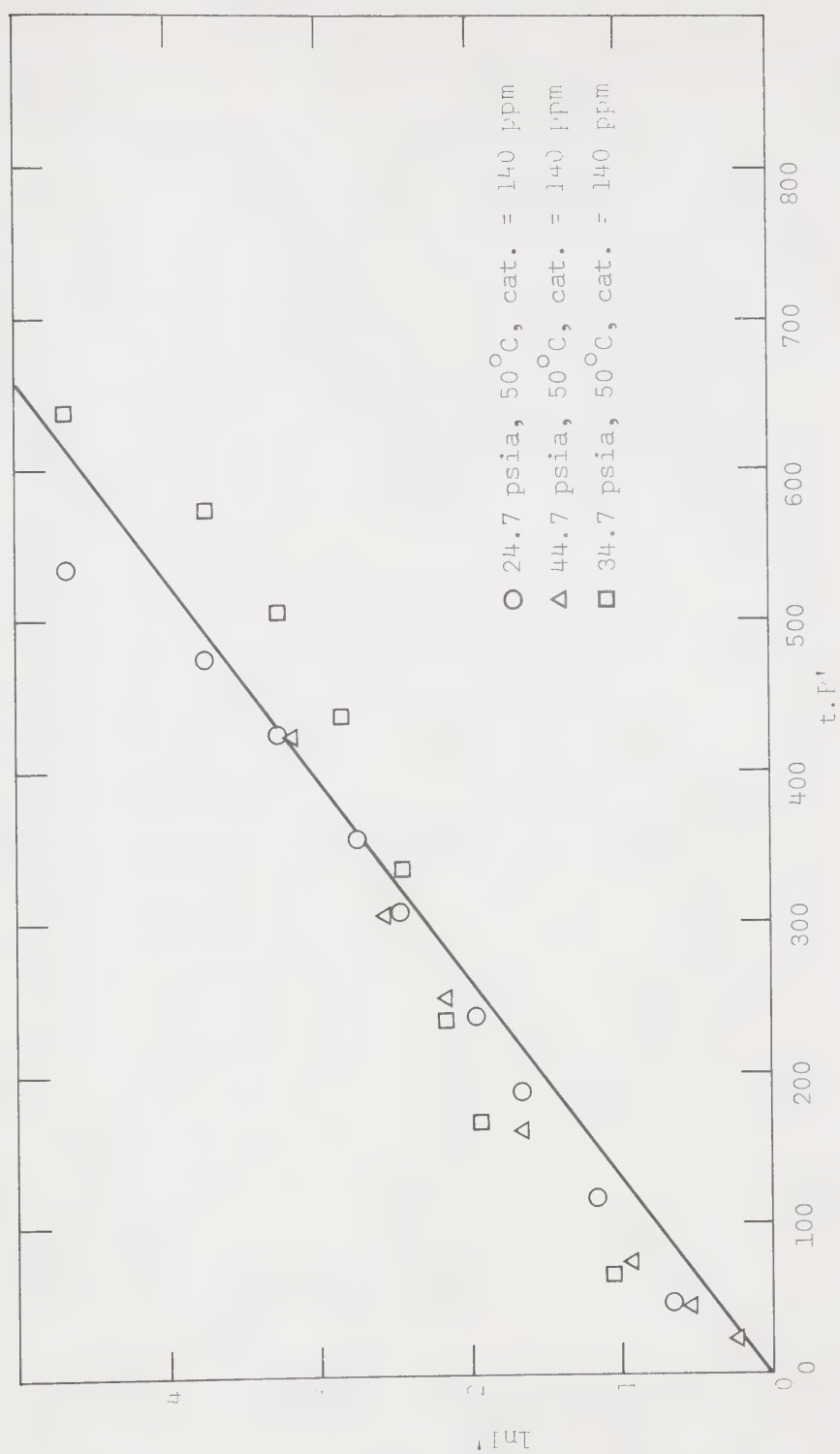


FIG. VII.8 VERIFICATION OF THE ASSUMED RATE EXPRESSION BY THE INTEGRAL METHOD.



reaction rate at 44.7 psia and 50°C, data were integrated starting from 95% (by volume) acetic acid.

Tables B.11 and B.12 show the processed data from runs at 34.7 psia, 140 ppm catalyst concentration but at 40°C and 30°C, respectively.  $\ln I'$  vs  $tP'$  plots for the data in tables B.10, B.11 and B.12 are shown in figure VII.9, which give three different straight lines for three different temperatures. Slopes of these lines thus give the reaction rate constants at the corresponding temperatures:-

From figure VII.9,

$$K_{R, 30^{\circ}\text{C}} = 1.90 \times 10^{-3} \text{ l/psia min.}$$

$$K_{R, 40^{\circ}\text{C}} = 3.46 \times 10^{-3} \text{ l/psia min.}$$

$$K_{R, 50^{\circ}\text{C}} = 7.64 \times 10^{-3} \text{ l/psia min.}$$

#### Arrhenius' Equation Fit for Temperature Dependency of $K_R$ :-

Arrhenius' equation is

$$K_R = K_R^{\circ} e^{-E/RT}$$

where,  $K_R^{\circ}$  = frequency factor

$E$  = activation energy

$R$  = gas-law constant

$T$  = temperature.

The above equation can easily be reduced to:

$$-\ln K_R = E/RT - \ln K_R^{\circ}$$

Thus, if  $-\ln K_R$  vs  $1/T$  is plotted, it should give a straight line.

The slope of the line =  $E/R$ .

A plot of  $\log K_R$  vs  $1/T$  is shown in figure VII.10 and from this plot  $E/R = 6.9 \times 10^3 / ^{\circ}\text{K}$ .





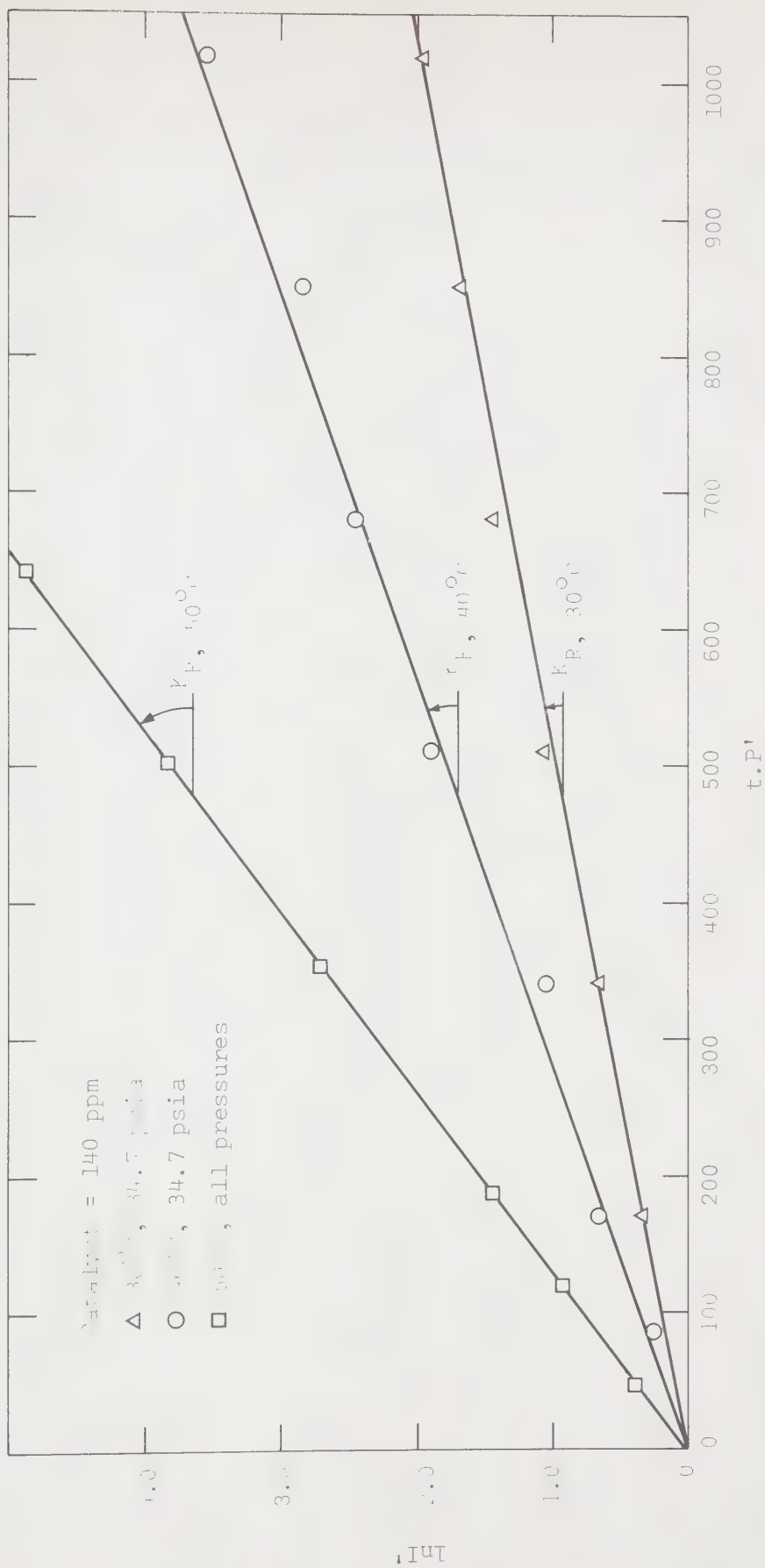


FIG. VII.3 EFFECT OF TEMPERATURE ON REACTION RATE CONSTANT.



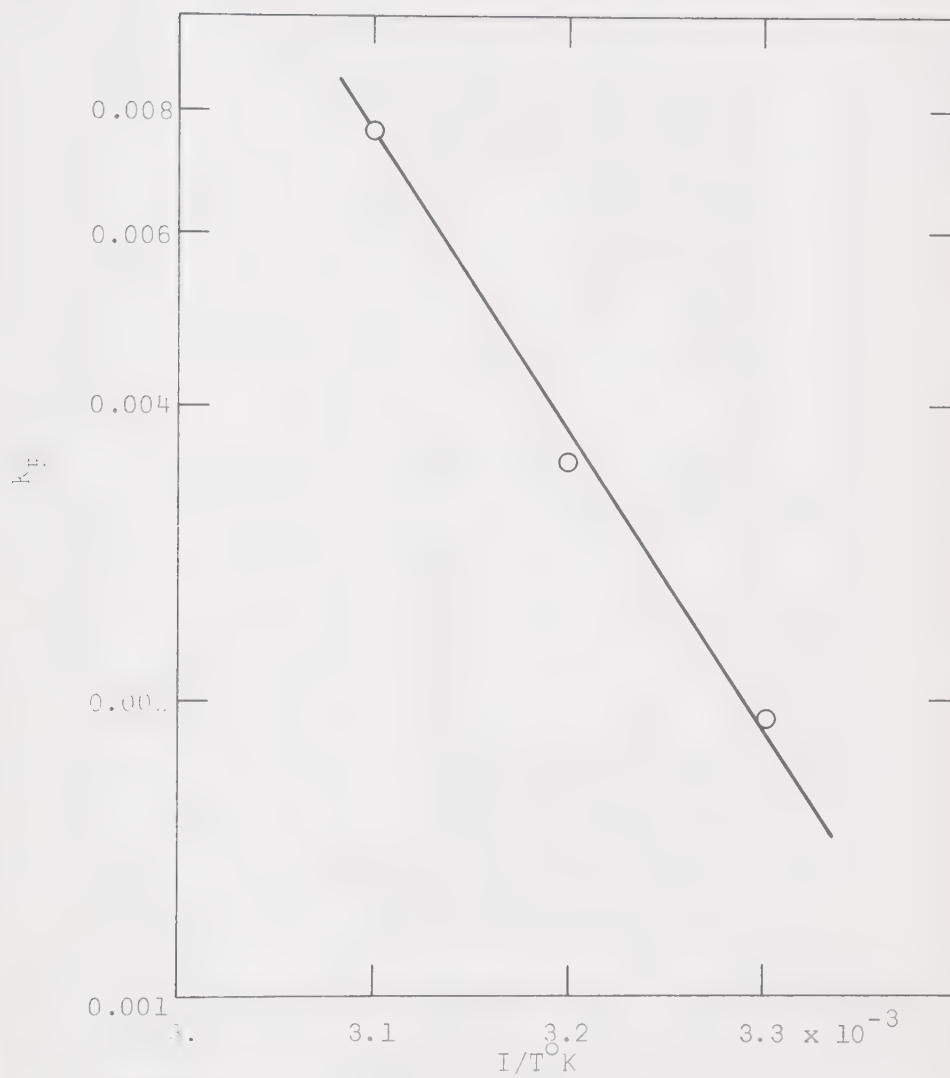


FIGURE VI.10 EFFECT OF TEMPERATURE ON  $K_R$



∴ E = activation energy

$$= 13.8 \times 10^3 \text{ cal/g-mole}$$

$K_R^0$  is calculated to be  $1.48 \times 10^7$ , l/psia min, and the Arrhenius' equation can be written as  $K_R = 1.48 \times 10^7 e^{-13.8 \times 10^3 / RT}$

#### Dependence on Catalyst Concentration:-

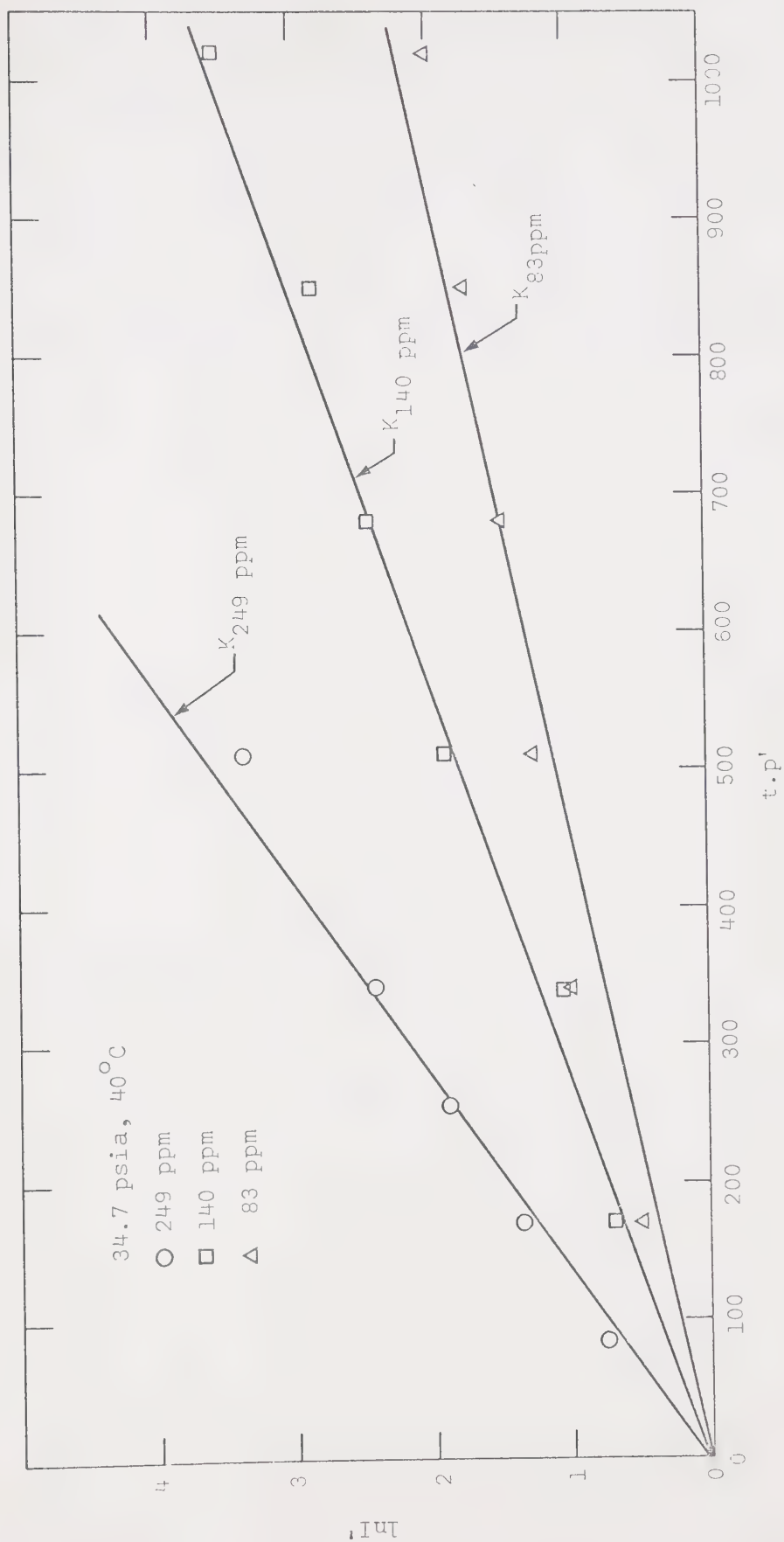
Tables B.13 and B.14 show the processed data for the reactions at 34.7 psia, 40°C and at two different catalyst concentrations, 83 ppm and 249 ppm.  $\ln I'$  vs  $tP'$  plots for these data and also for 140 ppm catalyst concentration are shown in figure VII.11. Straight lines are obtained for each catalyst concentration, which agrees with the assumed rate expression. Slopes of these lines (i.e.  $K_R$ ) are given below:

| Source     | T°C  | P,psia | Catalyst Concentration,ppm | $K_R$ ,l/psia min     |
|------------|------|--------|----------------------------|-----------------------|
| Fig.VII.11 | 40°C | 34.7   | 83                         | $2.02 \times 10^{-3}$ |
|            |      |        | 140                        | $3.46 \times 10^{-3}$ |
|            |      |        | 249                        | $7.00 \times 10^{-3}$ |

Figure VII.12 shows a plot of  $K_R$  vs catalyst concentration on a log-log plot and the slope of the line is almost one. Thus the reaction rate can be assumed first order in catalyst concentration. Figure VII.13 shows a plot of  $K_R$  vs catalyst concentration which gives a straight line of slope  $(K_R') = 2.52 \times 10^{-5}$  l/(psia min ppm). Hence the general rate expression is

$$r_{\text{AcH}} = -9.08 \times 10^4 e^{\frac{-13.8 \times 10^3}{RT}} \cdot b_{\text{AcH}} \cdot P_{O_2} \cdot (\text{cat. concn., ppm}) \dots (7.1)$$



FIG. VII.11 EFFECT OF CATALYST CONCENTRATION ON  $K_R$ .





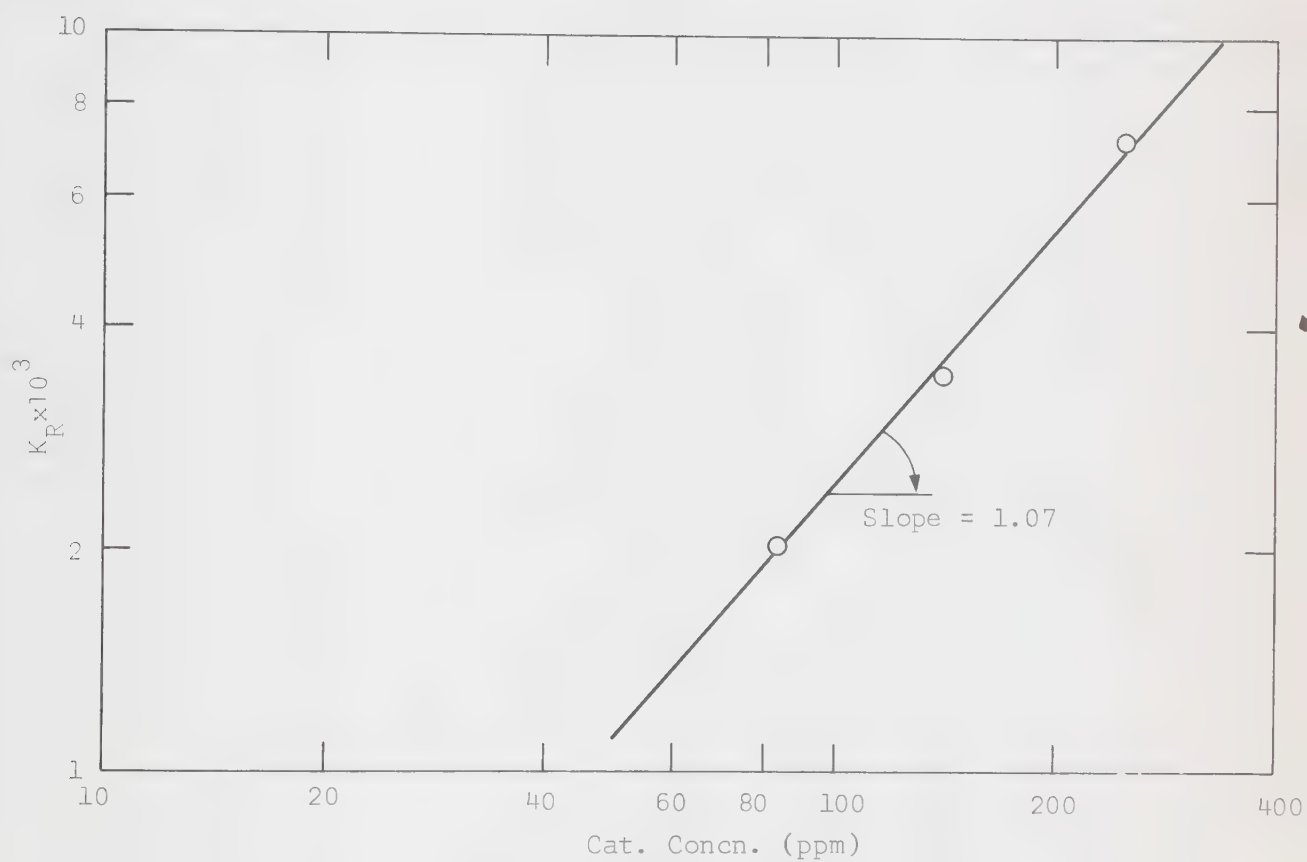


FIG. VII.12 CHECK OF THE REACTION ORDER IN CATALYST CONCENTRATION.



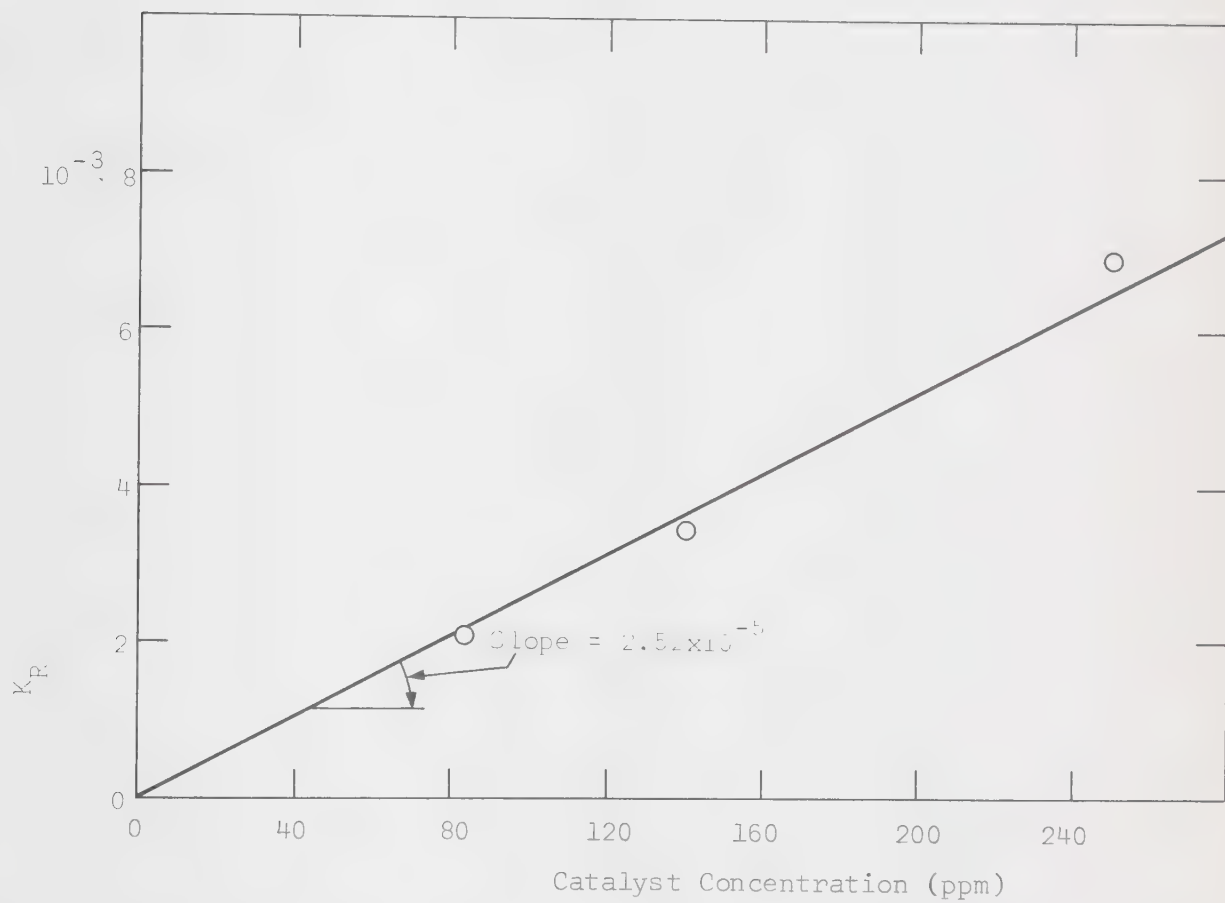


FIG. VII.13 DEPENDENCE OF THE REACTION RATE ON CATALYST CONCENTRATION.



### Comparison of Experimental and the Predicted Results:-

Consider the run number 15;  $P = 34.7$  psia,  $T = 40^{\circ}\text{C}$ ,  $b_{\text{AcH}}^{\circ} = 9.5\%$ ,  
catalyst = 140 ppm

$$\begin{aligned}\text{Predicted } K_R &= 9.08 \times 10^4 e^{\frac{-13.8 \times 10^3}{RT}} \quad (\text{cat. concn., ppm}) \\ &= 2.52 \times 10^{-5} (140 \text{ ppm}) \\ &= 3.46 \times 10^{-3} \text{ l/psia min.}\end{aligned}$$

Table B.15 shows the comparison of the predicted and the experimental data for  $t$  vs  $b_{\text{AcH}}$  and figure VII.14 shows the calculated and the experimental  $t$  vs.  $b_{\text{AcH}}$  plots, from which it can be seen that the rate expression presented here is quite satisfactory.

### Visual Observation:

The reaction mixture which was colourless at the start of the reaction turned brown after the reaction started. This observation is in conformity with that of other workers (5,6). The color change noted is associated with a change in the valence of the catalyst from  $\text{Mn}^{++}$  to  $\text{Mn}^{+++}$  (or  $\text{Co}^{++}$  to  $\text{Co}^{+++}$ ). If there is no color change, there is no subsequent reaction.

### B. Sparged Reactor Study:

#### (a) Hold-up Measurements:-

The oxygen-acetic acid system was considered to be representative of the reaction mixture and hold-up measurements were made for this system at  $40^{\circ}\text{C}$  and 20 psig. A liquid circulation rate of 1.83 gallons per minute was used. Results are given in table B.16 in appendix B and are plotted on figure VII.15 as  $\epsilon$  vs  $U_{\text{SG}} \left( \frac{62.4}{\rho_L} \cdot \frac{72}{\sigma} \right)^{1/3}$  so that they can be compared to Hughmark's correlation (57).



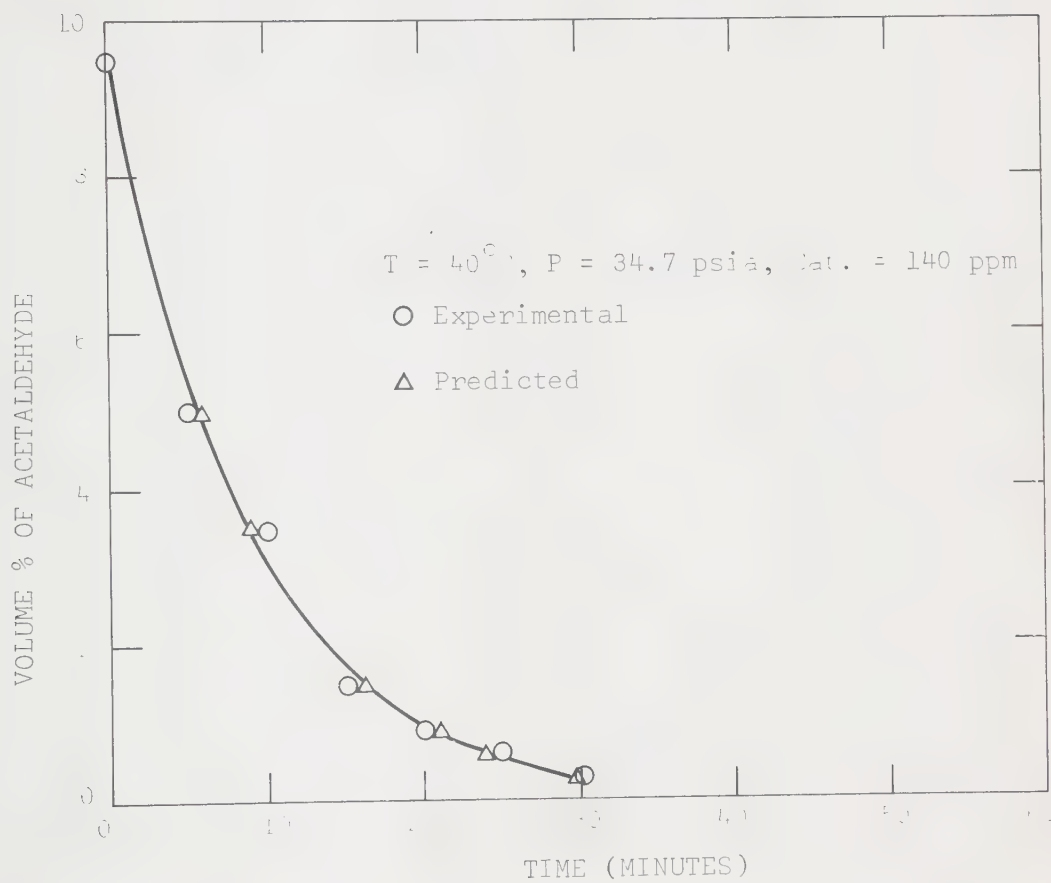


FIG. VII.14 COMPARISON OF THE PREDICTED AND THE EXPERIMENTAL KINETIC RESULTS.





○ Experimental (P = 20 psig, T = 40°C,  $U_{SL} = 1.83$  GPM)

□ From Hughmark's Correlation

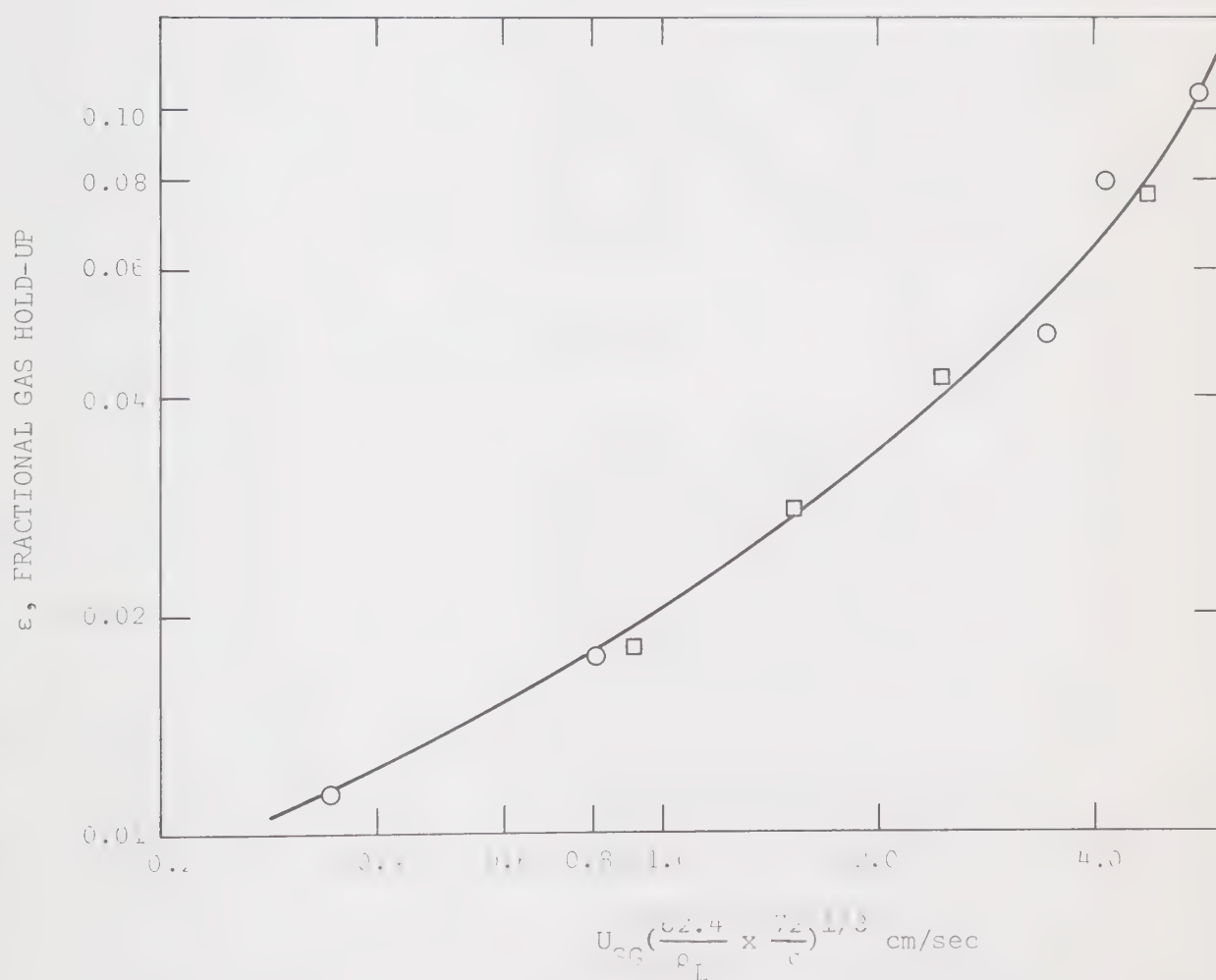


FIG. VII.15 HOLD-UP CORRELATION FOR  $O_2$ -AcOH SYSTEM AND COMPARISON WITH HUGHMARK'S CORRELATION.



### Comparison With Hughmark's Correlation:-

Hughmark's data take into account the effect of liquid physical properties on hold-up. The data indicated that hold-up for different systems can be correlated with the term  $U_{SG} \left( \frac{62.4}{\rho_L} \cdot \frac{72}{\sigma} \right)^{1/3}$ . Hughmark's data, however, were taken with zero liquid flow. From Hughmark's correlation for  $\epsilon'$  vs  $U_{SG} \left( \frac{62.4}{\rho_L} \cdot \frac{72}{\sigma} \right)^{1/3}$ ,  $\epsilon$  can be back-calculated from equation (5.19), as shown in section V.C, by trial and error for any particular  $U_{SG}$  and  $U_{SL}$ . Thus the data in the present work could be compared to Hughmark's data. Table B.17 in the appendix shows the results for  $U_{SG} \left( \frac{62.4}{\rho_L} \cdot \frac{72}{\sigma} \right)^{1/3}$  vs  $\epsilon$  (experimental) and  $\epsilon$  (predicted from Hughmark's correlation) and figure VII.15 shows the comparison of the two. It can be concluded that the experimental results are in good agreement with Hughmark's correlation.

### (b) Bubble Diameter and Interfacial Area:-

#### Bubble Diameter:-

It was noted visually that the bubbles formed in the oxygen-acetic acid system were much smaller than those formed in the air-water system. This demonstrated that the correlations available in the literature for the air-water system may not be suitable for the oxygen-acetic acid system.

Bubble diameters were measured from photographs taken of the oxygen-acetic acid system at various oxygen flow rates at 20 psig and 40°C. The oxygen flow rate was in the range of 47 ccs/sec to 334 ccs/sec. The flow regime was determined from Govier's chart (30) and the system was found to be operating in the bubble regime. The bubble sizes were determined by scaling maximum (l) and minimum (w) dimensions



of the individual bubbles on the photographs. In general, most of the observed bubbles were oblate spheroids; the diameter of a sphere equal in volume to the oblate spheroid, given by the following equation, was taken to be the diameter of a bubble:

$$d_b = (lw^2)^{1/3}$$

The volume surface mean diameter was calculated by the following equation

$$d_{vs} = \frac{\sum n_i d_{l,i}^3}{\sum n_i d_{b,i}^2}$$

Processed data for the bubble diameters are given in tables B.18 to B.22 in appendix B. The results are shown in table VII.1 and plotted in figure VII.16 as the superficial gas velocity of oxygen vs  $d_{vs}$ . The mean bubble diameters calculated from the empirical correlation (5.4) are also shown in table VII.1 for the comparison purposes. It must be noted that the experimental bubble diameters are much smaller than those calculated from equation (5.4). This was expected since the bubble diameter in electrolytes are smaller than in the air-water system.

#### Interfacial Area:-

The interfacial area in the bubble column is given in figure VII.17 as a function of the oxygen flow rate. The values of interfacial area were calculated using the following equation:

$$a' = \frac{6\varepsilon}{d_{vs}}$$

The processed data and the results are shown in table VII.1. Calderbank's equation (5.22) was also used for calculating the interfacial area and the values are given in table VII.1. They are smaller than the experimental values, demonstrating the fact that the empirical equations may only be suitable for the air-water system.



TABLE VII.I

BUBBLE DIAMETERS, HOLD-UP AND INTERFACIAL AREA AS A FUNCTION OF SUPERFICIAL GAS VELOCITY

| $O_2$ Flow<br>Rate<br>ccs/sec | Superficial<br>gas velocity<br>$U_{SG}$ , cm/sec | $d_{vs}$<br>cm | $\epsilon$ | $a'$<br>$\frac{cm^2}{cm^3}$ | 'a' from<br>Calderbank's<br>equation,<br>$cm^2/cm$ | 'a' from<br>Calder-<br>bank's<br>equation | $d_{vs}$<br>(Eqn.<br>5.4) |
|-------------------------------|--|----------------|------------|-----------------------------|--|---|---------------------------|
| 47                            | 0.579  | 0.139          | .0174      | 0.75                        |  |   |                           |
| 85                            | 1.048  | 0.223          | .0265      | 0.72                        | 0.666  | 0.648                                     | 0.41 cm                   |
| 177                           | 2.18   | 0.172          | 0.051      | 1.78                        |  |   |                           |
| 215                           | 2.64   | 0.176          | 0.062      | 2.12                        |  |   |                           |
| 334                           | 4.11   | 0.163          | 0.112      | 4.12                        | 2.29   | 2.04                                      | 0.357 cm                  |





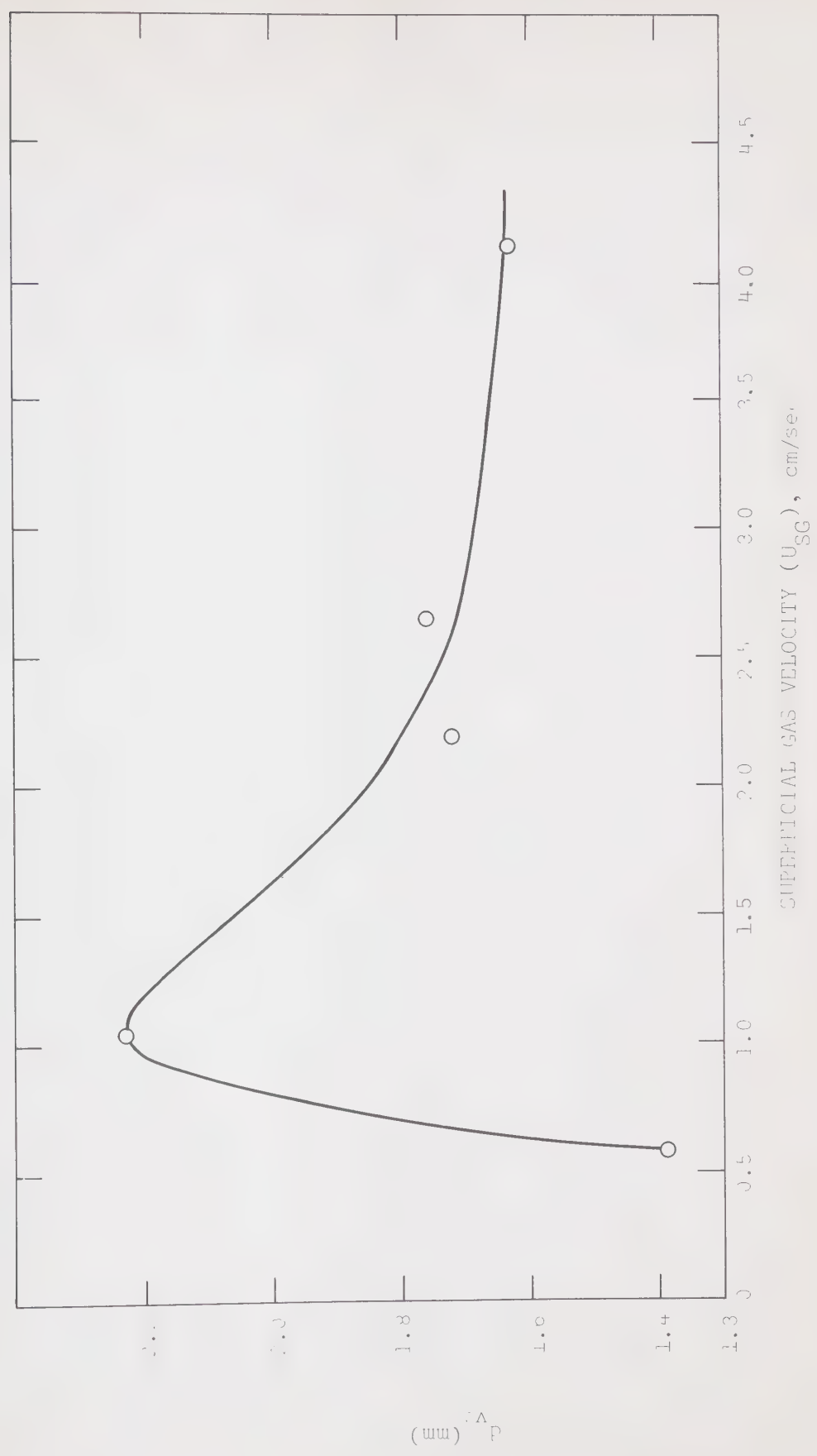


FIG. VII.16 SUPERFICIAL GAS VELOCITY OF  $O_2$  VS.  $d_{vs}$ .



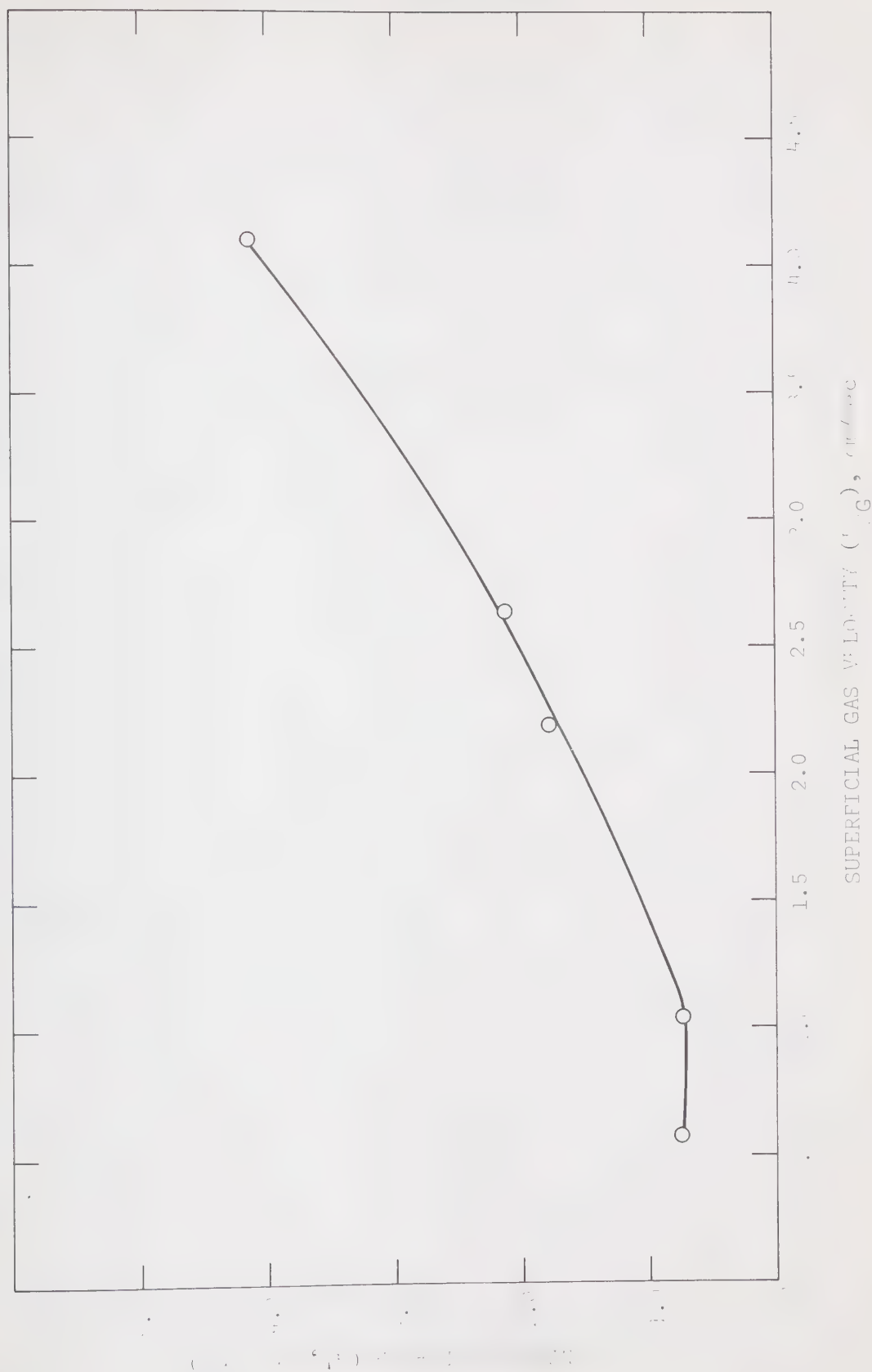


FIGURE VII.17 SUPERFICIAL GAS VELOCITY OF  $O_2$  IN WATER.



(c) Conversion of Acetaldehyde to Acetic Acid:-

(1) Experimental Results:-

Two runs, one at an oxygen flow rate of 85 ccs/sec and the other at 334 ccs/sec were made for the oxidation of acetaldehyde to acetic acid at  $40^{\circ}\text{C}$ , 20 psig, 140 ppm catalyst concentration, 10% (volume) initial concentration of acetaldehyde and 40 inches liquid level in the bubble reactor. The data are shown in tables B.23 and B.24 in appendix B and the results are plotted in figure VII.18 as concentration of acetaldehyde vs time for both oxygen flow rates.

(2) Modelling Sparged Reactor:-

In order to select an appropriate model for the sparged reactor it was necessary to determine the reaction regime consistent with the experimental operating conditions. To do so, it was essential to estimate some parameters, i.e. Henry's constant (H) for the oxygen-acetic acid system, the diffusivity of oxygen in acetic acid (D) and the physical mass transfer coefficient ( $K_L^{\circ}$ ). For these purposes, the reaction mixture was assumed to have properties of pure acetic acid.

Solubility of Oxygen in Acetic Acid:-

There are no data available for the solubility of oxygen in acetic acid. However, it was calculated from Prausnitz and Shair's equation (73) using the limited data available for the solubility of nitrogen in acetic acid. Calculations are shown in appendix A and the Henry's constant (H) for oxygen-acetic acid system at 20 psig and  $40^{\circ}\text{C}$  was estimated to be 1660 atmospheres/g-mole  $\text{O}_2$ /g-mole AcOH.

Diffusivity of Oxygen in Acetic Acid:-

Because of the lack of the data available in the literature for



the diffusivity of oxygen in acetic acid, it was calculated from Kuloor's equation (74) as shown in appendix A. It was estimated to be  $2.35 \times 10^{-5} \text{ cm}^2/\text{sec}$  at  $40^\circ\text{C}$ .

#### Physical Mass Transfer Coefficient, $K_L^O$ :-

Calderbank and Moo-Young's (51) and Hughmark's (57) equations were used for estimating  $K_L^O$  for the oxygen-acetic acid system. The results are shown in table VII.2.

#### Determination of the Reaction Regime:-

The diffusion time and the reaction time were calculated, as shown in appendix A, for the complete range of experimental conditions. The results are given below:

$$t_R = 13.8 \text{ sec}$$

$$t_D = 0.0125 \text{ sec} - 0.554 \text{ sec.}$$

Thus  $t_D \ll t_R$ , indicating that the bubble reactor was operating in the slow reaction regime.

#### Mathematical Model:-

The following assumptions were made in order to analyze the reactor:

- (1) Liquid phase is well mixed and operated as a batch
- (2) Gas is passed through the liquid phase in the form of bubbles
- (3) Pure oxygen gas (99%+) is used as the gas phase
- (4) Gas phase resistance is negligible
- (5) Axial dispersion is neglected
- (6) Reactor volume is constant.

In the slow reaction regime,  $K_L = K_L^O$  and the general equation (4.1) for this regime, given in section 4, reduces to the following equation:





$$K_L^O \frac{a'}{1-\epsilon} (C' - C_O) - 1/2 K_R b_{AcH} C_O = \frac{dC_O}{dt} \dots \dots \dots (7.2)$$

and the kinetic equation at a particular catalyst concentration is given by:

$$-K_R b_{AcH} C_O = \frac{db_{AcH}}{dt} \dots \dots \dots (7.3)$$

The above two equations were solved simultaneously by the Runge-Kutta method of fourth order to predict the performance of the reactor. The following initial conditions were used:

- (i) at  $t = 0$ ,  $C_O = 0$
- (ii) at  $\tau = 0$ ,  $b_{AcH} = b_{AcH}^O$ .

The values of  $a'$ ,  $K_R$  and  $\epsilon$  used in the model are given in table VII.2. The best-fit values for  $K_L^O$  were determined by fitting the model to the experimental data for the acetaldehyde concentration profile in the sparged reactor. The computer program is given in appendix A and the model results are given in tables B.25 and B.26 in appendix B. Figure VII.18 shows both the model prediction and the experimental curve for acetaldehyde concentration vs time. The model seems to fit the experimental data real good. The best-fit values for  $K_L^O$  are 0.015 cm/sec and 0.0065 cm/sec for oxygen flow rates of 85 ccs/sec and 334 ccs/sec, respectively. It can be seen from table VII.2 that the values of  $K_L^O$  predicted by Hughmark's equation for bubble swarms (57) and Calderbank and Moo-Young's equation (51) for bubble swarms of average bubble diameter less than 0.25 cm are in reasonably good agreement with those required for the best-fit.



TABLE VII.2

PHYSICAL MASS TRANSFER COEFFICIENTS

For  $O_2 = 85$  ccs/sec,  $\epsilon = 0.0265$ ;

$$K_R = 4.92 \times 10^3 \frac{\text{ccs of liquid}}{\text{g-mole AcH.min}}$$

The best fit values:  $K_L^O a' = 0.0107$  1/sec;  $a' = 0.712 \frac{\text{cm}^2}{\text{cm}^3}$ ;  $K_L^O = 0.015$  cm/sec.

For  $O_2 = 334$  ccs/sec,  $\epsilon = 0.112$

The best fit values:  $K_L^O a' = 0.267$  1/sec;  $a' = 4.12 \frac{\text{cm}^2}{\text{cm}^3}$ ;  $K_L^O = 0.0065$  cm/sec.

| Source  | 85 cc/sec<br>$K_L^O$<br>cm/sec | 334 cc/sec<br>$K_L^O$<br>cm/sec | 85 cc/sec<br>$K_L^O \cdot a'$<br>1/sec | 334 cc/sec<br>$K_L^O \cdot a'$<br>1/sec |
|---|--------------------------------|---------------------------------|--|---|
| Calderbank's equation<br>for $d_b < 0.25$ cm. | 0.0115                         | 0.0115                          | 0.0082                                 | 0.0474                                  |
| Calderbank's equation<br>for $d_b > 0.25$ cm  | 0.0433                         | 0.0433                          | 0.0308                                 | 0.178                                   |
| Hughmark's equation                           |                                |                                 |  |   |
| (1) for Single Bubbles                        | 0.0265                         | 0.0232                          | 0.01885                                | 0.0775                                  |
| (2) for Bubble Swarms                         | 0.0087                         | 0.00756                         | 0.0062                                 | 0.0312                                  |



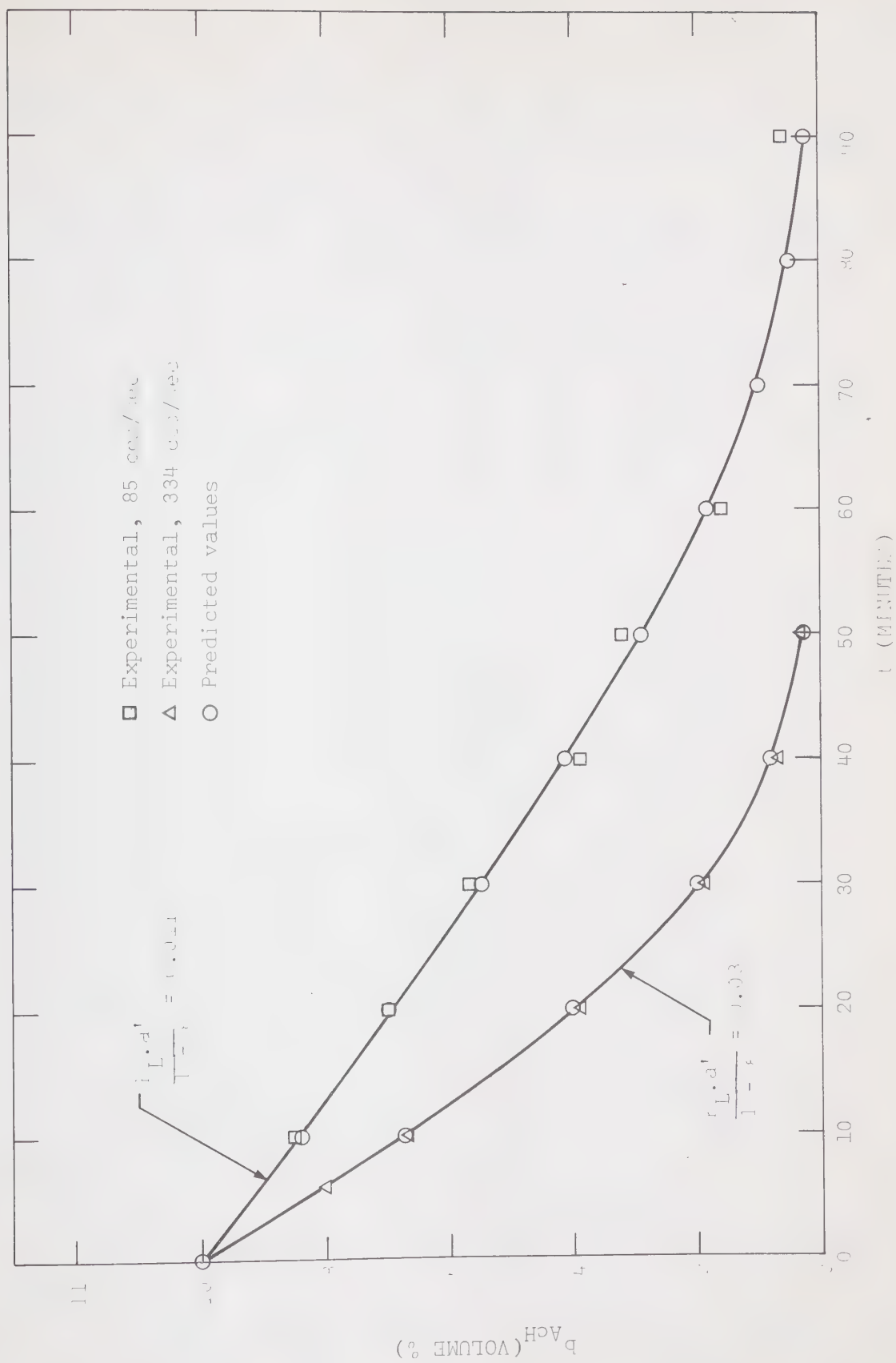


FIG. VII.18 LIQUID CONCENTRATION PROFILES IN THE SPARGED REACTOR.



## CHAPTER VIII

### DISCUSSION AND CONCLUSIONS:

The performance of a two-phase sparged reactor can be estimated if the following information is available.

- (1) Description of the chemical reactions occurring and kinetic rate data.
- (2) A model which adequately describes the mixing pattern in the reactor.
- (3) Interfacial area.
- (4) Gas hold-up.
- (5) Physical mass transfer coefficients.

For this study of the catalytic oxidation of acetaldehyde to acetic acid, since the reaction mechanism is complex, a simplified approach was used in that only the overall reaction was studied. A kinetic rate expression to describe the overall reaction was obtained which is first order in acetaldehyde - in agreement with the results of other workers who have studied the oxidation of aldehydes (4, 11, 20, 21, 22), first order in catalyst concentration, which is also in agreement with studies made by other workers (2, 11, 16, 23) and first order in catalyst concentration, which is supported by the works of Bawn and Williamson (4) and Allen (9). The catalyst concentration used was in the industrial range (i.e. 80-250  $\text{Mn}^{++}$  ppm, equivalent to 0.0253 - 0.079 wt % of  $\text{Mn}^{++}$  in acetaldehyde).

The rate expression obtained in this work is given below:

$$\frac{db_{\text{AcH}}}{dt} = r_{\text{AcH}} = -9.08 \times 10^4 e^{-13.8 \times 10^3 / RT} \cdot b_{\text{AcH}} \cdot p_{\text{O}_2} \cdot (\text{Cat. concn., ppm})$$





where,  $b_{\text{AcH}}$  = volume % of acetaldehyde in the liquid phase

and  $p_{\text{O}_2}$  = partial pressure of  $\text{O}_2$  in the reactor, psia.

Venugopal et. al. (11) concluded that the catalytic oxidation of acetaldehyde to acetic acid was independent of the catalyst concentration which appears to be highly doubtful. Further, it is not at all clear what units are used in their rate expression (11) and there are inconsistencies in their paper, which make it impossible to use their rate expression even for comparison purposes.

Studies in the four-inch bubble column provide information on bubble size, gas hold-up and interfacial area for the  $\text{AcH-AcOH-O}_2$  system.

The fractional gas hold-up results are in excellent agreement with those predicted from Hughmark's graphical correlation (57) which is claimed to hold for various systems covering a wide range of physical properties of liquid.

The measured bubble sizes are smaller than would be predicted from empirical estimating procedures in the literature but these were developed only for the air-water system. Yoshida and Akita (61) noted smaller bubble sizes in electrolytes and this could possibly be expected with the organic system dealt with here. The interfacial areas predicted from Calderbank's equation for interfacial area in agitated vessels, are smaller than the experimental values obtained in this work, though for the lower flow rate of oxygen (i.e. 85 ccs/sec), the difference is small. Hence one must be careful in using the available correlations for systems other than the air-



water system.

The best-fit values of physical mass transfer coefficient ( $K_L^0$ ), obtained from the model predictions and the experimental data for the acetaldehyde concentration profile in the sparged reactor, seem to be in reasonably good agreement with those predicted from Calderband's equation (5.14) for bubble swarms of average bubble diameter less than 0.25 cm and from Hughmark's equation (5.9) for bubble swarms.

For the ideal operating conditions, i.e. well-mixed liquid and pure gas, used in this work, a simple model suffices and can be used to predict the performance of the laboratory column with a good degree of accuracy. However, for an industrial column air would probably be used and a significant depletion of oxygen would occur. In such a case, the spatial variation of bubbles over the reactor length and the decrease in partial pressure of the reacting gas component must be considered. Equation (4.18) then provides the gas-phase model for a semi-flow reactor.

$$K_G a_b^{RT} \left( Y_C - \frac{CH}{P} \right) + \frac{U_b}{(1-Y_C)} \cdot \frac{dY_C}{dz} = 0 \quad \dots \dots (4.18)$$

and can be solved for  $Y_C(z)$ , mole-fraction of component C in the gas phase, as a function of reactor height  $z$ , and then average values of  $\bar{a}_b$ ,  $\bar{V}_b$  and  $\bar{Y}_C$  must be used in the liquid-phase model of interest to solve for  $c(t)$  or  $b(t)$ , as mentioned in chapter IV.



# LIST OF SYMBOLS

$a_1, a_2, a_3$  = empirical constants in eqn. (5.7)

$a_b$  = ratio of surface area to volume of a single bubble,  $L^{-1}$

$\bar{a}_b$  = average value of  $a_b$

$a$  = interfacial area per unit volume of liquid,  $L^{-1}$

$a'$  = interfacial area per unit volume of liquid-gas mixture,  $L^{-1}$

$A$  = integration constant in eqn. (3.18)

$a_k, b_k$  = empirical constants used in equation (5.9)

$b$  = concentration of liquid-phase reactant,  $mL^{-3}$

$b_o$  = bulk-liquid value of  $b$ ,  $mL^{-3}$

$b_{AcH}$  = volume % of acetaldehyde in liquid

$b_{AcH}^o$  = volume % of acetaldehyde in the liquid feed.

$C$  = concentration of reacting gas component in the liquid,  $mL^{-3}$

$C_{O_2}$  = gm-moles of  $O_2$  per cc of solution,  $mL^{-3}$

$C_i$  = inlet concentration of  $C$  in the liquid,  $mL^{-3}$

$C'$  = equilibrium value of  $C$ ,  $mL^{-3}$

$C'_o$  = interfacial value of  $C$ ,  $mL^{-3}$

$C_o$  = bulk-liquid value of  $C$ ,  $mL^{-3}$

$C_{O_2}^i$  = volume % of  $O_2$  in the gas-mixture.

$d_b$  = bubble diameter,  $L$

$d_{ob}$  = bubble diameter at the orifice,  $L$ .

$d_{bi}$  = bubble diameter of  $i$  number of bubbles in a sample,  $L$

$d'_b$  = bubble diameter read by microscope (Uncorrected),  $L$

$d_o$  = diameter of the orifice,  $L$

$d_{vs}$  = volume surface mean diameter of bubbles,  $L$



$d_t$  = tower (column) diameter, L

$D$  = diffusivity,  $L^2T^{-1}$

$D_1$  = diffusivity of the reacting gas component into the liquid,  $L^2T^{-1}$

$D_2$  = diffusivity of the liquid-phase reactant,  $L^2T^{-1}$

$E$  = activation energy

$f_2^O$  = fugacity of pure gas at initial conditions taken as  
1 atmosphere.

$f_2^L$  = fugacity of hypothetical liquid at 1 atmosphere.

$F$  = a variable defined by equation (4.15)

$g$  = acceleration due to gravity,  $LT^{-2}$

$G$  = volumetric flow of gas,  $L^3T^{-1}$

$G_1$  = molar gas flow rate at inlet,  $mT^{-1}$

$G_2$  = molar gas flow rate at outlet,  $mT^{-1}$

$H$  = Henry's constant

$I'$  = a parameter used in the integration of the rate expression.

$K_G$  = overall gas-phase mass transfer.

$K_r$  = first or pseudo first order reaction rate constant,  $T^{-1}$

$K_R$  = reaction rate constant, units depend on the order of  
reaction.

$K_R^O$  = frequency factor

$K_L$  = liquid-side mass transfer coefficient,  $LT^{-1}$

$K_g$  = gas-side mass transfer coefficient, moles/area-time-pressure

$L$  = reactor length, L

$l$  = length of a bubble, L

$L_S$  = latent heat of solvent, cal/gm





$L_{SO}$  = latent heat of solute, cal/gm

$M$  = molecular weight, m

$M_S$  = molecular weight of solvent, m

$N$  = instantaneous rate of chemical absorption,  $\text{mL}^{-2}\text{T}^{-1}$

$\bar{N}$  = average rate of chemical absorption,  $\text{mL}^{-2}\text{T}^{-1}$

$N_b$  = total number of bubbles per unit volume of liquid

$n$  = order of reaction

$n_i$  = number of bubbles of diameter  $d_{bi}$  in a sample

$p$  = partial pressure, force/area

$P$  = total pressure, force/area

$P' = (P - V_2)$ , force/area

$P_c$  = critical pressure, force/area

$P_a$  = agitator shaft power during dispersion.

$q$  = stoichiometric coefficient

$Q$  = volumetric liquid flow rate,  $\text{L}^3\text{T}^{-1}$

$r$  = kinetic rate of reaction

$R$  = Universal gas-law constant

$S$  = Dackwert's model parameter,  $\text{T}^{-1}$

$S_1$  = a constant =  $6^{2/3}\pi^{1/3}$

$t$  = time, T

$t^*$  = total time elapsed from the moment the surface element considered has been brought to the surface, T

$t_R$  = reaction time, T

$t_D$  = diffusion time, T

$T$  = temperature,  $^{\circ}\text{K}$



$T_r$  = reduced temperature

$T_c$  = critical temperature

$U_L$  = characteristic of the liquid velocity,  $LT^{-1}$

$U_{SG}$  = superficial gas velocity,  $LT^{-1}$

$U_{SL}$  = superficial liquid velocity,  $LT^{-1}$

$U_b$  = rise velocity of a bubble,  $LT^{-1}$

$U_s$  = slip velocity,  $LT^{-1}$

$U_{L,G}$  = linear liquid or gas velocity,  $LT^{-1}$

$V_t$  = terminal velocity,  $LT^{-1}$

$V_a$  = volume of agitated mass,  $L^3$

$V_m$  = molar volume of the solute,  $L^3$

$V_1$  = vapor pressure of AcH at reactor temperature, force/area

$V_2$  = vapor pressure of AcOH at reactor temperature, force/area

$V_L$  = volume of liquid in the reactor,  $L^3$

$V_{ob}$  = volume of a bubble at the orifice,  $L^3$

$V_b$  = volume of a single bubble in the reactor,  $L^3$

$W$  = a constant defined by eqn. (4.2)

$w$  = width of a bubble,  $L$

$X$  = mole fraction in the liquid

$x$  = average inside diameter of the column, calculated  
photographically

$x'$  = solubility of gas in liquid, g-moles of gas/g-mole of liquid

$Y_{ic}$  = mole fraction of component C in the inlet gas

$Z$  = distance along the axis of the reactor,  $L$ .



$Z_f$  = the aerated liquid height

$Z_l$  = the clear liquid height

### Greek Symbols:

$\alpha$  = a variable used in equation (3.20)

$\delta$  = pore diameter, L

$\delta'_1$  &  $\delta'_2$  = solubility parameters

$\epsilon$  = fractional gas hold-up without liquid flow

$\epsilon'$  = fractional gas hold-up with liquid flow

$\xi = (C_o - C') / (C'_o - C')$

$\mu$  = viscosity,  $ML^{-1}T^{-1}$

$\mu_c$  = viscosity of continuous phase,  $ML^{-1}T^{-1}$

$\nu_L$  = kinematic viscosity of liquid,  $L^2T^{-1}$

$\rho_{l,g}$  = specific gravity of liquid and gas, respectively

$\rho_d$  = specific gravity of dispersed phase

$\sigma$  = surface tension of liquid, force/length

$\phi_1$  = association parameter

### Dimensionless Numbers:

$W_{Fr}$  = Froude number =  $u^2/g\delta$

$N_{Pe}$  = Peclet number =  $d_b U_L / D$

$N_{Re}$  = Reynold's number =  $D U_p / \mu$

$N_{Sc}$  = Schmidt number =  $\mu / \rho D$

$N_{Sh}$  = Sherwood number =  $K_L^o d_b / D$

$N_{We}$  = Weber number,  $g u^2 \rho / \sigma$



BIBLIOGRAPHY

1. Hydrocarbon Processing and Petrol. Refiner., 44, No. 11, 157, (1965).
2. McNesby, J.R. and Heller, C.A. Jr., Chem. Reviews, 54, 325, (1954).
3. Bawn, C.E.H., Hobin, T.P. and Raphael, L., Proc. Roy. Soc., 237A, 313, (1956).
4. Bawn, C.E.H., and Williamson, J.B., Trans. Farad. Soc. 47, 721, (1951).
5. Kagan, M.J., and Lubarsky, G.D., J. Phys. Chem., 39, 837, (1935).
6. Emanuel, D., and Emanuel, M., "Liquid-Phase Oxidation of Hydrocarbons", Plenum Press , New York, 1967.
7. Yau, A.Y., Hamielec, A.E., Johnson, A.I., "Co-current gas-liquid Flow Symposium", Waterloo, 607, (1969).
8. Carpenter, B.H., I & EC Proc. Des. & Dev., 4, No. 1, 105, (1965)
9. Allen, G.C., "Private Communication", Celanese Chemical Corporation, Texas.
10. Gobron, L.G., Alheritiere, L.A., CEP, 60, No. 9, 55, (1964).
11. Venugopal, B., Kumar, R., and Kuloor, N.R., I & EC Proc. Des. & Dev., 6, No. 1, 139, (1967).
12. Fair, J.R., Chem. Engg., 7, 67, (1967).
13. Vanterpool, A., "Private Communication", Chemcell Limited, Edmonton, Canada.
14. Levenspiel, O., "Chemical Reaction Engineering", John Wiley and Sons, Inc., New York, 1962.





15. Astarita, G., "Mass Transfer With Chemical Reaction", Elsevier, New York, (1967).
16. Mulcahy, M.F.R., and Watt, I.C., Proc. Roy. Soc. (London), 216A, 10 & 30, (1953).
17. Van De Vuss, J.G., Chem. Eng. Sci., 16, 21, (1961)
18. Cooper, H.R. and Melville, H.W., J. Chem. Soc., 1984, (1951).
19. Raymond, E., J. Chem. Phys., 28, 316, (1931)
20. Bowen, E.J., and Tietz, E.L., J. Chem. Soc., p. 234, (1930)
21. Mulcahy, M.F.R., and Walt, I.C., Nature, 168, 123, (1951)
22. Ingles, T.A., and Melville, H.W., Proc. Roy. Soc. (London), 218A, 175, (1953).
23. Almquist, H.J. and Branch, G.E.K., J. Am. Chem. Soc., 54, 2293, (1932).
24. Schaftlein, R.W., and Russel, T.W.F., I & EC, 60, No. 5, 12, (1968).
25. Astarita, G. and Beek, W.J., Chem. Eng. Sci., 17, 665, (1962).
26. Davidson, J.F., Harrison, D., "Fluidized Particles", Cambridge University Press, Cambridge, 1963.
27. Roseheart, R.G., Rhodes, F., Ray, W.H., "Mass Transfer With Chemical Reaction in a Gas-Liquid Co-current Flow Reactor".  
- paper presented in the 19th CICH Conference, Edmonton, 1969.
28. Baker, O., Oil and Gas Journal, 53, No. 7, 185, (1954).
29. Tong, L.S., "Boiling Heat Transfer and Two-Phase Flow", Wiley, N.Y., 1965.
30. Cichy, P.T., and Russel, T.W.F., I & EC, 61, No. 8, 6, (1969).



31. Valentine, F.H.H., "Absorption in Gas-Liquid Dispersions", E & F.N. Spon, London, 1967.
32. Datta, R.L., Napier, D.H. and Newitt, D.M., Trans. Inst. Chem. Engrs., 28, 14, (1950).
33. Hughes, R.R., others, CEP, 51, 557, (1955).
34. Coppock, P.D., and Meicklejohn, G.T., Trans. Inst. Chem. Engrs., 29, 75, (1956).
35. Benzing, R.J. and Myers, J.E., I & EC Engg. Des. & Equip., 47, 20807, (1955).
36. Leibson, I., Holcomb, E.G., Cocoso, A.G., and Jacmic, J.J., AIChE J., 2, 296, (1956).
37. Davidson, L. and Amick E.H., AIChE J., 2, 337, (1956)
38. Davidson, J.F., and Shüler, B.O.G., Trans. Inst. Chem. Engrs., 38, 335, (1960)
39. Eversale, W.G., Wagnu, G.H., and Stockhouse, E., I & EC 33, 1459, (1941).
40. Calderbank, P.H., Brit. Chem. Eng., 1, 206 & 267, (1956).
41. Perry, J.H., "Chemical Engineering Handbook", 4th Ed., McGraw Hill Co., New York.
42. Siemes, W. and Kaufman, J.F., Chem. Eng. Sci., 5, 127, (1956)
43. Rennie, J. and Evans, F., Brit. Chem. Eng., 7, 498, (1962).
44. Koide, K.T., Kiraha, T., and Kubota, H., Chem. Engg. (Japan), 30, 712, (1966).
45. Baker, J.L., and Chao, B.T., AIChE J., 11, No. 2, 269, (1965)
46. Peebles, F.N., and Garber, J., CEP, 49, No. 2, 88, (1953)



47. Galore, B., Klinzing, G.E., and Tavelarides, L.L., I & EC, 61, No. 2, 21, (1969).
48. Houghton, G., McLean, A.M., and Ritchie, P.D., Chem. Eng. Sci., 17, 40, (1957).
49. Galore, B., and Hoelscher, H.E., AIChE J., 12, No. 3, 499, (1966).
50. Ho, G.E. and Prince, R.G.H., Chem. Eng. Sci., 23, 948, (1968)
51. Calderbank, P.H. and Moo-Young, M.B., Chem. Eng. Sci., 16, 34, (1961).
52. Griffith, R.M., Chem. Eng. Sci., 12, 198, (1960).
53. Johnson, A.I., Akheta, T., Can. J. Chem. Engg., 43, 10, (1965).
54. Miller, D.N., IEC, 56, No. 10, 18, (1964).
55. Soo, S.L., "Fluid Dynamics of Multiple Systems", Blaisdell, Waltham, Mass., 1967.
56. Teller, A.J., Chem. Eng., 67, July 11, 111, (1960)
57. Hughmark, G.A., I & EC Proc. Des. & Dev., 6, (2), 218, (1967).
58. Lochiel, A.C. and Calderbank, P.H., Chem. Eng. Sci., 19, 471, (1964).
59. Sharma, M.M. and Mashelkar, R.A., paper presented in Tripartite Chemical Engineering Conference held in Montreal, Canada, September, 1968.
60. Braulick, W.J., Fair, J.R. and Lerner, B.J., AIChE J., 11, 73, (1965).



61. Yoshida, F., and Akita, K., AIChE J., 11, No. 1, 9, (1965)
62. Fair, J.R., Lambright, A.J. and Andersen, J.W., I & EC Proc. Des. & Dev., 1 No. 1, 35, (1962).
63. Nicklin, D.J., Chem. Eng. Sci., 17, 693, (1962).
64. Towell, G.D., Strand, C.P., Ackerman, G.H., "AIChE Instn. Chem. Engrs. joint meeting", London, England, June, 1965.
65. Neusen, K.F., "ASME-AIChE Heat Transfer Conference", Los Angeles, August, 1965.
66. Vermeulen, J., Williams, G.M., and Langlois, G.E., Chem. Eng. Progr., 51, 85, (1955).
67. Kalra, H. "A Reivew on Measurement of Interfacial Area" - Deptt. of Chem & Pet. Engg., University of Alberta - Term Paper, (1966).
68. Baker, O., Oil and Gas Journal, 53, 7, 185, (1954).
69. Tadao, I. & Takeya, G., Chem. Engg. (Japan), English Translation, 5, 212, (1967).
70. Marruci, G., Nicodemo, L., Chem. Engg. Sci., 22, 1257, (1967).
71. Calderbank, P.H., Trans. Inst. Chem. Engrs., 37, 173, (1959)
72. Q.V.F. Glass Manual.
73. Prausnitz, J.M., and Shair, F.M., AIChE J., 7, No. 4, 682, (1962).
74. Sitaraman, R. Ibrahim, S., and Kuloor, N.R., Journal of Chem. and Engg. Data, 8, No. 2, 198, (1963).
75. International Critical Tables, section 11-2.

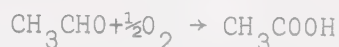




## APPENDIX A

### DERIVATION OF THE CHEMICAL REACTION RATE EXPRESSION

Assuming that the reaction in a stirred-tank reactor can be run under the kinetic regime, it is desired to derive the rate expression for a batch gas and liquid reaction:



The pressure in the reactor is maintained constant and the reaction is assumed to be a first order in oxygen and also a first order in acetaldehyde concentration.

$$\text{Hence, } \frac{db_{\text{AcH}}}{dt} = -K_R b_{\text{AcH}} \cdot P_{\text{O}_2}$$

It is assumed that the reactor contains only oxygen, acetaldehyde and acetic acid.

$$\therefore P = P_{\text{O}_2} + P_{\text{AcH}} + P_{\text{AcOH}}$$

$$\text{or, } P_{\text{O}_2} = P - P_{\text{AcH}} - P_{\text{AcOH}} = P - X_{\text{AcH}}(V_1) - X_{\text{AcOH}}(V_2)$$

where  $X_i$  = mole fraction of  $i$  in the liquid

$V_1$  = vapor pressure of AcH

$V_2$  = vapor pressure of AcOH

$b_{\text{AcH}}$  = volume % of AcH and AcOH in the liquid mixture of AcH and AcOH.

$$\therefore X_{\text{AcH}} = \frac{b_{\text{AcH}}(.78)}{44} / \left( \frac{b_{\text{AcH}}(.78)}{44} + \frac{(100-b_{\text{AcH}}) 1.05}{60} \right)$$

(specific gravity of AcH = 0.78 and specific gravity of AcOH = 1.05)

It is assumed that there is no change in volume when acetaldehyde and acetic acid are mixed.



$$\therefore X_{AcH} = \frac{1.77 \times 10^{-2} b_{AcH}}{1.77 \times 10^{-2} b_{AcH} - 1.75 \times 10^{-2} b_{AcH} + \frac{105}{60}}$$

$$= \frac{1.77 \times 10^{-2} b_{AcH}}{1.75} \approx 1.015 \times 10^{-2} b_{AcH}$$

Hence,  $p_{O_2} = P - 1.015 \times 10^{-2} b_{AcH} (V_1 - V_2) - V_2$

Substituting for  $p_{O_2}$  in the rate equation, one has

$$\frac{db_{AcH}}{dt} = -K_R b_{AcH} \{P - 1.015 \times 10^{-2} b_{AcH} (V_1 - V_2) - V_2\}$$

At a constant temperature, say  $T = 40^\circ\text{C}$ ,  $V_1 = 26$  psia,  $V_2 = 0.657$  psia

$$\therefore \frac{db_{AcH}}{dt} = -K_R b_{AcH} \{P - 0.266 b_{AcH} - 0.657\}$$

$$= -K_R b_{AcH} \{(P - 0.657) - 0.266 b_{AcH}\}$$

$$= -K_R b_{AcH} (P' - 0.266 b_{AcH})$$

where  $P' = P - V_2 = P - 0.657$

Integrating the above equation, one has,

$$\int_{b_0}^b \frac{db_{AcH}}{b_{AcH} (P' - 0.266 b_{AcH})} = \int_0^t -K_R dt$$

$$\text{or, } \frac{1}{P'} \int_{b_0}^b \left( \frac{1}{b_{AcH}} + \frac{0.266}{P' - 0.266 b_{AcH}} \right) db_{AcH} = -K_R t$$

$$\text{or, } \frac{1}{P'} \left\{ \ln \frac{P' - 0.266 b_{AcH}}{b_{AcH}} \right\}_{b_0}^{b_{AcH}} = K_R t$$



$$\text{or, } \ln \left( \frac{P' - 0.266b_{\text{AcH}}}{P' - 0.266b_{\text{AcH}}^{\circ}} \right) \left( \frac{b_{\text{AcH}}^{\circ}}{b_{\text{AcH}}} \right) = K_R t P'$$

In general at any temperature,

$$\ln \left\{ \frac{P' - 1.015 \times 10^{-2} (V_1 - V_2) b_{\text{AcH}}}{P' - 1.015 \times 10^{-2} (V_1 - V_2) b_{\text{AcH}}^{\circ}} \right\} \left\{ \frac{b_{\text{AcH}}^{\circ}}{b_{\text{AcH}}} \right\} = K_R t P'$$

#### Determination of Solubility of Oxygen in Acetic Acid:-

Solubility of oxygen in acetic acid is not available in the literature and the following equation proposed by Shair and Prausnitz (73) was used to estimate it, using the solubility of nitrogen in acetic acid (to get the solubility parameter for acetic acid) at 25°C and atmosphere pressure as 0.109 cc N<sub>2</sub> per cc liquid (75).

$$\frac{1}{x'_2} = \frac{f_2^L}{f_2^O} \exp \left\{ \frac{V_m (\delta'_1 - \delta'_2)^2 \phi_1^2}{RT} \right\}$$

where  $f_2^L$  = fugacity of hypothetical liquid at 1 atm.

$f_2^O$  = fugacity of pure gas at initial conditions taken as 1 atmosphere

$P_c$  = critical pressure

$\delta'_1, \delta'_2$  = solubility parameters

$\phi_1$  = association parameter

$V_m$  = molar volume of solute

$x'_2$  = solubility of gas in liquid.

#### Acetic Acid

CH<sub>3</sub>COOH,  $\rho_{25^\circ\text{C}} = 1.05 \text{ gms/cc}$ ;  $M = 60.05$



Nitrogen

$$\text{Solubility} = 0.109 \frac{\text{cc N}_2}{\text{cc liquid}}$$

∴ Solubility of nitrogen in mole fraction,

$$x' = \frac{0.109 \times 60.05}{2.24 \times 10^4 \times 1.044} \frac{\text{gm-mole N}_2}{\text{gm-mole AcOH}} = 2.79 \times 10^{-4}$$

$$\text{At } 25^\circ\text{C}, RT = 1.9872 \times 298.15 = 592.5 \text{ cal/gm-mole}$$

$$\text{For Nitrogen, } V_m = 32.4, T_c = 126.2^\circ\text{K}, T_r = \frac{298.15}{126.2} = 2.36$$

$$\delta'_2 = 2.58, f_2^L/P_c = 6.5$$

$$\therefore f_2^L = 6.5 \times 33.5 = 218 \text{ atm.}$$

$$\text{For Oxygen, } T_c = 154.4^\circ\text{K}, T_r = \frac{298.15}{154.4} = 1.93,$$

$$\delta'_2 = 4.0, f_2^L/P_c = 5.5$$

$$\therefore f_2^L = 5.5 \times 49.7 = 273 \text{ atm.}$$

Nitrogen

$$\frac{1}{2.79 \times 10^{-4}} = 218 \exp \left\{ \frac{32.4(\delta'_1 - \delta'_2)^2}{592.5} \right\}$$

$$\therefore \delta'_1 - \delta'_2 = 7.16; \delta'_1 = 7.16 + 2.58 = 9.74$$

where  $\delta'_1$  is the solubility parameter for acetic acid.

For Oxygen at  $25^\circ\text{C}$ 

$$\frac{1}{x'_2} = 273 \text{ atm} \exp \left\{ \frac{33}{592.5} (9.74 - 4.0)^2 \right\}$$

$$\therefore x'_2 = 5.83 \times 10^{-4} \text{ gm mole O}_2/\text{gm mole AcOH}$$





For  $O_2$  at  $40^\circ C$ ,  $RT = 1.987 \times 313 = 622$

$$T_r = \frac{313}{154.4} = 2.02; f_2^L = 5.8 \times 49.7 = 288 \text{ atm.}$$

$$\frac{1}{x_2'} = 288 \exp \left\{ \frac{33(5.74)^2}{622} \right\}$$

$$\therefore x_2' = 6.04 \times 10^{-4} \text{ gm mole } O_2 / \text{gm-mole AcOH}$$

Henry's Law:  $P = x_2' H$

$$\therefore H = \frac{1 \text{ atm}}{6.04 \times 10^{-4} \text{ g mole } O_2 / \text{g mole AcOH}} = 1660 \text{ atm} / \frac{\text{g mole } O_2}{\text{g mole AcOH}}$$

At 34.7 psia

$$x_2' = \frac{P_{O_2}}{H} = \frac{34.7}{14.7 \times 1660} = 1.42 \times 10^{-3} \frac{\text{g mole } O_2}{\text{g mole AcOH}}$$

$\therefore$  Solubility of oxygen at 34.7 psia and  $40^\circ C$

$$= 1.42 \times 10^{-3} \frac{\text{moles } O_2}{\text{mole AcOH}} \times \frac{1 \text{ mole}}{60.05 \text{ gm}} \times 1.05 \frac{\text{gms}}{\text{cc}}$$

$$= 2.425 \times 10^{-5} \text{ moles } O_2 / \text{cc solution}$$

$$C_{O_2} = \frac{P_{O_2}}{H} \times \frac{1.0271}{60.05} \frac{\text{g moles } O_2}{\text{cc solution}}$$

$$\therefore P_{O_2} = C_{O_2} \times \frac{1660 \times 14.7 \times 60.05}{1.05}$$

$$P_{O_2} = 1.423 \times 10^6 C_{O_2} \text{ psia}$$

#### Diffusivity of Oxygen in Acetic Acid:-

The following equation, proposed by Sitaraman, Ibrahim and Kuloor

(74) appears to be the best for estimating the diffusivity:



$$D = 5.4 \times 10^{-8} \left\{ \frac{M_S^{1/2} L_S^{1/2} T}{\mu_S V_m^{0.5} L_{SO}^{0.3}} \right\}^{0.93}$$

where  $D$  = diffusion coefficient,  $\text{cm}^2/\text{sec}$

$\mu_S$  = viscosity of solvent, cp

$V_m$  = molecular volume of solute,  $\text{ccs/g-mole}$

$M_S$  = molecular weight of solvent

$L_S$  = latent heat of vaporisation of solvent at normal boiling point, cal/gm.

$L_{SO}$  = latent heat of solute, cal/gm.

Here,  $T = 273 + 40^\circ\text{C} = 313^\circ\text{K}$

$M_S = 60$

$\mu = 0.98$  cp (41)

$L_S = 96.75$  cal/gm (41)

$V_m$  = molecular volume of  $\text{O}_2 = 25.6 \text{ cm}^3/\text{gm}$

$L_{SO} = 50.8$  cal/gm

$$\therefore D_{\text{O}_2 - \text{AcOH}} = 5.4 \times 10^{-8} \left\{ \frac{M_S^{1/2} L_S^{1/3} T}{\mu_S V_m^{0.5} L_{SO}^{0.3}} \right\}^{0.93}$$

$$= 5.4 \times 10^{-8} \left\{ \frac{7.75(4.57)(313)}{0.98(5.05)(3.25)} \right\}^{0.93}$$

$$D_{\text{O}_2 - \text{AcOH}} = 2.35 \times 10^{-5} \text{ cm}^2/\text{sec}$$

#### Determination of the Reaction Regime

$T = 40^\circ\text{C}$ ,  $P = 34.7$  psia, Catalyst concentration = 140 ppm

$$K_R = 3.46 \times 10^{-3} \text{ l/psia.min}$$



Initial concentration of acetaldehyde = 10 vol % = 0.00177 g mole/  
cc solution.

$$H = 1.423 \times 10^6 \text{ psi/gm-mole } O_2/\text{cc solution.}$$

$$\therefore r_{O_2} = \frac{1}{2} \frac{db_{AcH}}{dt} = \frac{-3.46 \times 10^{-3} \times 1.423 \times 10^6 C_{O_2} b_{AcH}}{2}$$

$$\therefore \frac{dC_{O_2}}{dt} = -2.46 \times 10^3 C_{O_2} b_{AcH}$$

$\therefore$  Initial rate (pseudo first order in  $O_2$ )

$$\frac{dC_{O_2}}{dt} = -2.46 \times 10^3 \times 1.77 \times 10^{-3} C_{O_2} = -4.36 C_{O_2} \therefore K_r = 4.36 \text{ min}^{-1}$$

$$\therefore t_R = \frac{1}{K_r} = \frac{1}{4.36} \text{ min} = 13.8 \text{ sec}$$

$$t_D = \frac{1}{(K_L^O)^2}$$

$$(1) \text{ For } K_L^O = 0.0065 \text{ cm/sec, } t_D = \frac{2.35 \times 10^{-5}}{(0.0065)^2} = 0.554 \text{ sec.}$$

$$\therefore t_D \ll t_R$$

$$(2) \text{ For } K_L^O = 0.0433 \text{ cm/sec, } t_D = \frac{2.35 \times 10^{-5}}{(0.0433)^2} \text{ sec} = 0.0125 \text{ sec}$$

$$\therefore t_D \ll t_R$$

Hence, the operation is in slow reaction regime.

















APPENDIX B

TABLE B.1

THE EFFECT OF AGITATION ON REACTION RATE

P = Pressure = 24.7 psia

T = Temperature = 50°C

AcH = 50 ccs, AcOH = 450 ccs.

Catalyst = 17 mgs = 140 ppm ( $Mn^{++}$  in AcH)

| Run Number | Stirrer RPM | Time<br>(Mins) | Volume % AcOH |
|------------|-------------|----------------|---------------|
| 1          | 2135        | 0              | 90.5          |
|            |             | 5              | 95.0          |
|            |             | 10             | 96.9          |
|            |             | 15             | 97.4          |
|            |             | 25             | 100.0         |
| 2          | 1125        | 0              | 90.5          |
|            |             | 5              | 94.2          |
|            |             | 10             | 96.1          |
|            |             | 21             | 98.5          |
|            |             | 25             | 98.8          |
|            |             | 40             | 100.0         |
|            |             | 75             | 100.0         |

Cont'd.



TABLE B.1 CONTINUED

| Run Number | Stirrer RPM | Time<br>(Mins) | Volume % AcOH |
|------------|-------------|----------------|---------------|
| 3          | 2910        | 0              | 90.5          |
|            |             | 5              | 93.9          |
|            |             | 10             | 95.1          |
|            |             | 15             | 95.7          |
|            |             | 25             | 97.9          |
|            |             | 40             | 98.5          |
|            |             | 60             | 100.0         |
| 4          | 600         | 0              | 90.5          |
|            |             | 5              | 91.3          |
|            |             | 12             | 91.6          |
|            |             | 17             | 92.2          |
|            |             | 25             | 92.4          |
|            |             | 40             | 93.6          |
|            |             | 60             | 97.1          |
|            |             | 90             | 100.0         |
| 5          | 1600        | 0              | 90.5          |
|            |             | 5              | 97.1          |
|            |             | 11             | 98.8          |
|            |             | 18             | 99.4          |
|            |             | 25             | 100.0         |
|            |             | 40             | 100.0         |

Cont'd.





TABLE B.1 CONTINUED

| Run Number | Stirrer RPM                      | Time<br>(Mins) | Volume % AcOH |
|------------|----------------------------------|----------------|---------------|
| 6          | 1125<br>(Reproducibility<br>Run) | 0              | 90.5          |
|            |                                  | 5              | 94.2          |
|            |                                  | 10             | 96.6          |
|            |                                  | 15             | 98.0          |
|            |                                  | 25             | 100.0         |
|            |                                  | 40             | 100.0         |



TABLE B.2

THE EFFECT OF AGITATION ON REACTION RATE

P = 34.7 psia

T = 50°C

AcH = 50 ccs, AcOH = 450 ccs

Catalyst = 17 mgms = 140 ppm

| Run Number | Stirrer RPM | Time<br>(Mins) | Volume % AcOh |
|------------|-------------|----------------|---------------|
| 7          | 1600        | 0              | 90.5          |
|            |             | 5              | 98.5          |
|            |             | 10             | 99.1          |
|            |             | 15             | 99.4          |
|            |             | 20             | 100.0         |
| 8          | 2135        | 0              | 90.7          |
|            |             | 5              | 98.2          |
|            |             | 10             | 98.8          |
|            |             | 15             | 99.4          |
|            |             | 20             | 99.7          |
| 9          | 2190        | 25             | 100.0         |
|            |             | 0              | 91.3          |
|            |             | 5              | 97.1          |
|            |             | 10             | 98.8          |
|            |             | 15             | 99.1          |
|            |             | 20             | 99.4          |
|            |             | 25             | 99.7          |
|            |             | 30             | 100.0         |



TABLE B.3

THE EFFECT OF AGITATION ON REACTION RATE

P = 44.7 psia

T = 50°C

AcH = 50 ccs, AcOH = 450 ccs.

Catalyst = 17 mgms = 140 ppm

| Run Number | Stirrer RPM | Time<br>(Mins) | Volume % AcOH |
|------------|-------------|----------------|---------------|
| 10         | 2135        | 0              | 90.5          |
|            |             | 3              | 98.0          |
|            |             | 5              | 99.4          |
|            |             | 10             | 99.7          |
|            |             | 15             | 100.0         |
| 11         | 2910        | 0              | 90.7          |
|            |             | 3              | 97.6          |
|            |             | 5              | 99.4          |
|            |             | 10             | 99.7          |
|            |             | 15             | 100.0         |
| 12         | 1600        | 0              | 90.5          |
|            |             | 5              | 98.2          |
|            |             | 10             | 98.8          |
|            |             | 15             | 99.1          |
|            |             | 20             | 99.5          |
|            |             | 25             | 100.0         |



TABLE B.4

THE EFFECT OF SAMPLE SIZE AND AGITATION ON REACTION RATE

P = 24.7 psia

T = 50°C

Catalyst = 140 ppm

AcOH = 900 ccs, AcH = 100 ccs

Total Reaction Mixture = 1000 ccs

| Run Number | Stirrer RPM | Time<br>(Mins) | Volume % AcOH |
|------------|-------------|----------------|---------------|
| 13         | 1600        | 0              | 90.5          |
|            |             | 5              | 96.9          |
|            |             | 10             | 98.1          |
|            |             | 15             | 98.8          |
|            |             | 25             | 100.0         |
|            |             | 40             | 100.0         |
| 14         | 2135        | 0              | 90.5          |
|            |             | 5              | 96.0          |
|            |             | 10             | 96.5          |
|            |             | 15             | 96.7          |
|            |             | 30             | 97.5          |
|            |             | 45             | 98.6          |
|            |             | 90             | 100.0         |





TABLE B.5

EFFECT OF TEMPERATURE ON REACTION RATE

P = 34.7 psia

RPM = 1600

Catalyst Concn. = 140 ppm.

| Run Number | Temperature | Time<br>(Mins) | Volume % AcOH |
|------------|-------------|----------------|---------------|
| 15         | 40°C        | 0              | 90.5          |
|            |             | 5              | 95.0          |
|            |             | 10             | 97.0          |
|            |             | 15             | 98.5          |
|            |             | 20             | 99.1          |
|            |             | 25             | 99.4          |
|            |             | 30             | 99.7          |
|            |             | 35             | 100.0         |
| 16         | 30°C        | 0              | 90.5          |
|            |             | 5              | 93.0          |
|            |             | 10             | 94.9          |
|            |             | 15             | 96.8          |
|            |             | 20             | 97.7          |
|            |             | 30             | 98.5          |
|            |             | 40             | 99.0          |
|            |             | 50             | 99.7          |
|            |             | 60             | 100.0         |



TABLE B.6

THE EFFECT OF CATALYST CONCENTRATION ON REACTION RATE

P = 34.7 psia

T = 40°C

RPM = 1600

| Run Number | Catalyst ppm | Time<br>(Mins) | Volume % AcOH |
|------------|--------------|----------------|---------------|
| 17         | 83           | 0              | 90.5          |
|            |              | 5              | 94.0          |
|            |              | 10             | 96.5          |
|            |              | 15             | 97.1          |
|            |              | 20             | 97.7          |
|            |              | 30             | 98.2          |
|            |              | 35             | 98.8          |
|            |              | 40             | 99.4          |
|            |              | 45             | 99.7          |
|            |              | 50             | 100.0         |
| 18         | 249          | 0              | 90.5          |
|            |              | 5              | 97.5          |
|            |              | 10             | 99.4          |
|            |              | 15             | 99.7          |
|            |              | 20             | 100.0         |



TABLE B.7

CHECK OF THE REPRODUCIBILITY

T = 40°C

P = 34.7 psia

RPM = 1600

| Run Number | Time<br>(Mins) | Volume % AcOH | Volume % AcH | Comments  |
|------------|----------------|---------------|--------------|---|
| 19         | 0              | 90.5          | 9.5          | Check the<br>Reproducibility<br>of Run Number<br>15 |
|            | 5              | 94.8          | 5.2          |   |
|            | 10             | 97.1          | 2.9          |   |
|            | 15             | 98.6          | 1.4          |   |
|            | 20             | 99.1          | 0.9          |   |
|            | 25             | 99.4          | 0.6          |   |
|            | 35             | 100.0         | 0.0          |   |



TABLE B.7'  
THE CATALYST ACTIVITY

$T = 40^{\circ}\text{C}$

$P = 34.7 \text{ psia}$

Catalyst = 140 ppm

$b_{\text{AcH}}^{\circ} = 20\% \text{ by volume}$

RPM = 1600

| Run Number | Time<br>(Mins) | Volume % AcOH | Comments             |
|------------|----------------|---------------|----------------------|
| 20         | 0              | 80.5          |                      |
|            | 5              | 89.0          |                      |
|            | 10             | 93.0          |                      |
|            | 15             | 96.7          |                      |
|            | 20             | 98.3          |                      |
|            | 25             | 98.8          |                      |
|            | 35             | 99.4          |                      |
|            | 40             | 100.0         |                      |
| 21         | 0              | 80.5          | AcOH formed above in |
|            | 5              | 86.7          | Run No. 20 was used, |
|            | 10             | 90.5          | Fresh AcH was used   |
|            | 15             | 91.5          | and make-up catalyst |
|            | 25             | 92.5          | was added to bring   |
|            | 35             | 93.0          | the catalyst concn.  |
|            | 50             | 93.6          | to 140 ppm.          |





TABLE B.8

THE EFFECT OF AcH AND O<sub>2</sub> CONCENTRATIONS ON REACTION RATE

$P = 24.7 \text{ psia}$ ,  $T = 50^\circ\text{C}$ ,  $V_2 = 1.045 \text{ psia}$ ,  $V_1 = 34 \text{ psia}$ ,  $P' = P - V_2 = (24.7 - 1.045)$   
 $= 23.655 \text{ psia}$ ,  $V_1 - V_2 = 32.955 \text{ psia}$

$\therefore 1.015 \times 10^{-2} (32.955) = 0.334 \text{ psia}$ ;  $b_{\text{AcH}}^\circ = 9.5\%$

$$\text{Rate Equation: } \ln \left( \frac{P' - 0.334 b_{\text{AcH}}}{b_{\text{AcH}}} \cdot \frac{b_{\text{AcH}}^\circ}{P' - 0.334 b_{\text{AcH}}^\circ} \right) = K.t.P'$$

$$\frac{b_{\text{AcH}}^\circ}{P' - 0.334 b_{\text{AcH}}^\circ} = \frac{9.5}{23.655 - 0.334(9.5)} = 0.46$$

$$\text{or, } \ln \left\{ \frac{(P' - 0.334 b_{\text{AcH}})}{b_{\text{AcH}}} \cdot (0.46) \right\} = Kt.P'$$

Catalyst = 140 ppm

| Run No. | Time (Mins) | $b_{\text{AcOH}}$ | $b_{\text{AcH}}$ | $0.334 b_{\text{AcH}}$ | $\frac{P' - 0.334 b_{\text{AcH}}}{b_{\text{AcH}}}$ | $\frac{P' - 0.334 b_{\text{AcH}}^\circ}{b_{\text{AcH}}^\circ}$ | $\ln \frac{P' - 0.334 b_{\text{AcH}}}{b_{\text{AcH}}} \cdot \frac{b_{\text{AcH}}^\circ}{P' - 0.334 b_{\text{AcH}}^\circ}$ | $t.P'$  |
|---------|-------------|-------------------|------------------|------------------------|--|--|---|---------|
| 5       | 2           | 94.6              | 5.4              | 1.80                   | 21.855   | 1.861  | 0.62  | 47.31   |
|         | 5           | 96.8              | 3.2              | 1.07                   | 22.585   | 3.246  | 1.175   | 118.272 |
|         | 8           | 98.0              | 2.0              | 0.668                  | 22.987   | 5.29   | 1.665   | 189.24  |
|         | 10          | 98.5              | 1.5              | 0.50                   | 23.155   | 7.162  | 1.968   | 236.55  |
|         | 13          | 99.1              | 0.9              | 0.30                   | 23.355   | 11.936   | 2.48  | 307.515 |
|         | 15          | 99.3              | 0.7              | 0.234                  | 23.421   | 15.390   | 2.72  | 354.82  |
|         | 18          | 99.6              | 0.4              | 0.134                  | 23.521   | 27.047   | 3.29  | 425.79  |
|         | 20          | 99.75             | 0.25             | 0.0835                 | 23.571   | 43.368   | 3.77  | 473.10  |
|         | 22.5        | 99.9              | 0.10             | 0.0334                 | 23.621   | 108.650  | 4.68  | 532.24  |



TABLE B.9

THE EFFECT OF AcH and O<sub>2</sub> CONCENTRATIONS ON REACTION RATE

$$P = 34.7 \text{ psia}, T = 50^{\circ}\text{C} \quad P' = 34.7 - 1.045 = 33.655 \text{ psia}$$

$$b_{\text{AcH}}^{\circ} = 9.5$$

$$\therefore \frac{b_{\text{AcH}}^{\circ}}{P' - 0.334 b_{\text{AcH}}^{\circ}} = \frac{9.5}{33.655 - 3.17} = 0.312$$

$$\ln \left\{ \frac{P' - 0.334 b_{\text{AcH}}^{\circ}}{b_{\text{AcH}}} (0.23) \right\} = KtP'$$

Catalyst = 140 ppm

| Run No. | Time (Mins) | $b_{\text{AcOH}}$ | $b_{\text{AcH}}$ | $0.334 b_{\text{AcH}}$ | $P_0 = \frac{P' - 0.334 b_{\text{AcH}}}{b_{\text{AcH}}}$ | $P_0 (.312)$<br>$\frac{P_0}{b_{\text{AcH}}}$ | $P_0 (.23)$<br>$\ln \frac{P_0}{b_{\text{AcH}}}$ | $t \cdot P'$ |
|---------|-------------|-------------------|------------------|------------------------|--|--|---|--------------|
| 7       | 2           | 96.5              | 3.5              | 1.169                  | 32.486   | 2.895  | 1.063   | 67.310       |
|         | 5           | 98.5              | 1.5              | 0.501                  | 33.154   | 6.895  | 1.93  | 168.275      |
|         | 7           | 98.8              | 1.2              | 0.400                  | 33.255   | 8.646  | 2.16  | 235.585      |
|         | 10          | 99.1              | 0.9              | 0.300                  | 33.355   | 11.563                                       | 2.44  | 336.55       |
|         | 13          | 99.4              | 0.6              | 0.20                   | 33.455   | 17.395                                       | 2.85  | 437.51       |
|         | 15          | 99.6              | 0.4              | 0.133                  | 33.522   | 26.145                                       | 3.26  | 504.825      |
|         | 17          | 99.75             | 0.25             | 0.083                  | 33.572   | 41.896                                       | 3.73  | 572.135      |
|         | 19          | 99.9              | 0.10             | 0.0334                 | 33.622   | 104.490                                      | 4.69  | 639.44       |



TABLE B.10

THE EFFECT OF AcH and O<sub>2</sub> CONCENTRATIONS ON REACTION RATE

P = 44.7 psia, T = 50°C, 140 ppm, 2135 RPM

$b_{AcH}^0 = 5\%$

$$\frac{b_{AcH}^0}{P' - .334 b_{AcH}^0} = \frac{5}{43.655 - .334(5)} = \frac{5}{41.985} = .119$$

| Run No. | Time (Mins) | $b_{AcOH}$ | $b_{AcH}$ | $0.334 b_{AcH}$ | $P_{O_2} - P' - .334 b_{AcH}$ | $\frac{P_{O_2} (.119)}{b_{AcH}}$ | $\ln \frac{P_{O_2} (.119)}{b_{AcH}}$ | t.p'   |
|---------|-------------|------------|-----------|-----------------|-------------------------------|----------------------------------|--------------------------------------|--------|
| 10      | 0.0         | 95         | 5         | 1.67            | 41.985                        | 1.0                              | 0                                    | 0      |
|         | 0.5         | 96         | 4         | 1.337           | 42.318                        | 1.26                             | 0.231                                | 21.8   |
|         | 1.0         | 97         | 3         | 1.00            | 42.655                        | 1.69                             | 0.525                                | 43.655 |
|         | 1.7         | 98         | 2         | 0.668           | 42.987                        | 2.56                             | 0.94                                 | 74.2   |
|         | 3.7         | 99         | 1         | 0.334           | 43.321                        | 5.16                             | 1.64                                 | 161.5  |
|         | 5.7         | 99.4       | 0.6       | 0.20            | 43.455                        | 8.62                             | 2.155                                | 249.0  |
|         | 7.0         | 99.6       | 0.4       | 0.134           | 43.521                        | 12.95                            | 2.56                                 | 306.0  |
|         | 9.7         | 99.8       | 0.2       | 0.0668          | 43.588                        | 25.9                             | 3.26                                 | 424.0  |



TABLE B.11

THE EFFECT OF TEMPERATURE ON REACTION RATE

$P = 34.7$  psia, Catalyst = 140 ppm,  $T = 40^{\circ}\text{C}$ ,  $V_1 = 26$  psia,  $V_2 = 0.657$  psia,

$V_1 - V_2 = 25.347$  psia,  $P' = 34.7 - 0.657 = 34.043$  psia

$$\therefore 1.015 \times 10^{-2} (V_1 - V_2) = 1.015 \times 10^{-2} (25.347) = 0.258$$

$$b_{\text{AcH}}^{\circ} = 9.5$$

$$\therefore \frac{b_{\text{AcH}}^{\circ}}{P' - 0.258 b_{\text{AcH}}^{\circ}} = \frac{9.5}{31.493}$$

$$\ln \left\{ \frac{P' - 0.258 b_{\text{AcH}}^{\circ}}{b_{\text{AcH}}^{\circ}} (0.302) \right\} = Kt \cdot P' = 0.302$$

| Run No. | Time (Mins) | $b_{\text{AcOH}}$ | $b_{\text{AcH}}$ | $.258 b_{\text{AcH}}$ | $P_2 = P' - .258 b_{\text{AcH}}$ | $P_2 (.302) = \frac{P_2 (.302)}{b_{\text{AcH}}}$ | $P_2 (.302) = \ln \frac{P_2 (.302)}{b_{\text{AcH}}}$ | $t \cdot P'$ |
|---------|-------------|-------------------|------------------|-----------------------|----------------------------------|--|--|--------------|
| 15      | 5           | 95.0              | 5.0              | 1.290                 | 32.753                           | 1.978  | 0.682  | 170.215      |
|         | 10          | 96.5              | 3.5              | 0.903                 | 33.140                           | 2.859  | 1.05   | 340.43       |
|         | 15          | 98.5              | 1.5              | 0.387                 | 33.656                           | 6.776  | 1.91   | 510.645      |
|         | 20          | 99.1              | 0.9              | 0.232                 | 33.811                           | 11.344   | 2.43   | 680.86       |
|         | 25          | 99.4              | 0.6              | 0.154                 | 33.889                           | 17.056   | 2.84   | 851.075      |
|         | 30          | 99.7              | 0.3              | 0.077                 | 33.966                           | 34.190   | 3.53   | 1021.290     |





TABLE B.12

THE EFFECT OF TEMPERATURE ON REACTION RATE

$P = 34.7$  psia, Catalyst = 140 ppm,  $T = 30^{\circ}\text{C}$ ,  $V_1 = 20$  psia,  $V_2 = 0.387$  psia,

$V_1 - V_2 = 19.613$  psia,  $P' = P - V_2 = 34.7 - 0.387 = 34.313$  psia

$\therefore 1.015 \times 10^{-2}(V_1 - V_2) = 1.015 \times 10^{-2}(19.613) = 0.199$  psia

$$b_{\text{AcH}}^0 = 9.5; \quad \frac{b_{\text{AcH}}^0}{P' - 0.199 b_{\text{AcH}}} = \frac{9.5}{34.313 - 1.89} = 0.294$$

$$\ln \left\{ \frac{P' - 0.199 b_{\text{AcH}}}{b_{\text{AcH}}} (0.294) \right\} = K.t.P'$$

| Run No. | Time (Mins) | $b_{\text{AcOH}}$ | $b_{\text{AcH}}$ | $0.199 b_{\text{AcH}}$ | $P_0 = P' - 0.199 b_{\text{AcH}}$ | $\frac{P_0 (0.294)}{b_{\text{AcH}}}$ | $\ln \frac{P_0 (0.294)}{b_{\text{AcH}}}$ | $t.P'$ |
|---------|-------------|-------------------|------------------|------------------------|-----------------------------------|--------------------------------------|--|--------|
| 16      | 5           | 93.0              | 7                | 1.393                  | 32.920                            | 1.382                                | 0.323                                    | 170.2  |
|         | 10          | 95.0              | 5.0              | 0.995                  | 33.318                            | 1.959                                | 0.672                                    | 340.5  |
|         | 15          | 96.6              | 3.4              | 0.676                  | 33.637                            | 2.908                                | 1.07                                     | 515    |
|         | 20          | 97.6              | 2.4              | 0.477                  | 33.836                            | 4.144                                | 1.42                                     | 682    |
|         | 25          | 98.15             | 1.85             | 0.368                  | 33.945                            | 5.40                                 | 1.68                                     | 857    |
|         | 30          | 98.6              | 1.4              | 0.278                  | 34.035                            | 7.147                                | 1.965                                    | 1022   |
|         | 35          | 98.9              | 1.1              | 0.218                  | 34.095                            | 9.111                                | 2.21                                     | 1200   |
|         | 40          | 99.2              | 0.8              | 0.159                  | 34.154                            | 12.551                               | 2.53                                     | 1367   |



TABLE B.13

THE EFFECT OF CATALYST CONCENTRATION ON REACTION RATE

$P = 34.7$  psia,  $T = 40^{\circ}\text{C}$ , Catalyst = 83 ppm,  $V_1 = 26$  psia,  $V_2 = 0.657$  psia,

$V_1 - V_2 = 25.347$  psia,  $P' = 34.7 - 0.657 = 34.043$  psia

$$\therefore 1.015 \times 10^{-2} (V_1 - V_2) = 1.015 \times 10^{-2} (25.347) = 0.258$$

$$b_{\text{AcH}}^{\circ} = 9.5, \therefore \frac{b_{\text{AcH}}^{\circ}}{P' - 0.258 b_{\text{AcH}}^{\circ}} = \frac{9.5}{31.493} = 0.302$$

$$\ln \left\{ \frac{P' - 0.258}{b_{\text{AcH}}} (0.302) \right\} = K t P'$$

| Run No. | Time (Mins) | $b_{\text{AcOH}}$ | $b_{\text{AcH}}$ | $.258 b_{\text{AcH}}$ | $P_0 = \frac{P' - .258 b_{\text{AcH}}}{b_{\text{AcH}}}$ | $\frac{P_0 (.302)}{b_{\text{AcH}}}$ | $\ln \frac{P_0 (.302)}{b_{\text{AcH}}}$ | $t \cdot P'$ |
|---------|-------------|-------------------|------------------|-----------------------|---|-------------------------------------|---|--------------|
| 17      | 5           | 94.0              | 6.0              | 1.548                 | 32.495  | 1.635                               | 0.492                                   | 170.2        |
|         | 10          | 96.3              | 3.7              | 0.954                 | 33.089  | 2.700                               | 0.992                                   | 340.5        |
|         | 15          | 97.1              | 2.9              | 0.748                 | 33.295  | 3.467                               | 1.24                                    | 511.0        |
|         | 20          | 97.7              | 2.3              | 0.593                 | 33.450  | 4.391                               | 1.48                                    | 682          |
|         | 25          | 98.2              | 1.8              | 0.464                 | 33.579  | 5.633                               | 1.73                                    | 852          |
|         | 30          | 98.6              | 1.4              | 0.361                 | 33.682  | 7.265                               | 1.98                                    | 1022         |
|         | 35          | 98.9              | 1.1              | 0.283                 | 33.76   | 9.268                               | 2.22                                    | 1192         |
|         | 40          | 99.35             | 0.65             | 0.167                 | 33.876  | 15.738                              | 2.76                                    | 1365         |



TABLE B.14

THE EFFECT OF CATALYST CONCENTRATION ON REACTION RATE

P = 34.7 psia, T = 40°C, Catalyst = 249 ppm, P' = 34.043 psia

$$b_{\text{AcH}}^{\circ} = 9.5\% \therefore \frac{b_{\text{AcH}}^{\circ}}{P' - 0.258 b_{\text{AcH}}^{\circ}} = \frac{9.5}{31.493} = 0.302$$

| Run No. | Time (Mins) | $b_{\text{AcOH}}$ | $b_{\text{AcH}}$ | $0.258 b_{\text{AcH}}$ | $P_2 = \frac{P_2}{P' - 0.258 b_{\text{AcH}}}$ | $\frac{P_2(.302)}{b_{\text{AcH}}}$ | $\ln \frac{P_2(.302)}{b_{\text{AcH}}}$ | t.P'  |
|---------|-------------|-------------------|------------------|------------------------|---|------------------------------------|--|-------|
| 18      | 0           | 90.5              | 9.5              | 2.45                   | 31.593  | 1                                  | 0                                      | 0     |
|         | 2.5         | 95.5              | 4.5              | 1.16                   | 32.883  | 2.2                                | 0.79                                   | 85.2  |
|         | 5           | 97.5              | 2.5              | 0.645                  | 33.398  | 4.07                               | 1.395                                  | 170.2 |
|         | 7.5         | 98.5              | 1.5              | 0.387                  | 33.656  | 6.75                               | 1.91                                   | 255.0 |
|         | 10          | 99.15             | 0.85             | 0.22                   | 33.823  | 11.3                               | 2.43                                   | 340.5 |
|         | 15          | 99.65             | 0.35             | 0.090                  | 33.953  | 29.4                               | 3.38                                   | 510.0 |



TABLE B.15

COMPARISON OF THE PREDICTED AND EXPERIMENTAL RESULTS

$$P' = 34.043 \text{ psia}$$

$$K_R = 3.46 \times 10^{-3} \text{ at } 40^\circ\text{C}, 34.7 \text{ psia, 140 ppm}$$

$$P' \cdot K_R = 0.118$$

| Source     | Volume %<br>of AcH | $\ln \frac{P_{O_2}(.302)}{b_{AcH}}$ | Experi-<br>mental<br>'t'<br>(Mins) | Calculated 't',<br>$\ln \frac{P_{O_2}(.302)}{b_{AcH}} \cdot \frac{P' \cdot K_R}{P}$ (Mins) |
|------------|--------------------|-------------------------------------|------------------------------------|--|
| Run No. 15 | 9.5                | 0                                   | 0                                  | 0  |
| and        | 5                  | 0.683                               | 5                                  | 5.85   |
| table B.11 | 3.5                | 1.05                                | 10                                 | 8.90   |
|            | 1.5                | 1.91                                | 15                                 | 16.7   |
|            | 0.9                | 2.43                                | 20                                 | 20.6   |
|            | 0.6                | 2.84                                | 25                                 | 24.1   |
|            | 0.3                | 3.53                                | 30                                 | 29.9   |





TABLE B.16

OXYGEN FLOW RATE VS FRACTIONAL GAS HOLD-UP

P = 20 psig, T = 40°C

| Observation<br>No. | O <sub>2</sub> Flow<br>Rate at<br>40°C and<br>34.7 psia,<br>ccs/sec. | Z <sub>L</sub><br>cm. | Z <sub>F</sub><br>cm. | Z <sub>F</sub> -Z <sub>L</sub><br>cm | $\alpha = \frac{Z_F - Z_L}{Z_F}$ | H <sub>2</sub> O<br>cm/<br>sec. | 1.3911<br>3 |
|--------------------|--|-----------------------|-----------------------|--------------------------------------|----------------------------------|---------------------------------|-------------|
| 1                  | 20.0   | 101.60                | 102.757               | 1.157                                | 0.0113                           | 0.247                           | 0.343       |
| 2                  | 47.0   | 101.60                | 103.40                | 1.800                                | 0.0174                           | 0.58                            | 0.806       |
| 3                  | 200.0  | 101.60                | 106.781               | 5.181                                | 0.0486                           | 2.47                            | 3.43        |
| 4                  | 242.0  | 101.60                | 110.39                | 8.800                                | 0.0796                           | 2.99                            | 4.15        |
| 5                  | 325.0  | 101.60                | 113.60                | 12.000                               | 0.1058                           | 4.01                            | 5.59        |



TABLE B.17

COMPARISON OF THE EXPERIMENTAL  $\epsilon$  WITH THE VALUE GIVEN BY HUGHMARK'S EQUATION

| Observation<br>No. | $U_{SG} \left( \frac{62.4}{\rho_L} \times \frac{72}{\sigma} \right)^{1/3}$ | $\epsilon$ (Expt)<br>(from graph) | $\epsilon'$ (Hughmark)<br>(from Hughmark's<br>graph) | $\epsilon$ (Hughmark)<br>(back-<br>calculated) |
|--------------------|--|-----------------------------------|--|--|
| 1                  | 0.914  | 0.019                             | 0.025  | 0.018  |
| 2                  | 1.525  | 0.028                             | 0.039  | 0.028  |
| 3                  | 2.440  | 0.040                             | 0.0585   | 0.040  |
| 4                  | 4.670  | 0.080                             | 0.106  | 0.079  |



TABLE B.18

INDIVIDUAL BUBBLE DIAMETERS

$O_2$  flow rate = 334 ccs/sec, magnification = 10, column diameter in photo = 3.0",

$$d_b = \frac{d_b'}{10} \cdot \frac{3.45}{3.0}$$

| 1  | w  | Number of<br>Bubbles, $n_i$ | $d_b'$ | $d_b$ | $n_i d_b^2$ | $n_i d_b^3$ |
|----|----|-----------------------------|--------|-------|-------------|-------------|
| 18 | 15 | 4                           | 16.9   | 1.94  | 15.04       | 29.17       |
| 12 | 10 | 27                          | 11.3   | 1.3   | 45.63       | 59.31       |
| 12 | 12 | 4                           | 12     | 1.38  | 7.60        | 8.74        |
| 10 | 10 | 38                          | 10     | 1.15  | 50.16       | 57.68       |
| 14 | 11 | 1                           | 12.9   | 1.49  | 2.22        | 3.30        |
| 14 | 10 | 1                           | 12.5   | 1.44  | 2.07        | 2.98        |
| 7  | 7  | 1                           | 7      | 0.805 | 0.64        | 0.51        |
| 15 | 13 | 2                           | 14.3   | 1.64  | 5.36        | 8.79        |
| 13 | 13 | 1                           | 13     | 1.49  | 2.22        | 3.30        |
| 20 | 20 | 4                           | 20     | 2.3   | 21.16       | 48.66       |
| 10 | 8  | 7                           | 9.3    | 1.07  | 7.98        | 8.53        |
| 20 | 8  | 1                           | 14.7   | 1.69  | 2.85        | 4.81        |
| 15 | 10 | 9                           | 13.1   | 1.51  | 20.52       | 30.98       |
| 15 | 15 | 24                          | 15     | 1.725 | 70.80       | 121.77      |
| 10 | 9  | 1                           | 9.64   | 1.11  | 1.23        | 1.36        |
| 20 | 15 | 7                           | 18.2   | 2.09  | 30.52       | 63.78       |
| 20 | 12 | 3                           | 16.86  | 1.94  | 11.28       | 21.88       |
| 15 | 12 | 1                           | 13.92  | 1.60  | 2.56        | 4.09        |
| 20 | 18 | 2                           | 19.3   | 2.22  | 9.84        | 21.84       |
| 18 | 8  | 1                           | 13.7   | 1.575 | 2.46        | 3.86        |

Cont'd.



TABLE B.18 CONTINUED

| l  | w  | Number of<br>Bubbles, $n_i$ | $d_b'$ | $d_b$ | $n_i d_b^2$     | $n_i d_b^3$     |
|----|----|-----------------------------|--------|-------|-----------------|-----------------|
| 20 | 7  | 1                           | 14.7   | 1.69  | 2.85            | 4.89            |
| 20 | 10 | 2                           | 15.9   | 1.83  | 6.68            | 12.22           |
| 30 | 15 | 1                           | 23.8   | 2.74  | 7.50            | 20.55           |
| 30 | 20 | 1                           | 26.2   | 3.02  | <u>9.12</u>     | <u>27.54</u>    |
|    |    |                             |        |       | $\Sigma=348.31$ | $\Sigma=570.46$ |

$$d_{vs} = \frac{570.46}{348.31} = 1.63 \text{ mm}$$





TABLE B.19

INDIVIDUAL BUBBLE DIAMETERS

$O_2$  flow rate = 215 ccs/sec, magnification = 10, Column diameter in photo = 2.2",

$$d_b = \frac{d_b'}{10} \cdot \frac{3.45}{2.2}$$

| 1  | w  | Number of<br>Bubbles, $n_i$ | $d_b'$ | $d_b$ | $n_i d_b^2$     | $n_i d_b^3$     |
|----|----|-----------------------------|--------|-------|-----------------|-----------------|
| 5  | 5  | 34                          | 5      | .784  | 20.40           | 15.91           |
| 6  | 6  | 1                           | 6      | .94   | 0.88            | 0.82            |
| 8  | 4  | 8                           | 6.3    | .989  | 7.68            | 7.60            |
| 8  | 5  | 1                           | 6.8    | 1.065 | 1.12            | 1.19            |
| 8  | 8  | 8                           | 8      | 1.25  | 12.48           | 15.60           |
| 10 | 8  | 1                           | 9.3    | 1.46  | 2.13            | 3.10            |
| 15 | 4  | 40                          | 9.6    | 1.50  | 90.0            | 135.00          |
| 10 | 10 | 2                           | 10     | 1.57  | 4.92            | 7.62            |
| 12 | 8  | 1                           | 10.2   | 1.60  | 2.56            | 4.09            |
| 10 | 10 | 11                          | 11.3   | 1.77  | 34.43           | 60.94           |
| 20 | 4  | 10                          | 11.7   | 1.83  | 33.40           | 61.12           |
| 10 | 6  | 1                           | 8.44   | 1.32  | 1.74            | 2.29            |
| 10 | 5  | 1                           | 7.92   | 1.24  | 1.53            | 1.89            |
| 12 | 12 | 1                           | 12     | 1.88  | 3.53            | 6.63            |
| 15 | 10 | 1                           | 13.1   | 2.05  | 4.20            | 8.61            |
| 30 | 10 | 2                           | 20.8   | 3.26  | 21.24           | 69.24           |
| 30 | 15 | 1                           | 23.3   | 3.68  | 13.54           | 49.82           |
|    |    |                             |        |       | $\Sigma=255.78$ | $\Sigma=451.66$ |

$$d_{vs} = \frac{451.66}{255.78} = 1.76 \text{ mm.}$$



TABLE B.20

INDIVIDUAL BUBBLE DIAMETERS

O<sub>2</sub> flow rate = 177 ccs/sec, magnification = 10, Column diameter in photo = 2.50".

$$d_b = \frac{d_b'}{10} \cdot \frac{3.45}{2.50}$$

| l  | w  | Number of<br>Bubbles, $n_i$ | $d_b'$ | $d_b$ | $n_i d_b^2$      | $n_i d_b^3$      |
|----|----|-----------------------------|--------|-------|------------------|------------------|
| 8  | 8  | 2                           | 8      | 1.104 | 2.436            | 2.682            |
| 8  | 6  | 1                           | 7.26   | 1.001 | 1.002            | 1.003            |
| 10 | 8  | 5                           | 9.3    | 1.283 | 8.23             | 10.559           |
| 12 | 6  | 1                           | 9.5    | 1.311 | 1.718            | 2.252            |
| 10 | 10 | 8                           | 10     | 1.38  | 15.232           | 21.020           |
| 12 | 8  | 1                           | 10.2   | 1.407 | 1.979            | 2.784            |
| 12 | 10 | 5                           | 11.3   | 1.559 | 12.150           | 18.941           |
| 12 | 12 | 3                           | 12     | 1.656 | 8.226            | 13.622           |
| 15 | 10 | 10                          | 13.1   | 1.807 | 32.65            | 58.998           |
| 20 | 10 | 1                           | 15.86  | 2.188 | 4.788            | 10.476           |
| 18 | 18 | 1                           | 18     | 2.484 | 6.170            | 15.326           |
| 20 | 15 | 1                           | 18.2   | 2.511 | 6.305            | 15.831           |
|    |    |                             |        |       | $\Sigma=100.886$ | $\Sigma=173.494$ |

$$d_{vs} = \frac{173.494}{100.886} = 1.719 \text{ mm.}$$



TABLE B.21

INDIVIDUAL BUBBLE DIAMETERS

O<sub>2</sub> flow rate = 85 ccs/sec, magnification = 10, Column diameter in photo = 2.0",

$$d_b = \frac{d_b'}{10} \cdot \frac{3.45}{2.0}$$

| 1  | w  | Number of<br>Bubbles, n <sub>i</sub> | d <sub>b</sub> ' | d <sub>b</sub> | n <sub>i</sub> d <sub>b</sub> <sup>2</sup> | n <sub>i</sub> d <sub>b</sub> <sup>3</sup> |
|----|----|--------------------------------------|------------------|----------------|--|--|
| 6  | 6  | 9                                    | 6                | 1.035          | 9.54                                       | 9.82                                       |
| 8  | 8  | 47                                   | 8                | 1.38           | 89.30                                      | 123.23                                     |
| 9  | 9  | 8                                    | 9                | 1.55           | 19.20                                      | 29.76                                      |
| 10 | 8  | 2                                    | 9.28             | 1.60           | 5.12                                       | 8.19                                       |
| 10 | 10 | 31                                   | 10               | 1.72           | 91.45                                      | 157.29                                     |
| 12 | 10 | 4                                    | 11.28            | 1.945          | 15.04                                      | 29.17                                      |
| 13 | 10 | 2                                    | 11.90            | 2.05           | 8.40                                       | 17.22                                      |
| 12 | 12 | 2                                    | 12               | 2.07           | 8.56                                       | 17.71                                      |
| 15 | 10 | 11                                   | 13.08            | 2.26           | 56.10                                      | 126.78                                     |
| 15 | 12 | 3                                    | 13.90            | 2.40           | 17.20                                      | 41.28                                      |
| 16 | 12 | 1                                    | 14.52            | 2.50           | 6.25                                       | 15.62                                      |
| 11 | 17 | 1                                    | 14.70            | 2.53           | 6.40                                       | 16.19                                      |
| 18 | 10 | 1                                    | 14.80            | 2.55           | 6.50                                       | 16.57                                      |
| 16 | 15 | 1                                    | 15.64            | 2.70           | 7.29                                       | 19.68                                      |
| 18 | 12 | 1                                    | 15.70            | 2.71           | 7.34                                       | 19.89                                      |
| 15 | 15 | 1                                    | 15.00            | 2.58           | 6.65                                       | 17.15                                      |
| 20 | 10 | 3                                    | 15.86            | 2.73           | 22.35                                      | 61.01                                      |
| 16 | 14 | 1                                    | 15.3             | 2.64           | 6.96                                       | 18.37                                      |
| 15 | 15 | 1                                    | 15.0             | 2.59           | 6.70                                       | 17.35                                      |

(cont'd.)



TABLE B.21 CONTINUED

| 1  | w  | Number of<br>Bubbles, $n_i$ | $d_b'$ | $d_b$ | $n_i d_b^2$     | $n_i d_b^3$      |
|----|----|-----------------------------|--------|-------|-----------------|------------------|
| 14 | 10 | 1                           | 12.52  | 2.16  | 4.66            | 10.06            |
| 20 | 12 | 1                           | 16.86  | 2.91  | 8.46            | 24.61            |
| 20 | 15 | 1                           | 18.16  | 3.13  | 9.79            | 30.64            |
| 25 | 10 | 1                           | 18.4   | 3.18  | 10.11           | 32.14            |
| 20 | 17 | 1                           | 18.9   | 3.26  | 10.62           | 34.62            |
| 24 | 15 | 1                           | 20.4   | 3.52  | 12.39           | 43.61            |
| 30 | 12 | 1                           | 22.2   | 3.83  | 14.66           | 55.95            |
| 40 | 12 | 1                           | 26.7   | 4.60  | 21.16           | 97.33            |
|    |    |                             |        |       | $\Sigma=488.11$ | $\Sigma=1091.24$ |

$$d_{vs} = \frac{1091.24}{488.11} = 2.23 \text{ mm.}$$





TABLE B.24

INDIVIDUAL BUBBLE DIAMETERS

O<sub>2</sub> flow rate = 47 ccs/sec, magnification = 14, Column diameter in photo=1.70 "

$$d_b = \frac{d_b'}{14} \left( \frac{3.45}{1.70} \right)$$

| 1  | w  | Number of<br>Bubbles, $n_i$ | $d_b'$ | $d_b$ | $n_i d_b^2$     | $n_i d_b^3$      |
|----|----|-----------------------------|--------|-------|-----------------|------------------|
| 5  | 5  | 1                           | 5      | 0.72  | 0.518           | 0.372            |
| 6  | 6  | 7                           | 6      | 0.864 | 5.222           | 4.511            |
| 8  | 6  | 4                           | 7.26   | 1.045 | 4.366           | 4.562            |
| 8  | 8  | 3                           | 8      | 1.152 | 3.981           | 4.586            |
| 10 | 6  | 10                          | 8.44   | 1.215 | 14.76           | 17.933           |
| 10 | 8  | 8                           | 9.3    | 1.339 | 14.336          | 19.195           |
| 10 | 10 | 9                           | 10     | 1.44  | 18.657          | 26.866           |
| 14 | 5  | 1                           | 10.04  | 1.445 | 2.088           | 3.017            |
| 16 | 5  | 1                           | 10.84  | 1.56  | 2.433           | 3.795            |
| 15 | 6  | 1                           | 11.4   | 1.641 | 2.692           | 4.417            |
| 12 | 10 | 1                           | 11.3   | 1.627 | 2.647           | 4.306            |
| 12 | 12 | 1                           | 12     | 1.728 | 2.985           | 5.158            |
| 12 | 8  | 1                           | 10.2   | 1.468 | 2.155           | 3.163            |
| 18 | 8  | 1                           | 13.7   | 1.972 | 3.888           | 7.667            |
| 15 | 13 | 1                           | 14.3   | 2.059 | 4.29            | 8.833            |
|    |    |                             |        |       | $\Sigma=84.969$ | $\Sigma=118.381$ |

$$d_{vs} = \frac{118.381}{84.969} = 1.393 \text{ mm.}$$



TABLE B.23

CONVERSION OF AcH to AcOH IN SPARGER REACTOR

$T = 40^{\circ}\text{C}$ ,  $P = 20$  psig, Catalyst concentration = 140 ppm, Liquid height = 40",  
 Diameter of column  $\approx 4$ ", Orifice diameter  $\approx 0.2$  cm., Liquid recycle rate =  
 1.83 U.S. G.P.M.,  $\text{O}_2$  flow rate = 334 ccs/sec;  $b_{\text{AcH}}^{\circ} = 10\%$  vol. at  $40^{\circ}\text{C}$  and  
 34.7 psia.

| Time<br>(Mins) | $b_{\text{AcOH}}$ | $b_{\text{AcH}}$ (volume %) |
|----------------|-------------------|-----------------------------|
| 0              | 90.0              | 10.0                        |
| 6              | 92.0              | 8.0                         |
| 10             | 93.3              | 6.7                         |
| 20             | 96.1              | 3.9                         |
| 30             | 98.1              | 1.9                         |
| 40             | 99.3              | 0.7                         |
| 50             | 99.7              | 0.3                         |



TABLE B.24

CONVERSION OF AcH to AcOH IN SPARGER REACTOR

O<sub>2</sub> flow rate = 85 ccs/sec, T = 40°C, P = 20 psig, Catalyst concentration = 140 ppm, b<sup>o</sup><sub>AcH</sub> = 10% volume.

| Observation Number | Time (Mins) | b <sub>AcOH</sub> (volume %) | b <sub>AcH</sub> (volume %) |
|--------------------|-------------|------------------------------|-----------------------------|
| 1                  | 0           | 90.0                         | 10.0                        |
| 2                  | 10          | 91.6                         | 8.4                         |
| 3                  | 20          | 93.0                         | 7.0                         |
| 4                  | 30          | 94.3                         | 5.7                         |
| 5                  | 40          | 96.1                         | 3.9                         |
| 6                  | 50          | 96.8                         | 3.2                         |
| 7                  | 60          | 98.4                         | 1.6                         |
| 8                  | 90          | 99.4                         | 0.6                         |



## CONCN-TIME PROFILE-EXIDN OF ACH IN BUBBLE REACTOR

MASS TR. COEFF\*VOL INTERFACIAL AREA= 0.01100

| TIME(MINS)  | CONCN-O2   | CONCN.-ACH  |
|-------------|------------|-------------|
| 0.00000010  | 0.00000000 | 10.00000000 |
| 1.99998379  | 0.00000327 | 9.71738815  |
| 3.99995327  | 0.00000337 | 9.40493488  |
| 5.99992275  | 0.00000347 | 9.09396648  |
| 7.99989223  | 0.00000357 | 8.78456020  |
| 9.99986172  | 0.00000368 | 8.47680569  |
| 11.99983120 | 0.00000379 | 8.17079526  |
| 13.99980068 | 0.00000392 | 7.86663342  |
| 15.99977016 | 0.00000405 | 7.56442547  |
| 17.99972824 | 0.00000418 | 7.26429653  |
| 19.99969456 | 0.00000433 | 6.96637440  |
| 21.99966027 | 0.00000448 | 6.67079067  |
| 23.99962679 | 0.00000465 | 6.37770748  |
| 25.99959371 | 0.00000482 | 6.08728409  |
| 27.99956043 | 0.00000501 | 5.79971218  |
| 29.99952715 | 0.00000521 | 5.51517200  |
| 31.99949387 | 0.00000543 | 5.23389149  |
| 33.99946059 | 0.00000566 | 4.95609760  |
| 35.99942731 | 0.00000590 | 4.68205166  |
| 37.99939402 | 0.00000617 | 4.41203213  |
| 39.99936074 | 0.00000645 | 4.14634228  |
| 41.99932746 | 0.00000676 | 3.88530922  |
| 43.99929418 | 0.00000709 | 3.62930012  |
| 45.99926090 | 0.00000745 | 3.37870884  |
| 47.99922762 | 0.00000783 | 3.13397026  |
| 49.99919434 | 0.00000825 | 2.89553642  |
| 51.99916106 | 0.00000870 | 2.66390038  |
| 53.99912777 | 0.00000918 | 2.43959236  |
| 55.99909449 | 0.00000970 | 2.22317696  |
| 57.99906121 | 0.00001026 | 2.01524258  |
| 59.99902793 | 0.00001086 | 1.81637573  |
| 61.99899465 | 0.00001149 | 1.62719917  |
| 63.99896137 | 0.00001217 | 1.44828892  |
| 65.99892809 | 0.00001289 | 1.28027058  |
| 67.99889481 | 0.00001364 | 1.12362862  |
| 69.99886152 | 0.00001442 | 0.97874540  |
| 71.99882824 | 0.00001522 | 0.84592372  |
| 73.99879496 | 0.00001604 | 0.72532558  |
| 75.99876168 | 0.00001686 | 0.61694050  |
| 77.99872840 | 0.00001766 | 0.52056825  |





## CONCN-TIME PROFILE-OXIDN OF ACH IN BUBBLE REACTOR

MASS TR. COEFF\*VOL INTERFACIAL AREA= 0.03000

| TIME(MINS)   | CONCN-O2   | CONCN.-ACH  |
|--------------|------------|-------------|
| 0.00000010   | 0.00000000 | 10.00000000 |
| 1.99998379   | 0.00000742 | 9.36505699  |
| 3.99995327   | 0.00000781 | 8.68914986  |
| 5.99992275   | 0.00000823 | 8.03003502  |
| 7.99989223   | 0.00000868 | 7.38908291  |
| 9.99986172   | 0.00000917 | 6.76775646  |
| 11.99983120  | 0.00000970 | 6.16762447  |
| 13.99980068  | 0.00001027 | 5.59034252  |
| 15.99977016  | 0.00001089 | 5.03763008  |
| 17.999728284 | 0.00001155 | 4.51126957  |
| 19.99879456  | 0.00001225 | 4.01299381  |
| 21.99830627  | 0.00001299 | 3.54451847  |
| 23.99781799  | 0.00001377 | 3.10738754  |
| 25.99732971  | 0.00001458 | 2.70293427  |
| 27.99684143  | 0.00001541 | 2.33217430  |
| 29.99635315  | 0.00001625 | 1.99571037  |
| 31.99586487  | 0.00001710 | 1.69362545  |
| 33.99537659  | 0.00001793 | 1.42545605  |
| 35.99488831  | 0.00001873 | 1.19020748  |
| 37.99440002  | 0.00001948 | 0.98619944  |
| 39.99391174  | 0.00002018 | 0.81130332  |
| 41.99342346  | 0.00002082 | 0.66302514  |
| 43.99293518  | 0.00002140 | 0.53862447  |
| 45.99244690  | 0.00002190 | 0.43526036  |
| 47.99195862  | 0.00002233 | 0.35011810  |
| 49.99147034  | 0.00002270 | 0.28052193  |
| 51.99098206  | 0.00002301 | 0.22401375  |
| 53.99049377  | 0.00002326 | 0.17839134  |
| 55.99000549  | 0.00002348 | 0.14173377  |
| 57.98951721  | 0.00002365 | 0.11239636  |
| 59.98902893  | 0.00002379 | 0.08899486  |
| 61.98854065  | 0.00002390 | 0.07038200  |
| 63.98805237  | 0.00002399 | 0.05560732  |
| 65.98756409  | 0.00002406 | 0.04389931  |
| 67.98707581  | 0.00002412 | 0.03463450  |
| 69.98658752  | 0.00002416 | 0.02731119  |
| 71.98609924  | 0.00002420 | 0.02152773  |
| 73.98561096  | 0.00002423 | 0.01696357  |
| 75.98512268  | 0.00002425 | 0.01336366  |
| 77.98463440  | 0.00002427 | 0.01052557  |















**B29949**